Dual little strings from F-theory and flop transitions

Stefan Hohenegger,[a,b] **Amer Iqbal**[a,c,d] **and Soo-Jong Rey**[a,e]

[a]*Fields, Gravity & Strings, CTPU, Institute for Basic Sciences,*
Seoul 08826, Korea

[b]*Université de Lyon, UMR 5822, CNRS/IN2P3, Institut de Physique Nucléaire de Lyon,*
4 rue Enrico Fermi, 69622 Villeurbanne Cedex, France

[c]*Abdus Salam School of Mathematical Sciences, Government College University,*
Lahore, Pakistan

[d]*Center for Theoretical Physics,*
Lahore, Pakistan

[e]*School of Physics and Astronomy & Center for Theoretical Physics,*
Seoul National University,
Seoul 08826, Korea

E-mail: s.hohenegger@ipnl.in2p3.fr, amer@alum.mit.edu,
rey.soojong@gmail.com

ABSTRACT: A particular two-parameter class of little string theories can be described by M parallel M5-branes probing a transverse affine A_{N-1} singularity. We previously discussed the duality between the theories labelled by (N, M) and (M, N). In this work, we propose that these two are in fact only part of a larger web of dual theories. We provide evidence that the theories labelled by (N, M) and $(\frac{NM}{k}, k)$ are dual to each other, where $k = \gcd(N, M)$. To argue for this duality, we use a geometric realization of these little string theories in terms of F-theory compactifications on toric, non-compact Calabi-Yau threefolds $X_{N,M}$ which have a double elliptic fibration structure. We show explicitly for a number of examples that $X_{NM/k,k}$ is part of the extended moduli space of $X_{N,M}$, i.e. the two are related through symmetry transformations and flop transitions. By working out the full duality map, we provide a simple check at the level of the free energy of little string theories.

Contents

1 Introduction

Little string theories are a class of interacting, non-local, ultraviolet complete quantum theories in six dimensions (or lower), which nevertheless has a well-defined energy-momentum tensor. These theories have recently attracted a lot of renewed attention from various viewpoints [1–11]. They can be obtained from string theory through a particular decoupling limit that preserves numerous 'stringy' properties, but suppresses gravitational interactions. The limit in type II string theory requires to take the string coupling constant to zero ($g_{st} \to 0$), while keeping the string length ℓ_{st} fixed. Depending on the details, we can construct various types of little string theories [12–19].

Maximally supersymmetric little string theories have sixteen supercharges (for a review, see [20]) and come in two different incarnations that are related by T-duality upon circle compactification:

- type IIa little string theory of A_{N-1} type with $\mathcal{N} = (1,1)$ supersymmetry:
  This non-chiral LST can be obtained through the decoupling limit of a stack of N NS5-branes in type IIB string theory, or through the decoupling limit of an $\mathbb{R}^4/\mathbb{Z}_N$ orbifold background in type IIA string theory,

- type IIb little string theory of A_{N-1} type with $\mathcal{N} = (2,0)$ supersymmetry:
  This chiral LST can be obtained through the decoupling limit of a stack of N NS5-branes in type IIA string theory, or through the decoupling limit of an $\mathbb{R}^4/\mathbb{Z}_N$ orbifold background in type IIB string theory.

One way to make T-duality between these two theories tangible is through a nonperturbative construction of little string theories within the framework of F-theory compactification [21, 22]. Indeed, the theories mentioned above can be described in terms of toric, non-compact Calabi-Yau threefolds that feature a double elliptic fibration structure. We studied these Calabi-Yau threefolds in previous papers [8, 10] and denoted them by $X_{N,1}$. In this F-theory framework, the little string T-duality corresponds to the exchange of the two elliptic fibrations [8, 9], relating type IIa and type IIb little string theories of type A_{N-1}.

More recently, little string theories with eight supercharges have been studied [9, 10, 23, 24]. A two-parameter class of such theories can be obtained from type IIa or IIb little string theories of type A_{N-1} through a particular orbifolding procedure [9, 10, 25]. Specifically, we consider the decoupling limit of a stack of NS5-branes that probe an orbifold singularity (rather than flat $\mathbb{R}^4$ as above), i.e. for generic $N, M \in \mathbb{N}$, we have

- $\mathbb{Z}_N$ orbifold of IIa little string theory of type A_{M-1}:
  This little string theory generically preserves $\mathcal{N} = (1,0)$ supersymmetry and is described through the decoupling limit of M NS5-branes in type IIB string theory probing an $\mathbb{R}^4/\mathbb{Z}_N$ orbifold background.

- $\mathbb{Z}_M$ orbifold of IIb little string theory of type A_{N-1}:
  This little string theory generically preserves $\mathcal{N} = (1,0)$ supersymmetry and is described through the decoupling limit of N NS5-branes in type IIA string theory probing an $\mathbb{R}^4/\mathbb{Z}_M$ orbifold background.

Extending the discussion in [26], the type IIb orbifolded little string theory can also be described as a decoupling limit of N parallel NS5-branes that probe an affine A_{M-1} ALE space. By lifting to M-theory, this realisation allows a description of the BPS excitations of the little string theories through systems of parallel M5-branes with M2-branes stretched between them. For the latter, the partition functions can be computed in a very efficient manner, using either the world-sheet theory of the M-string (which is the one-dimensional intersection between the M5- and M2-branes) [25, 27] or a dual realisation in terms of (p, q)-brane webs in type II string theory [28, 29].

The description we will mostly focus on in this paper, however, is in terms of F-theory on a two-parameter class of toric, non-compact Calabi-Yau threefolds $X_{N,M}$, generalising the geometric approach to the little string theories with sixteen supercharges mentioned above. Indeed, denoting by $Z_{\text{IIa}}^{(N,M)}$ and $Z_{\text{IIb}}^{(M,N)}$ the little string partition functions and by $\mathcal{Z}_{X_{N,M}}(\mathbf{t}, \mathbf{T}, m, \epsilon_{1,2})$ the refined topological string partition function[1] on $X_{N,M}$, we proposed in the previous work [10]

$$Z_{\text{IIa}}^{(N,M)}(\mathbf{T}, \mathbf{t}, m, \epsilon_{1,2}) = \mathcal{Z}_{X_{N,M}}(\mathbf{t}, \mathbf{T}, m, \epsilon_{1,2}), \quad Z_{\text{IIb}}^{(M,N)}(\mathbf{T}, \mathbf{t}, m, \epsilon_{1,2}) = \mathcal{Z}_{X_{M,N}}(\mathbf{T}, \mathbf{t}, m, \epsilon_{1,2}),$$

which makes T-duality manifest in the sense that $Z_{\text{IIa}}^{(N,M)}(\mathbf{T}, \mathbf{t}, m, \epsilon_{1,2}) = Z_{\text{IIb}}^{(N,M)}(\mathbf{t}, \mathbf{T}, m, \epsilon_{1,2})$. This connection between little string theories and the Calabi-Yau threefolds $X_{N,M}$ also reveals a number of other additional dualities. For example, since $X_{N,M}$ can be represented as a particular resolution of a $\mathbb{Z}_N \times \mathbb{Z}_M$ orbifold of $X_{1,1}$ (which at the boundary of the moduli space resembles the resolved conifold), it follows that $X_{N,M}$ and $X_{M,N}$ are dual to each other. This duality also implies that the $\mathbb{Z}_N$ orbifolds of IIa LST of type A_{M-1} (and respectively the $\mathbb{Z}_M$ orbifolds of IIb LST of type A_{N-1}) are self-dual under T-duality [10] in certain regions of the $(\mathbf{t}, \mathbf{T})$ moduli space. This has been checked explicitly at the level of the free energies associated with the partition functions $Z_{\text{IIa}}^{(N,M)}$ and $Z_{\text{IIb}}^{(M,N)}$ [10].

In this paper, we consider further duality relations between theories that are characterised by different (N, M). Based on a number of explicit examples, we propose that theories characterised by (N, M) (with generic $M, N \in \mathbb{N}$ and $\gcd(M, N) = k$) and $(\frac{NM}{k}, k)$ are dual to each other. The corresponding Calabi-Yau threefolds are related through a chain of transformations involving flop transitions:[2]

$$X_{N,M} \quad \sim \quad X_{NM/k,k}, \qquad \text{for} \qquad k = \gcd(M, N).$$

Moreover, we make a proposal for the full duality map, i.e. we provide the Kähler parameters of $X_{NM/k,k}$ completely in terms of the Kähler parameters of $X_{N,M}$. Finally, based on results of our previous work [10], we perform a simple check at the level of the free energies $\Sigma_{N,M}$ associated with the partition functions $\mathcal{Z}_{X_{N,M}}$. Indeed, in [10], we proposed that the free energies $\Sigma_{N,M}$ enjoy a special property which we called *self-similarity*: in a particular region of the parameter space and in the Nekrasov-Shatashvili limit [30, 31], we have $\lim_{\epsilon_2 \to 0} \epsilon_2 \Sigma_{N,M} = NM \lim_{\epsilon_2 \to 0} \epsilon_2 \Sigma_{1,1}$. We show for generic $M, N \in \mathbb{N}$ that the

---

[1]Here $\mathbf{t}$ and $\mathbf{T}$ are two sets of Kähler parameters (associated with a double elliptic fibration of $X_{N,M}$) and $\epsilon_{1,2}$ as well as m are deformation parameters.

[2]By $\sim$, we will denote Calabi-Yau threefolds related by symmetry transformations and flop transitions.

proposed duality map, when restricted to the above mentioned region in parameter space, corresponds to an $\mathrm{Sp}(2,\mathbb{Z})$ transformation, under which $\mathcal{Z}_{X_{1,1}}$ is invariant. This is a strong indication that indeed $\mathcal{Z}_{X_{N,M}} = \mathcal{Z}_{X_{NM/k,k}}$ after application of the duality map.

This proposed duality has other consequences and in fact gives rise to a whole web of dual theories. Indeed, for any pair of integers (M,N) and (M',N') with $MN = M'N'$ and $\gcd(M,N) = k = \gcd(M',N')$, the proposed duality also implies

$$X_{N,M} \quad \sim \quad X_{N',M'} \,.$$

In this way, we have for example that the Calabi-Yau threefolds parametrised by $(30,1) \sim (15,2) \sim (10,3) \sim (6,5) \sim (5,6) \sim (3,10) \sim (2,15) \sim (1,30)$ are all related to one another. Reformulating this relation in a more abstract fashion, we propose that the theories parametrised by (M,N) and (M',N') as above are part of the extended moduli space [32–36] of the Calabi-Yau threefold $X_{NM/k,k}$. Little string theories described by $(N,1)$ brane configuration preserve sixteen supercharges. An additional twist (the m-deformation) breaks the supersymmetry down to eight supercharges [25, 27]. In M-theory description, this additional twist is needed for localizing M5-branes in transverse $\mathbb{R}^4$ and thus for unambiguously calculating the partition function using the M-string worldsheet theory. In F-theory description, this additional twist is needed for obtaining smooth geometries for various duality maps therein. From the viewpoint of little string theories, this means that $\mathbb{Z}_M$ orbifolds of type IIa or IIb little string theories of type A_{N-1} with $k = 1$ are dual to IIb or IIa little string theories of type A_{NM-1} with this additional twist given by parameter m, and both configurations preserve eight supercharges. However, as we shall discuss in detail, the little string theories labelled by (N,M) and $(NM,1)$ live in different points of the parameter space: the radii of the two transverse circles on which the little strings are compactified are different in the two cases.

This paper is organised as follows: in section 2, we review in more detail the relation between little string theories and toric Calabi-Yau threefolds $X_{N,M}$. We will also discuss flop transitions that define the extended moduli space of the latter. In section 3, we review the topological string partition functions of $X_{N,M}$ as well as its relation to $\mathcal{Z}_{X_{1,1}}$ in a particular region in the Kähler moduli space. In section 4, we present numerous explicit examples for the duality $X_{N,M} \sim X_{NM/k,k}$ (with $k = \gcd(N,M)$) and present checks for the duality at the level of the free energies. In section 5, we make a proposal of the duality map for generic (N,M) and show that it satisfies the same checks as all the examples of section 4. Finally, section 6 contains our conclusions.

2 Little strings and Calabi-Yau threefolds

Little string theories can be described in several different but U-dual equivalent ways. For example, they can be realised as ADE orbifold compactifications of type II string theory (in the presence of NS5-branes) subject to a particular limit in which gravity decouples [12–19]. Alternatively, LSTs can also be described by systems of M5-branes in M-theory that probe a transverse ADE orbifold. However, the description that is most useful for our current purposes uses the F-theory: indeed, by compactifying F-theory on appropriate elliptically

fibered Calabi-Yau threefolds, little string theories with both $\mathcal{N} = (2,0)$ and $\mathcal{N} = (1,0)$ supersymmetry can be obtained. In fact, a classification of little string theories using this F-theory approach was carried out recently in [9].

These Calabi-Yau threefolds are elliptically fibered over a two complex dimensional base, which in the decoupling limit becomes non-compact. In general, the charge lattice of the compactified theory is given by the lattice of two-cycles in the non-compact base, and BPS states are given by D3-branes wrapping holomorphic two curves in the base. The little strings in particular arise from D3-branes wrapping a curve of self intersection zero in the base. Calabi-Yau threefolds that have such a curve with vanishing self-intersection in the base actually have a double elliptic fibration, since the base itself is an elliptic fibration over the complex plane [37]. As was first discovered in [8, 9], this double fibration structure is crucially related to T-duality of the little string theory.

2.1 Calabi-Yau threefolds $X_{N,M}$

Calabi-Yau threefolds $X_{N,M}$ which realise type IIa little strings in an orbifold background of type A_N are toric and are given by the resolution of a $\mathbb{Z}_N \times \mathbb{Z}_M$ orbifold of $X_{1,1}$ [8]. Here $X_{1,1}$ is itself a Calabi-Yau threefold with a double elliptic fibration over the complex plane [38]. To understand this, we begin with a geometry that is similar to $X_{1,1}$, namely the (deformed) conifold. The latter can be described as a hypersurface in $\mathbb{C}^4$

$$xy - zw = \epsilon, \qquad \text{for} \qquad (x, y, z, w) \in \mathbb{C}^4. \qquad (2.1)$$

Here $\epsilon > 0$ corresponds to the deformation that regularises an otherwise singular geometry. To make the fibration structure visible, we re-write eq. (2.1) in the following manner

$$xy = u, \ \ zw = u - \epsilon, \qquad (2.2)$$

which corresponds to a $\mathbb{C}^\times \times \mathbb{C}^\times$ fibration over the u-plane: the first $\mathbb{C}^\times$ fibration degenerates at $u = 0$ and the second one at $u = \epsilon$. The $\mathbb{S}^1$'s of these two $\mathbb{C}^\times$ fibrations together with the path in the u-plane connecting the points $u = 0$ and $u = \epsilon$ give an $\mathbb{S}^3$. We can compactify the $\mathbb{C}^\times$ fibers to obtain a double elliptic fibration over the u-plane,

$$y^2 = x^3 + f_1(u)\,x + g_1(u), \quad w^2 = z^3 + f_2(u)\,z + g_2(u). \qquad (2.3)$$

Here $f_1(u), g_1(u), f_2(u), g_2(u)$ are holomorphic functions of u such that $\Delta_1(u) = 4f_1^3 + 27g_1^2$ vanishes only at $u = 0$ and $\Delta_2(u) = 4f_2^3 + 27g_2^2$ vanishes only at $u = \epsilon$ so that the two elliptic fibrations have fibers of type I_1 at $u = 0$ and $u = \epsilon$, respectively.

The geometry described above is singular in the limit $\epsilon \to 0$. Besides the deformation eq. (2.1), we have an alternative way of dealing with this singularity: we can also resolve the conifold to obtain a $\mathbb{P}^1$. Indeed, instead of eq. (2.1), we describe the resolution of the conifold through the equation

$$\begin{pmatrix} x & z \\ w & y \end{pmatrix} \begin{pmatrix} \lambda_1 \\ \lambda_2 \end{pmatrix} = 0, \qquad (2.4)$$

where $\lambda = \frac{\lambda_1}{\lambda_2}$ is the coordinate on the blowup $\mathbb{P}^1$ mentioned above. The resulting geometry can also be described as a $\mathbb{C}^4$ quotient by $\mathbb{C}^\times$,

$$(A_1, A_2, B_1, B_2) \mapsto (\lambda A_1, \lambda A_2, \lambda^{-1} B_1, \lambda^{-1} B_2), \tag{2.5}$$

where (A_1, A_2, B_1, B_2) are coordinates of $\mathbb{C}^4$ such that[3]

$$\begin{pmatrix} x & z \\ w & y \end{pmatrix} = \begin{pmatrix} A_1 \\ A_2 \end{pmatrix} \begin{pmatrix} B_1 & B_2 \end{pmatrix}. \tag{2.6}$$

The resolution is particularly useful for discussing orbifolds of the conifold: let $\Gamma_1 \times \Gamma_2 \subset \mathrm{SU}(2) \times \mathrm{SU}(2)$ be a pair of ADE subgroups of $\mathrm{SU}(2)$ which act on $(A_1, A_2, B_1, B_2) \in \mathbb{C}^4$ by embedding in $\mathrm{SU}(4)$:

$$\Gamma_1: \begin{pmatrix} A_1 \\ B_1 \end{pmatrix} \mapsto \gamma_1 \begin{pmatrix} A_1 \\ B_1 \end{pmatrix}, \qquad \text{for} \qquad \gamma_1 \in \Gamma_1$$

$$\begin{pmatrix} A_2 \\ B_2 \end{pmatrix} \mapsto \begin{pmatrix} A_2 \\ B_2 \end{pmatrix}$$

$$\Gamma_2: \begin{pmatrix} A_1 \\ B_2 \end{pmatrix} \mapsto \gamma_2 \begin{pmatrix} A_1 \\ B_2 \end{pmatrix}, \qquad \text{for} \qquad \gamma_2 \in \Gamma_2$$

$$\begin{pmatrix} A_2 \\ B_1 \end{pmatrix} \mapsto \begin{pmatrix} A_2 \\ B_1 \end{pmatrix}. \tag{2.7}$$

Modding the geometry (2.4) by this action we get the $\Gamma_1 \times \Gamma_2$ orbifold of the resolved conifold. In the particular case $\Gamma_1 \times \Gamma_2 = \mathbb{Z}_N \times \mathbb{Z}_M$ for $M, N \in \mathbb{Z}$ the action eq. (2.7) takes the form [39]:

$$(A_1, A_2, B_1, B_2) \mapsto (\omega_N^a \omega_M^b A_1, A_2, \omega_N^{-a} B_1, \omega_M^{-b} B_2), \tag{2.8}$$

where $(\omega_N, \omega_M) = (e^{\frac{2\pi i}{N}}, e^{\frac{2\pi i}{M}})$ and $a, b \in \mathbb{Z}$.[4]

In order to describe little string theories, we have to replace the deformed conifold by the doubly elliptically fibered Calabi-Yau manifold $X_{1,1}$ which can be understood as a compactification of $\mathbb{C}^\times \times \mathbb{C}^\times$ fibers of the resolved conifold to double elliptic fibers, as we shall discuss in the following section. In the general case of a $\Gamma_1 \times \Gamma_2$ orbifold of $X_{1,1}$ we obtain a geometry with two fibers of the corresponding ADE type in the two elliptic fibrations, which describes (Γ_1, Γ_2) little string theories.[5]

---

[3]Notice that the relation $\det \left[\begin{pmatrix} A_1 \\ A_2 \end{pmatrix} \begin{pmatrix} B_1 & B_2 \end{pmatrix} \right] = xy - zw = 0$ for the unresolved conifold is manifestly realised in this parametrisation.

[4]For completeness we mention that we can also describe $\mathbb{Z}_N \times \mathbb{Z}_M$ orbifolds of the deformed conifold. Indeed, when the $\mathbb{C}^\times \times \mathbb{C}^\times$ fibration of the deformed conifold is compactified to a double elliptic fibration, we can introduce the orbifold geometry

$$y^2 = x^3 + f_1(u^N) x + g_1(u^N), \quad w^2 = z^3 + f_2(u^M) z + g_2(u^M), \tag{2.9}$$

so that there is a I_N and I_M fiber in the two elliptic fibrations.

[5]For a recent discussions on multiple fibrations, see [40].

Figure 1. The Newton polygon of the resolved conifold (left) and the Calabi-Yau threefold $X_{1,1}$ (right). The polygon of the latter is obtained by tiling the plane with the Newton polygon of the resolved conifold. Equivalently, this tiling can be though of drawing the Newton polygon of the resolved conifold on a (doubly periodic) torus.
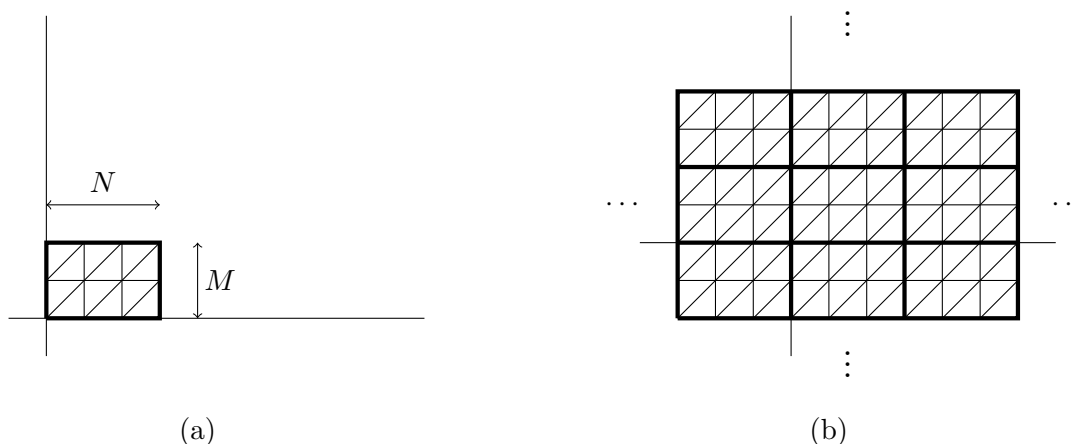

Figure 2. (a) The Newton polygon of the $\mathbb{Z}_N \times \mathbb{Z}_M$ orbifold of the resolved conifold. (b) The Newton polygon of $X_{N,M}$ is obtained through a tiling of the plane with the Newton polygon of the orbifold of the resolved conifold.

2.1.1 The dual brane webs

The toric Calabi-Yau threefolds $X_{N,M}$ obtained from $\mathbb{Z}_M \times \mathbb{Z}_N$ orbifolds of $X_{1,1}$, as described in the previous subsubsection, can be dualised to (p,q) 5-brane webs [41, 42] which in turn realise certain five- and six-dimensional gauge theories [38, 41]. This dual 5-brane web is in fact identical to the toric web of $X_{N,M}$, which is dual to the Newton polygon [41]. The Newton polygon of $X_{1,1}$ (as well as the one of the resolved conifold) are shown in figure 1. The $\mathbb{Z}_N \times \mathbb{Z}_M$ orbifold of the resolved conifold is also toric and the corresponding Newton polygon is given by a rectangle of size $N \times M$ [39]. Similar to $X_{1,1}$, the Newton polygon of $X_{N,M}$ is described by a tiling of the plane by the Newton polygon of the orbifolded resolved conifold, i.e. the rectangle of size $N \times M$ as shown in figure 2. The periodic tiling in figure 2(b) then implies that these webs are living on $\mathbb{T}^2$ rather than on $\mathbb{R}^2$, and the two elliptic fibrations of $X_{N,M}$ are dual to the two circles on which the 5-branes are wrapped. The web diagram of $X_{N,M}$ can be obtained as the dual graph of the Newton polygon and is shown in figure 3. The diagonal (blue) lines along the direction $(1,1)$ in figure 3 are due to the triangulation of the Newton polygon.
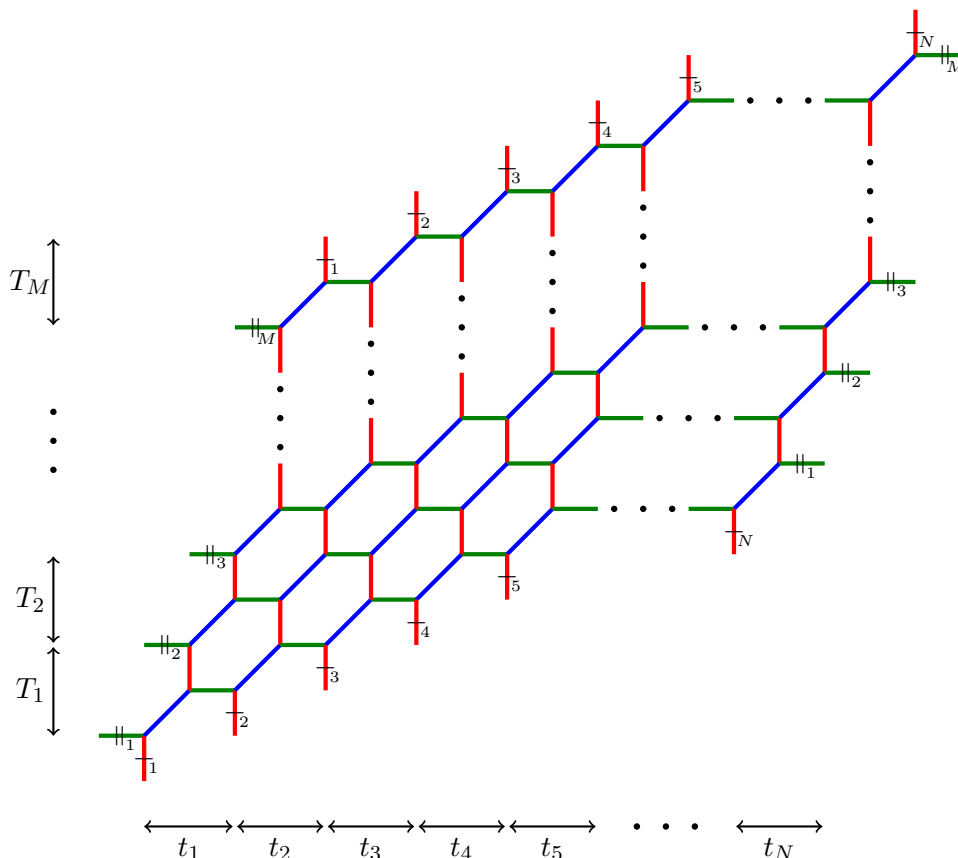
Figure 3. The 5-brane web dual to the Calabi-Yau threefold $X_{N,M}$.

Furthermore, the lengths of various lines in the 5-brane web correspond to Kähler parameters of $X_{N,M}$. From figure 3, it can be seen that there are $MN + 2$ independent parameters [25]. This counting arises as follows: the web is parametrised by $MN + M + N$ parameters, corresponding to the vertical and horizontal distances as well as the blue diagonal distances. However, there are also $M + N - 2$ constraints which arise from the gluing-conditions on $\mathbb{T}^2$, which impose that the vertical lines at the top and the bottom of the diagram and the horizontal lines at the left- and right end of the diagram can be glued together in a consistent fashion.

Specifically, we denote by T_i the separation between the horizontal lines (corresponding to D5-branes from the (p,q)-brane web perspectives) and by t_a the separation between the vertical lines (corresponding to NS5-branes). Furthermore, we will collectively denote

$$\mathbf{T} = (T_1, T_2, \ldots, T_M), \qquad \text{and} \qquad \mathbf{t} = (t_1, t_2, \ldots, t_N), \qquad (2.10)$$

and we denote the following quantities[6]

$$\tau = \frac{i}{2\pi}(T_1 + T_2 + \ldots + T_M), \qquad \text{and} \qquad \rho = \frac{i}{2\pi}(t_1 + t_2 + \ldots + t_N). \qquad (2.11)$$

---

[6]From the viewpoint of little string theories in five dimensions, τ and ρ play a distinguished role compared to the remaining moduli $(T_1, \ldots T_{M-1})$ and $(t_1, \ldots T_{N-1})$: depending on the precise duality frame, they respectively correspond to the coupling constant of little string theory and the radius of $\mathbb{S}^1$ on which the little string theory is compactified.

Notice, from the point of view of the Calabi-Yau threefold, τ and ρ are just a particular combination of the Kähler moduli $(\mathbf{t}, \mathbf{T})$. In fact [10], one may choose to parametrise the moduli space by $(\tau, T_1, \ldots, T_{M-1}, \rho, t_1, \ldots, t_{N-1})$. However, from the point of view of the dual little string theories, τ and ρ are the radii of two circles of the little string theory geometry. In this regard, they are treated as fixed (but generic) external parameters rather than moduli.

2.2 Flop transitions in $X_{N,M}$

In this section, we discuss flop transitions which connect topologically distinct Calabi-Yau threefolds. We also discuss the flop transition from the brane web perspectives.

2.2.1 Resolved conifold and flop transitions

A Calabi-Yau threefold can degenerate in many different ways including a divisor collapsing to a point or a curve collapsing to a point. The flop transition is of the latter type in the sense that a rational curve shrinks to a zero size. In the neighborhood of such a singularity, the Calabi-Yau threefold is described by

$$xy - zw = 0 \,, \qquad x = z_1 + iz_2 \,, y = z_1 - iz_2 \,, z = -z_3 - iz_4 \,, w = z_3 - iz_4 \,. \qquad (2.12)$$

which resembles the conifold as discussed above. As before, we can resolve the singularity

$$\frac{x}{z} = \frac{w}{y} \qquad \text{such that} \qquad x = \lambda\, z \qquad \text{and} \qquad w = \lambda\, y \,. \qquad (2.13)$$

Here, λ is the local coordinate on the blowup $\mathbb{P}^1$ and (x, w, λ) are the coordinates on the Calabi-Yau threefold in a patch over $\mathbb{P}^1$. In the second patch, the coordinates are (z, y, λ^{-1}). The two equations relating (x, w) to (z, y) in eq. (2.13) are the transition functions for the bundle $\mathcal{O}(-1) \oplus \mathcal{O}(-1)$ over $\mathbb{P}^1$.

However, there are two possible choices:

$$\frac{x}{z} = \frac{w}{y} \qquad \text{such that} \qquad x = \lambda y \quad \text{and} \quad w = \lambda y \,, \qquad (2.14)$$
$$\frac{x}{w} = \frac{z}{y} \qquad \text{such that} \qquad x = \lambda' w \quad \text{and} \quad z = \lambda' y \,.$$

The difference between the two choices corresponds to interchanging z and w, and this is known as a flop transition. Another way of describing this transition is through the quotient construction of the conifold in terms of $(A_1, A_2, B_1, B_2) \in \mathbb{C}^4$ (see eq. (2.5)),

$$|A_1|^2 + |A_2|^2 - |B_1|^2 - |B_2|^2 = r \,, \qquad (2.15)$$

where the parameter r determines the size of the resolved $\mathbb{P}^1$. The flop transition is given by $r \mapsto -r$ so that the roles of $A_{1,2}$ and $B_{1,2}$ are interchanged. Thus, in terms of the original Kähler class, if the $\mathbb{P}^1$ has area r, then, after the flop transition, it has area $-r$. However, in the flopped geometry, we can define a different Kähler class with respect to which the flopped curve has a positive area. Thus, at $r = 0$ we are at the boundary of the Kähler cone and the flop $r \mapsto -r$ takes us out of the Kähler cone of the Calabi-Yau we started with and into the Kähler cone of another Calabi-Yau threefold. This extended moduli space of the Kähler class is discussed in more detail in section 2.3.
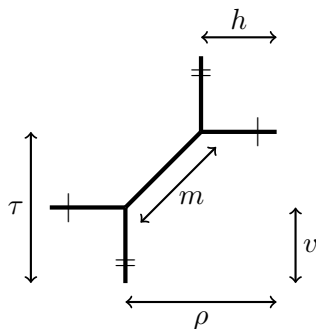
Figure 4. Toric diagram of the Calabi-Yau manifold $X_{1,1}$. The parameters (ρ, τ, m) are those appearing in the partition function with $\tau = v + m$ and $\rho = m + h$.

2.2.2 Flop transitions in $X_{1,1}$ and $\mathrm{Sp}(2, \mathbb{Z})$

In order to facilitate the computations in later part of this paper, we discuss the flop transition from the perspective of the brane web. The web diagram of $X_{1,1}$ is shown in figure 4 with a choice of the $NM + 2 = 1 + 2 = 3$ independent parameters (h, v, m) (which correspond to the Kähler parameters of three $\mathbb{P}^1$'s) or, equivalently, (ρ, τ, m). The local geometry of all three $\mathbb{P}^1$'s is that of the resolved conifold and hence these can undergo flop transitions. Indeed, the second figure in eq. (2.16) shows the 5-brane web after a flop of the curve corresponding to the parameter m. The last two figures of (2.16) give different ways of representing the web dual to the flopped geometry.[7] Eq. (2.16) also indicates the change in the Kähler parameters caused by the flop transition: the Kähler parameters of all curves intersecting the curve that undergoes a flop transition change depending on the intersection number [43].[8]

$$(2.16)$$
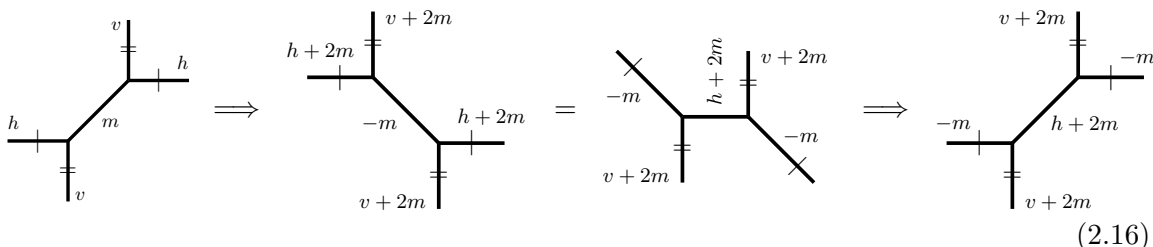
Furthermore, in the first diagram on the left in eq. (2.16), we have

$$\rho = h + m\,, \qquad\qquad \tau = v + m\,, \qquad\qquad (2.17)$$

while in the final diagram on the right of (2.16) we have

$$
\begin{aligned}
\rho' &= h + 2m - m = \rho\,,\\
\tau' &= v + h + 4m = \rho + \tau + 2m\,,\\
m' &= h + 2m = \rho + m\,.
\end{aligned}
\qquad (2.18)
$$

---

[7]In the last step, we have performed an $\mathrm{SL}(2, \mathbb{Z})$ transformation that acts in the following manner on the various lines: $(1, 0) \longrightarrow (1, 1)$, $(0, 1) \longrightarrow (0, 1)$ and $(1, -1) \longrightarrow (1, 0)$.

[8]Notice, since the vertical and horizontal lines are identified, both h and v touch at both ends the line m that is flopped (i.e. they have intersection number 2). This explains the shifts by $2m$ rather than simply m.

m The transformation $(\tau, \rho, m) \mapsto (\tau', \rho', m')$ corresponds to an automorphism of $X_{1,1}$ acting as an $\mathrm{Sp}(2, \mathbb{Z})$ transformation. To understand this, we recall that the geometry mirror to $X_{1,1}$ is a genus-two curve with period matrix given by

$$\Omega = \begin{pmatrix} \tau & m \\ m & \rho \end{pmatrix}. \tag{2.19}$$

The automorphism group of this curve is $\mathrm{Sp}(2, \mathbb{Z})$, which acts on the period matrix by the generalisation of the fractional linear transformations:

$$\Omega \mapsto (A\Omega + B)(C\Omega + D)^{-1}, \qquad \text{with} \qquad \begin{pmatrix} A & B \\ C & D \end{pmatrix} \in \mathrm{Sp}(2, \mathbb{Z}). \tag{2.20}$$

Specifically, the matrices A, B, C, D (with integer entries) satisfy

$$A^T D - C^T B = \mathbb{1}_{2 \times 2} = DA^T - CB^T, \qquad A^T C = C^T A, \qquad B^T D = D^T B. \tag{2.21}$$

Using the transformation of the parameters under a flop transition given by eq. (2.18), we can arrange them into a transformed period matrices

$$\Omega' = \begin{pmatrix} \tau' & m' \\ m' & \rho' \end{pmatrix}, \tag{2.22}$$

which is indeed related to eq. (2.20) by

$$\Omega' = (A\Omega + B)(C\Omega + D)^{-1}, \tag{2.23}$$

with

$$A = \begin{pmatrix} 1 & 1 \\ 0 & 1 \end{pmatrix}, \qquad B = \begin{pmatrix} 0 & 0 \\ 0 & 0 \end{pmatrix}, \qquad C = \begin{pmatrix} 0 & 0 \\ 0 & 0 \end{pmatrix}, \qquad D = \begin{pmatrix} 1 & 0 \\ -1 & 1 \end{pmatrix}. \tag{2.24}$$

These matrices satisfy eq. (2.21), as is required for a $\mathrm{Sp}(2, \mathbb{Z})$ transformation.[9] This indicates that the combined flop transition eq. (2.16) corresponds to an $\mathrm{Sp}(2, \mathbb{Z})$ transformation.

2.2.3 Flop transitions and constraints

The orbifold $X_{N,M}$ has many curves which can undergo flop transitions. In eq. (2.25), we show the generic case, where a generic such curve in the web diagram undergoes a flop, and the way the Kähler parameters change: the transformation not only changes the sign of the Kähler parameter of the curve that undergoes a flop, but also modifies the Kähler parameter of any curve with non-trivial intersection with the former eq. (2.25).

$$(2.25)$$
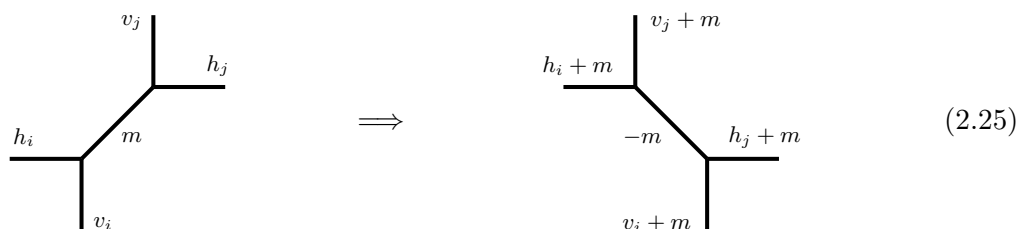
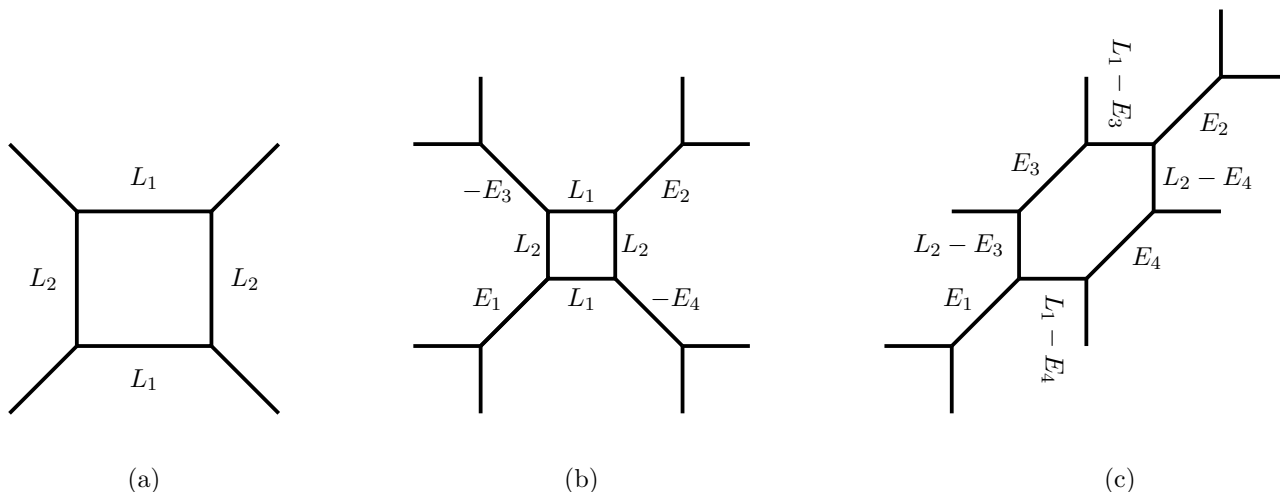[9] Notice also $\det \Omega = \rho \tau - m^2 = \det \Omega'$.

Figure 5. (a) Four-cycles of the type $\mathbb{P}^1 \times \mathbb{P}^1$ glued together. (b) The four-cycles are blown up with curves $E_{1,2}$ and $-E_{3,4}$. (c) The geometry after a flop of the lines $-E_3$ and $-E_4$.

We can apply the result of this generic transformation to more complex cases. For example, the Calabi-Yau threefolds $X_{N,M}$ are non-compact with a collection of four-cycles forming the compact part. These four-cycles S_a are all $\mathbb{P}^1 \times \mathbb{P}^1$ blown up at four points glued to each other, as depicted in figure 5. The six curves $(E_1, E_2, E_3, E_4, L_1, L_2)$ shown in figure 5 are all exceptional curves which are locally $\mathcal{O}(-1) \oplus \mathcal{O}(-1) \mapsto \mathbb{P}^1$. They have the following intersection form

$$L_i \cdot L_j = 1 - \delta_{ij}, \qquad L_i \cdot E_a = 0, \qquad E_a \cdot E_b = -\delta_{ab}, \qquad \text{for} \qquad \begin{matrix} i = 1, 2 \\ a, b = 1, 2, 3. \end{matrix} \qquad (2.26)$$

After the blow-ups, the areas of the curves can be represented as follows

$$A(E_a) = m_a, \qquad A(L_1 - E_4) = h_1, \qquad A(L_1 - E_3) = h_2,$$
$$A(L_2 - E_3) = v_1, \qquad A(L_2 - E_4) = v_2, \qquad (2.27)$$

for which the corresponding Kähler form is given by

$$\omega = (v_1 + m_3)L_1 + (h_1 + m_4)L_2 - m_1 E_1 - m_2 E_2 - m_3 E_3 - m_4 E_4. \qquad (2.28)$$

We can check that the above Kähler form gives areas for the curves $E_{1,2,3,4}$ and $L_1 - E_4$ and $L_2 - E_3$ that are consistent with eq. (2.27). However, the areas of $L_1 - E_3$ and $L_2 - E_4$ under this Kähler form give two constraints:

$$h_2 = h_1 + m_4 - m_3, \qquad \text{and} \qquad v_2 = v_1 + m_3 - m_4. \qquad (2.29)$$

The presence of two constraints is consistent with the fact that there are eight curves in figure 5, of which only six are independent. The canonical class of S_a is given by

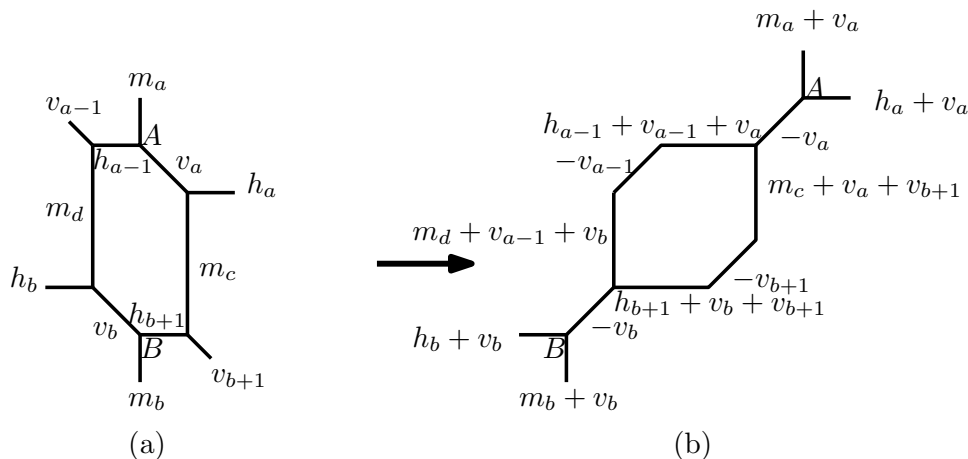$$-K_{S_a} = 2L_1 + 2L_2 - E_1 - E_2 - E_3 - E_4, \qquad (2.30)$$

Figure 6. Change of parameters and vertices A, B after a flop transition.

and its area is given by

$$
\begin{aligned}
s_a = \omega \cdot (-K_{S_a}) &= 2(h_1 + m_4 + v_1 + m_3) - m_1 - m_2 - m_3 - m_4 \\
&= 2h_1 + 2v_1 + m_3 + m_4 - m_1 - m_2 \\
&= h_1 + h_2 + v_1 + v_2 + m_3 + m_4 - m_1 - m_2 \, .
\end{aligned} \tag{2.31}
$$

Here, we have used the constraint eq. (2.29) to simplify the expression in the second line. The area of the canonical class remains the same as the various curves in the geometry undergo flop transitions.

Finally, another loop of cycles that is needed for the computations later on is shown in figure 6, which corresponds to a four-cycle S in the Calabi-Yau threefold, which is $\mathbb{P}^1 \times \mathbb{P}^1$ blown up at four points. The loop corresponds to the curve class which is the anti-canonical class of S, whose area is given by

$$
A := v_a + m_c + v_{b+1} + h_{b+1} + v_b + m_d + v_{a-1} + h_{a-1} \, . \tag{2.32}
$$

After a flop transition, the area of the curves in S changes but the area of the canonical class remains the same

$$
\begin{aligned}
A' = &-v_a + (m_c + v_a + v_{b+1}) - v_{b+1} + (h_{b+1} + v_b + v_{b+1}) - v_b + (m_d + v_{a-1} + v_b) \\
&- v_{a-1} + (h_{a-1} + v_{a-1} + v_a) = A \, .
\end{aligned} \tag{2.33}
$$

2.3 Calabi-Yau threefolds and extended moduli space

In the previous section, we discussed flop transition from the point of view of Calabi-Yau manifolds and the associated brane webs. To understand the physical implications of such transitions, we recall that propagating strings see the underlying geometry in a very different way than point particles. This extended nature of strings is responsible for physically smooth processes which lead to topology changes of the geometry. In [32], Reid conjectured (this conjecture is known as *Reid's fantasy*) that all Calabi-Yau threefolds are
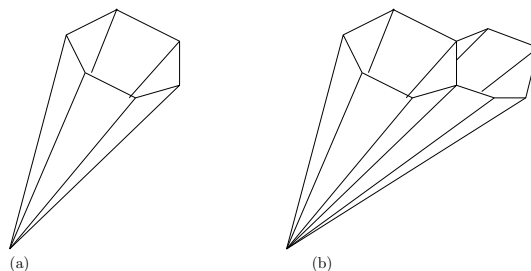
Figure 7. (a) Kähler cone of a CY3fold. (b) Extended Kähler cone connecting two distinct CY3folds.

connected to each other through singular, perhaps non-Kähler, manifolds. Many families of Calabi-Yau threefolds are now known to be connected by conifold and flop transitions, as discussed above [33–36]. The case of the conifold transition is well understood from string theory point of view that it requires non-perturbative effects to make the physics non-singular [44, 45]. The conifold transition also leads to a change in the Hodge numbers of the Calabi-Yau threefold [45].

To understand these transitions from the point of view of the Kähler moduli space of Kähler threefolds, we recall that the latter has the structure of a cone given by:

$$\int_X \omega \wedge \omega \wedge \omega > 0, \qquad \int_{P_a} \omega \wedge \omega > 0, \qquad \int_{\Sigma_i} \omega > 0, \qquad (2.34)$$

where ω is the Kähler form on X, P_a are two-dimensional complex submanifolds and Σ_i represent holomorphic curves in X. The walls of the Kähler cone are given by the shrinking of a rational curve or a divisor in the Calabi-Yau threefold [46]. In the case of rational curve resolving this degeneration as described above leads again to a rational curve but in a Calabi-Yau threefold which is outside the Kähler cone we started with. In terms of the original Kähler form the new rational curve has negative area. Therefore, such flop transitions connects two Calabi-Yau threefolds with same hodge numbers but different triple intersection numbers. By putting together the Kähler cones of the two Calabi-Yau threefolds, we get an extended moduli space, as shown in figure 7. In was shown recently that Calabi-Yau threefold related by flop transitions are connected by a path in the extended Kähler moduli space which consists of Ricci flat Calabi-Yau threefolds [47].

There are many known examples of families of Calabi-Yau threefolds which connect to each other via flop transitions (and conifold transitions) and therefore fit to an extended Kähler moduli space [33, 48–51]

3 Partition function: relation between (N, M) and $(1,1)$

In this section, we review some results in the literature, which will turn out to be important in the following.

3.1 Partition functions

In our previous works [8, 10], the topological string partition functions $\mathcal{Z}_{X_{N,M}}$ of the toric Calabi-Yau manifolds $X_{M,N}$ have been studied. The former can either be computed di-

rectly using the (refined) topological vertex formalism or alternatively as the M-string partition function.

The partition function $\mathcal{Z}_{X_{N,M}}$ depends on the $MN+2$ independent Kähler parameters of $X_{N,M}$ as well as two deformation parameters $\epsilon_{1,2}$. In [25, 27, 28], it has been computed for the particular case that the resolution of each intersection (called m) is the same. For the remaining parameters, the notation in figure 3 was used which appear in the following fashion

$$
\begin{aligned}
\bar{Q}_i &= e^{-T_i}, & &\forall i = 1, \ldots, M, \\
Q_a &= e^{-t_a}, & &\forall a = 1, \ldots, N, \\
Q_{ab} &= Q_a Q_{a+1} \ldots Q_{b-1}, & &\text{for } 1 \le a < b \le N,
\end{aligned}
\tag{3.1}
$$

as well as the two deformation parameters of the Ω-background $\epsilon_{1,2}$ which appear through

$$
q = e^{2\pi i \epsilon_1} \qquad \text{and} \qquad t = e^{-2\pi i \epsilon_2}. \tag{3.2}
$$

With this notation, the partition function takes the form [28]

$$
\mathcal{Z}_{X_{N,M}}(\mathbf{t}, \mathbf{T}, m, \epsilon_{1,2}) = W_N(\emptyset)^M \sum_{\alpha_a^{(i)}} Q_\tau^{\sum_a |\alpha_a^{(M)}|} \left(\prod_{i=1}^M \bar{Q}_i^{\sum_a \left(\left| \alpha_a^{(i)} \right| - \left| \alpha_a^{(M)} \right| \right)} \right) \tag{3.3}
$$

$$
\times \prod_{i=1}^M \prod_{a=1}^N \frac{\vartheta_{\alpha_a^{(i+1)} \alpha_a^{(i)}}(Q_m; \rho)}{\vartheta_{\alpha_a^{(i)} \alpha_a^{(i)}}(\sqrt{t/q}; \rho)} \prod_{1 \le a < b \le N} \prod_{i=1}^M \frac{\vartheta_{\alpha_a^{(i)} \alpha_b^{(i+1)}}(Q_{ab} Q_m^{-1}; \rho)\, \vartheta_{\alpha_a^{(i+1)} \alpha_b^{(i)}}(Q_{ab} Q_m; \rho)}{\vartheta_{\alpha_a^{(i)} \alpha_b^{(i)}}(Q_{ab} \sqrt{t/q}; \rho)\, \vartheta_{\alpha_a^{(i)} \alpha_b^{(i)}}(Q_{ab} \sqrt{q/t}; \rho)},
$$

with the prefactor

$$
W_N(\emptyset; \mathbf{t}, m, \epsilon_{1,2}) = \lim_{\tau \to i\infty} \mathcal{Z}_{X_{N,1}}(\tau, \rho, t_1, \cdots, t_{N-1}, m, \epsilon_{1,2}) \tag{3.4}
$$

$$
= \frac{1}{\prod_{n=1}^\infty (1 - Q_\rho^n)} \prod_{i,j,k} \prod_{a,b=1}^N \frac{1 - Q_\rho^{k-1} Q_{a,a+b} Q_m^{-1} t^{i-\frac{1}{2}} q^{j-\frac{1}{2}}}{1 - Q_\rho^{k-1} Q_{a,a+b}\, t^{i-1} q^j} \frac{1 - Q_\rho^{k-1} Q_{a,a+b-1} Q_m\, t^{i-\frac{1}{2}} q^{j-\frac{1}{2}}}{1 - Q_\rho^{k-1} Q_{a,a+b}\, t^i q^{j-1}}.
$$

Here, we have used the notation

$$
Q_\tau = e^{2\pi i \tau}, \qquad Q_\rho = e^{2\pi i \rho}, \qquad Q_m = e^{2\pi i m}, \tag{3.5}
$$

and $\alpha_a^{(i)}$ in eq. (3.3) for NM many independent integer partitions where, for a particular partition $\alpha_a^{(i)} = (\alpha_{a,1}^{(i)}, \alpha_{a,2}^{(i)}, \ldots, \alpha_{a,\ell}^{(i)})$ with total length ℓ,

$$
|\alpha_a^{(i)}| = \sum_{n=1}^\ell \alpha_{a,n}^{(i)}. \tag{3.6}
$$

Finally, for any two integer partitions μ and ν, the functions $\vartheta_{\mu\nu}$ in eq. (3.12) are defined as

$$
\vartheta_{\mu\nu}(x; \rho) := \prod_{(i,j) \in \mu} \vartheta\left(x^{-1} q^{-\mu_i + j - \frac{1}{2}} t^{-\nu_j^t + i - \frac{1}{2}}; \rho \right) \prod_{(i,j) \in \nu} \vartheta\left(x^{-1} q^{\nu_i - j + \frac{1}{2}} t^{\mu_j^t - i + \frac{1}{2}}; \rho \right), \tag{3.7}
$$

where (for $x = e^{2\pi i z}$)

$$\vartheta(x;\rho) := \left(x^{\frac{1}{2}} - x^{-\frac{1}{2}}\right) \prod_{k=1}^{\infty} (1 - x Q_\rho^k)(1 - x^{-1} Q_\rho^k) = \frac{i\,\theta_1(\rho,x)}{Q_\rho^{1/8} \prod_{k=1}^{\infty}(1 - Q_\rho^k)}\,. \tag{3.8}$$

Here, θ_1 is the Jacobi theta function and we refer the reader to [52] for the proper definition along with several useful identities.

Finally, we can also define the BPS partition function that counts single particle BPS states of the little string theories associated with $X_{N,M}$

$$\Sigma_{N,M}(\mathbf{t}, \mathbf{T}, m, \epsilon_{1,2}) = \mathrm{Plog}\, \mathcal{Z}_{X_{N,M}}(\tau, \rho, t_1, \ldots, t_{N-1}, T_1, \ldots, T_{M-1}, m, \epsilon_{1,2}) \tag{3.9}$$

$$= \sum_{k=1}^{\infty} \frac{\mu(k)}{k} \log \mathcal{Z}_{X_{N,M}}(k\tau, k\rho, k\,t_1, \ldots, k\,t_{N-1}, k\,T_1, \ldots, k\,T_{M-1}, k\,m, k\epsilon_{1,2})\,,$$

where Plog is the plethystic logarithm and $\mu(k)$ is the Möbius function. In [10], we have studied the BPS counting functions (3.9) at the particular region in the full string moduli space

$$Q_1 = Q_2 = \ldots = Q_N = Q_\rho^{\frac{1}{N}} \qquad \text{and} \qquad \overline{Q}_1 = \overline{Q}_2 = \ldots = \overline{Q}_M = Q_\tau^{\frac{1}{M}}\,. \tag{3.10}$$

For a large class of examples, we found that, in the Nekrasov-Shatashvili limit $\epsilon_2 \to 0$,

$$\lim_{\epsilon_2 \to 0} \epsilon_2\, \Sigma_{N,M}(\tfrac{\rho}{N}, \cdots, \tfrac{\rho}{N}, \tfrac{\tau}{M}, \cdots, \tfrac{\tau}{M}, m, \epsilon_{1,2}) = NM \lim_{\epsilon_2 \to 0} \epsilon_2\, \Sigma_{1,1}(\tfrac{\rho}{N}, \tfrac{\tau}{M}, m, \epsilon_{1,2})\,, \tag{3.11}$$

which we termed *self-similarity* and which we conjectured to hold for generic $M, N \in \mathbb{N}$. As a consequence, in the Nekrasov-Shatashvili limit and for eq. (3.10), the free energy of any configuration (N, M) can be completely obtained from $\mathcal{Z}_{X_{1,1}}$. In section 3.2, we will discuss $\mathcal{Z}_{X_{1,1}}$ in detail and show that it is invariant under $\mathrm{Sp}(2, \mathbb{Z})$. It then follows from eq. (3.11) that $\mathrm{Sp}(2, \mathbb{Z})$ symmetry is inherited by the partition function of the (N, M) case in the limit we discussed before.

3.2 The case $X_{1,1}$

The simplest configuration corresponds to the case $(N, M) = (1, 1)$, which will play an important role throughout this work.

3.2.1 The partition function $\mathcal{Z}_{X_{1,1}}$

As discussed in section 2, the Calabi-Yau threefold $X_{1,1}$ has three Kähler parameters (τ, ρ, m). Figure 4 shows the three parameters in the dual 5-brane web diagram. The topological string partition function $\mathcal{Z}_{X_{1,1}}$ depends on these three Kähler parameters and is given by [8, 27, 28]

$$\mathcal{Z}_{X_{1,1}}(\tau, \rho, m, \epsilon_{1,2}) = W_1(\emptyset) \sum_\alpha Q_\tau^{|\alpha|}\, \frac{\vartheta_{\alpha\alpha}(Q_m; \rho)}{\vartheta_{\alpha\alpha}(\sqrt{t/q}; \rho)}\,, \tag{3.12}$$

with the same notation as in (3.2) and (3.5). The prefactor (3.4) for $N = 1$ takes the form

$$W_1(\emptyset; \rho, m, \epsilon_{1,2}) = \lim_{\tau \to i\infty} \mathcal{Z}_{X_{1,1}}(\tau, \rho, m, \epsilon_{1,2})$$

$$= \frac{1}{\prod_{n=1}^{\infty}(1 - Q_\rho^n)} \prod_{i,j,k} \frac{1 - Q_\rho^k Q_m^{-1} t^{i-\frac{1}{2}} q^{j-\frac{1}{2}}}{1 - Q_\rho^k t^{i-1} q^j} \frac{1 - Q_\rho^{k-1} Q_m t^{i-\frac{1}{2}} q^{j-\frac{1}{2}}}{1 - Q_\rho^k t^i q^{j-1}}. \quad (3.13)$$

As was discussed in [38, 53] (see also [54]), the expansion of $\mathcal{Z}_{X_{1,1}}$ in a power series in Q_τ can be written in terms of the equivariant elliptic genus of the Hilbert scheme of points,

$$\mathcal{Z}_{X_{1,1}}(\tau, \rho, m, \epsilon_{1,2}) = W_1(\emptyset, \rho, m, \epsilon_{1,2}) \sum_{k=0}^{\infty} Q_\tau^k \chi_{\text{ell}}(\text{Hilb}^k[\mathbb{C}^2])$$

$$= \prod_{n,k,\ell,r,s} \left(1 - Q_\rho^n Q_\tau^k Q_m^\ell q^r t^s \right)^{-c(nk,\ell,r,s)}, \quad (3.14)$$

where the coefficients c are obtained from a Fourier expansion of the equivariant elliptic genus of $\mathbb{C}^2$

$$\chi_{\text{ell}}(\mathbb{C}^2) = \sum_{n,\ell,r,s} c(n,\ell,r,s) Q_\rho^n Q_m^\ell q^r t^s. \quad (3.15)$$

Notice that eq. (3.14) is manifestly invariant under the exchange $\rho \longleftrightarrow \tau$ since c only depends on the product nk. This is compatible with a particular Hecke structure [29] found for the associated free energy $\Sigma_{1,1}$.

Furthermore, as was discussed in [28], the partition function $\mathcal{Z}_{X_{1,1}}$ can be written as a sum over the Narain lattice $\Gamma_{3,2}$, which is manifestly invariant under $SO(3, 2, \mathbb{Z})$.[10] Since the latter is homeomorphic to $\text{Sp}(2, \mathbb{Z})$ as recalled below, the partition function $\mathcal{Z}_{X_{1,1}}$ is invariant under the latter. As a consequence of eq. (3.11), this property is also inherited by $\mathcal{Z}_{X_{N,M}}$ in the NS-limit and eq. (3.10).

Recall that an element of $\mathbb{R}^{3,2}$ that transform linearly under $SO(3, 2, \mathbb{Z})$ can be mapped to a (4×4) matrix that transform by conjugation under $\text{Sp}(2, \mathbb{Z})$. Denote

$$\vec{a} = (a_1, a_2, a_3, a_4, a_5) \in \mathbb{R}^{3,2} \quad \text{and} \quad M(\vec{a}) = \frac{1}{2} \begin{pmatrix} a_1 & a_2 - a_3 & 0 & -a_4 + a_5 \\ a_2 + a_3 & -a_1 & a_4 - a_5 & 0 \\ 0 & -a_4 - a_5 & a_1 & a_2 + a_3 \\ a_4 + a_5 & 0 & a_2 - a_3 & -a_1 \end{pmatrix}. \quad (3.16)$$

Then, the $SO(3, 2, \mathbb{Z})$ action on $\vec{a}$ is realized as an $\text{Sp}(2, \mathbb{Z})$ action on M given by $g\, M\, g^{-1}$, where $g \in \text{Sp}(2, \mathbb{Z})$ with invariant inner product given by $\text{Tr}(M(\vec{a})M(\vec{b})) = a_1 b_1 + a_2 b_2 - a_3 b_3 - a_4 b_4 + a_5 b_5$.

---

[10]It was shown in [55] that the generating function of the elliptic genus of Hilbert scheme of points on K3 can be expressed as a sum over the Narain lattice $\Gamma_{3,2}$ and is given in terms of the weight ten Igusa cusp form. The two are not unrelated as the genus-one amplitude of $\mathcal{Z}_{X_{1,1}}$ is precisely the generating function studied in [54, 55]. This is not a coincidence, as to be explained in [56].
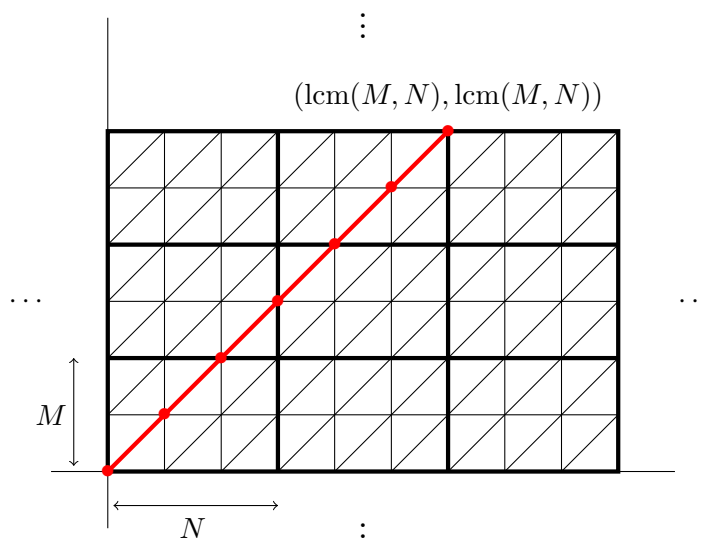
Figure 8. Newton polygon of $X_{N,M}$ (with $\gcd(M,N) = 1$) and a path following only diagonal lines. The two points at $(0,0)$ and $(\mathrm{lcm}(M,N), \mathrm{lcm}(M,N))$ are equivalent. Furthermore, since $\gcd(M,N) = 1$, this path maps out all inequivalent points of the polygon.

4 Mapping (N, M) to $(\frac{MN}{k}, k)$: examples

In this section, we compile evidences that the Calabi-Yau threefolds $X_{N,M}$ and $X_{\frac{NM}{k},k}$ are related through a series of flop transitions.

4.1 Relations between Newton polygons

Before presenting a series of examples, we first give a general argument to motivate that such a relation ought to exists. To this end, we consider the Newton polygon of $X_{N,M}$ tiling the plane $\mathbb{R}^2$. We start from the origin and follow a diagonal lines until we reach a point that is equivalent to the origin (see figure 8).

This point has coordinates

$$(\mathrm{lcm}(M,N), \mathrm{lcm}(M,N)) = \left(\tfrac{NM}{k}, \tfrac{NM}{k}\right), \qquad \text{with} \qquad k = \gcd(M,N). \qquad (4.1)$$

If $k = 1$ (as in the example in figure 8), this path has already mapped out all inequivalent points of the Newton polygon. If $k > 1$, we can continue the procedure by following one horizontal line from the origin and tracing another diagonal path until we hit again an equivalent point. Following this procedure for k steps maps out the entire Newton polygon (see figure 9). The fact that the Newton polygon can equivalently be mapped out by k lines of length $\frac{NM}{k}$ suggests that it is equivalent to the Newton polygon of size $\left(\frac{NM}{k}, k\right)$. In other words, it suggests that there exists a transformation which maps $X_{N,M}$ to $X_{\frac{NM}{k},k}$. In the following, we discuss numerous examples (using the toric webs of $X_{N,M}$) to show that such a transformation indeed exists.
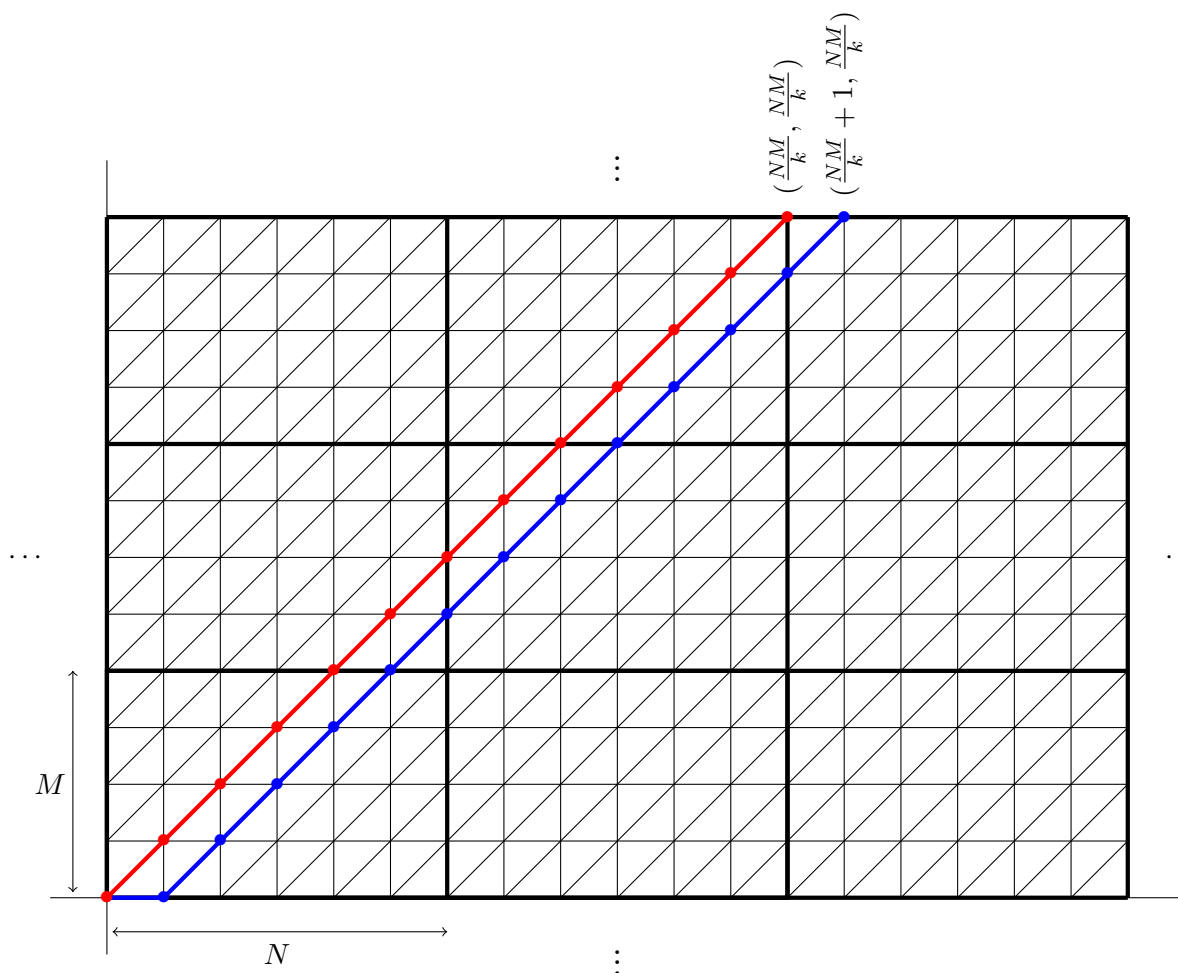
Figure 9. Newton polygon of $X_{N,M}$ with $\gcd(M,N) \geq 2$ and two paths following only diagonal lines (the specific case shown here is $(N,M) = (6,4)$ with $\gcd(6,4) = 2$). These two paths map out all inequivalent points of the Newton polygon.

4.2 Relation between $(N,M) = (3,2)$ and $(6,1)$

Our first example is the configuration $(N,M) = (3,2)$, which we show can be related to the case $(N,M) = (6,1)$. Since this is the simplest (non-trivial) example, we will work out this case in great detail.

4.2.1 Starting configuration $(N,M) = (3,2)$ and consistency conditions

The web diagram of the configuration $(N,M) = (3,2)$ is shown in figure 10 which is parametrised by 18 variables: h_i, v_i and m_i for $i = 1, \ldots, 6$. As discussed above, these parameters are not all independent. Indeed, for consistency, all lines of the same color in figure 10 have to be parallel to each other. With the blue lines oriented along the direction $(1,1)$, these conditions can be formulated locally for each of the 6 hexagons (see also the
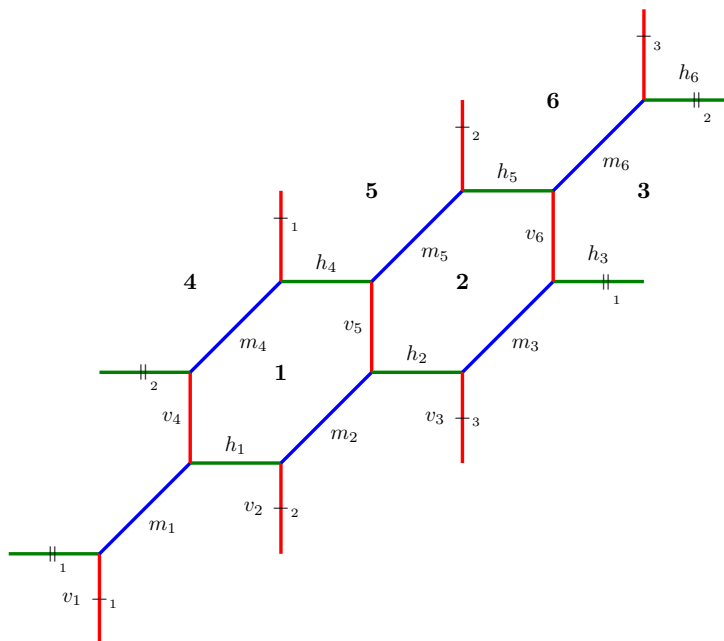
Figure 10. Parametrisation of the $(N, M) = (3, 2)$ web diagram. The parameters (h_i, v_i, m_i) with $i = 1, \ldots, 6$ are not all independent, but are subject to the conditions (4.2)–(4.7).

discussion in section 2.2.3)

- hexagon 1:

$$h_1 + m_2 = m_4 + h_4 \,, \qquad\qquad v_4 + m_4 = m_2 + v_5 \,, \qquad (4.2)$$

- hexagon 2:

$$h_2 + m_3 = m_5 + h_5 \,, \qquad\qquad v_5 + m_5 = m_3 + v_6 \,, \qquad (4.3)$$

- hexagon 3:

$$h_3 + m_1 = m_6 + h_6 \,, \qquad\qquad v_6 + m_6 = m_1 + v_4 \,, \qquad (4.4)$$

- hexagon 4:

$$h_6 + m_4 = m_3 + h_3 \,, \qquad\qquad v_3 + m_3 = m_4 + v_1 \,, \qquad (4.5)$$

- hexagon 5:

$$h_4 + m_5 = m_1 + h_1 \,, \qquad\qquad v_1 + m_1 = m_5 + v_2 \,, \qquad (4.6)$$

- hexagon 6:

$$h_5 + m_6 = m_2 + h_2 \,, \qquad\qquad v_2 + m_2 = m_6 + v_3 \,. \qquad (4.7)$$

These equations leave 8 independent parameters. This agrees with the result found in [27] (see also [10]) that a generic (M, N) web has $MN + 2$ independent parameters.
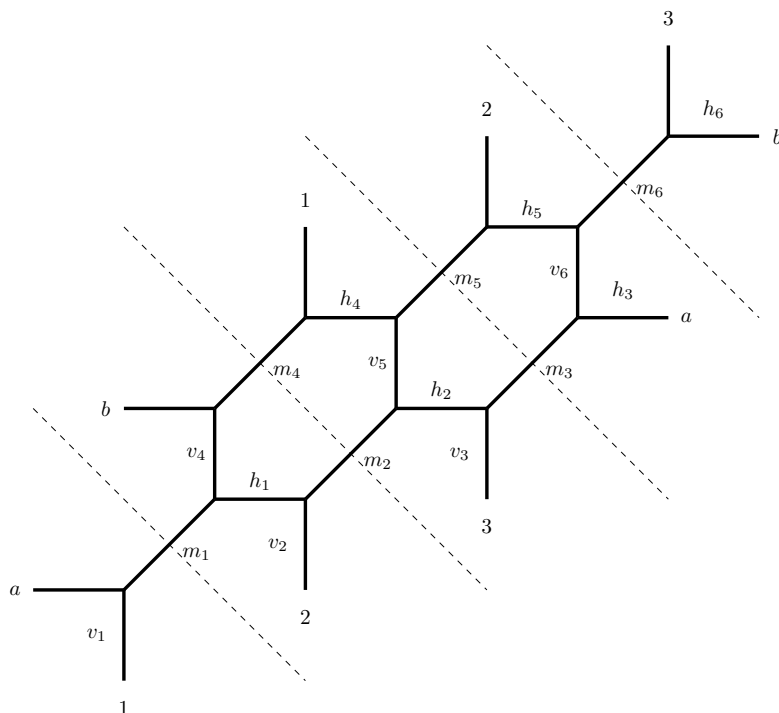
Figure 11. Cutting the $(N, M) = (3, 2)$ web diagram. The vertical lines $1, 2, 3$ and the horizontal lines a, b are identified respectively.

4.2.2 Duality transformation

To proceed, we cut the $(3, 2)$ diagram along the dashed lines shown in figure 11 and glue them back together in order to obtain figure 12. Cutting again along the dashed line and glueing the lines labelled by a together, we arrive at the web drawn in figure 13. Next, we perform an $\mathrm{SL}(2, \mathbb{Z})$ transformation. The latter does not change the length of a given line, however, it changes their orientation. Specifically, the transformation we consider rotates the lines as follows:

$$(1,0) \longrightarrow (1,1), \qquad (0,1) \longrightarrow (-1,0), \qquad (1,1) \longrightarrow (0,1), \qquad (4.8)$$

i.e. it rotates a horizontal line into a diagonal one, a diagonal into a vertical and a vertical into a horizontal. The resulting diagram is shown in figure 14. In order to be consistent, however, we have to impose two types of consistency conditions

- The vertical length of the line connecting the upper node 1 with the lower node 1 (denoted $L = m_4 + h_4 + h_2 + h_6$ in figure 14) must be equal to the length of the line connecting the upper node 2 with lower node 2 (denoted $L' = m_2 + h_2 + h_6 + h_1$ in figure 14) as well as 3 with 3 etc.:

$$m_4 + h_4 + h_2 + h_6 = m_2 + h_2 + h_6 + h_1 = m_6 + h_6 + h_1 + h_5 \qquad (4.9)$$
$$= m_1 + h_1 + h_5 + h_3 = m_5 + h_5 + h_3 + h_4 = m_3 + h_3 + h_4 + h_2 \,.$$
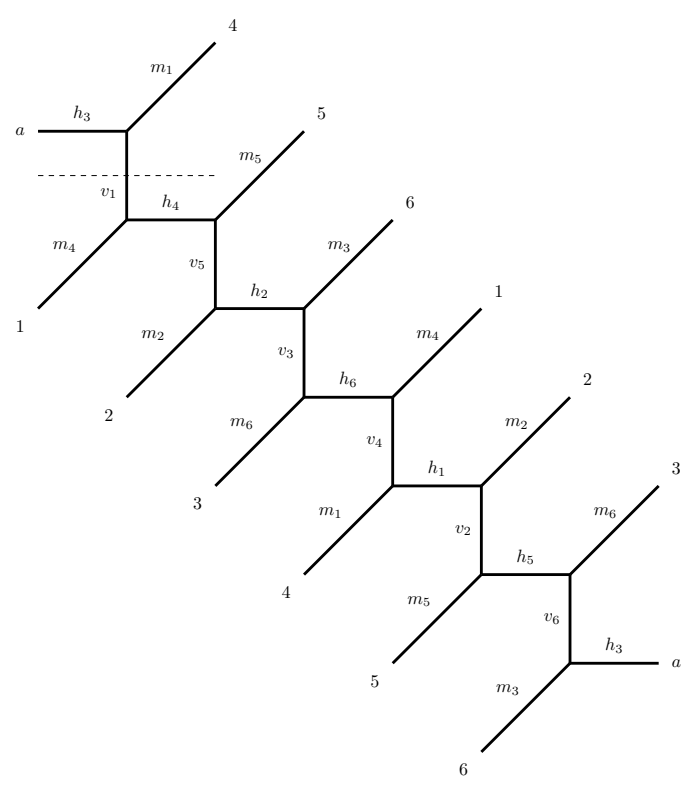
Figure 12. Re-gluing of the (2, 3) web-diagram. The lines labelled 1, 2, 3, 4, 5, 6 and a are identified, respectively. The dashed line signifies the cutting in order to obtain the web drawn in figure 13.
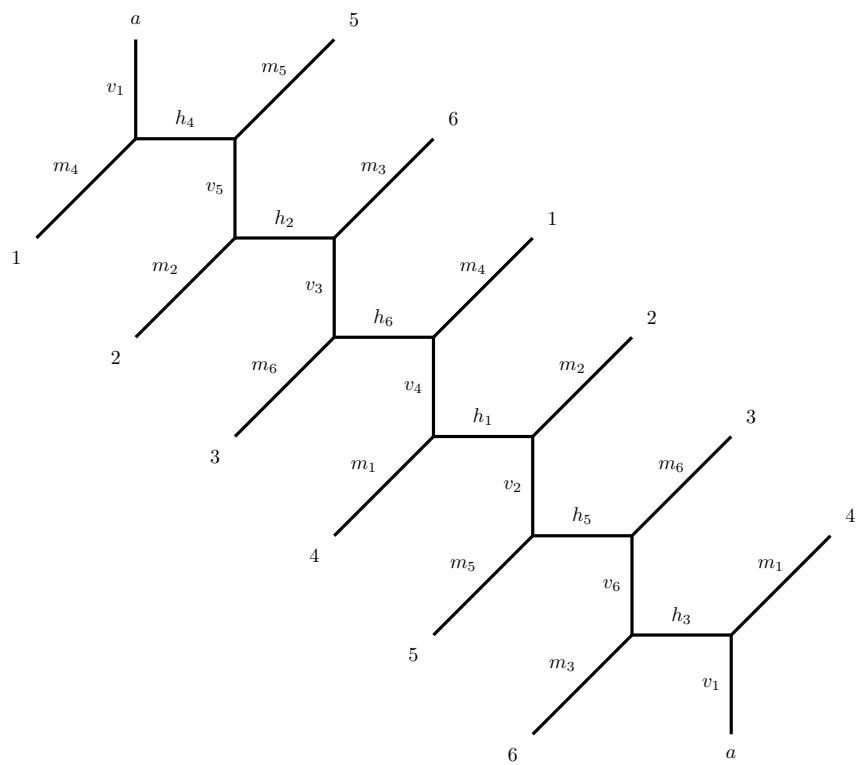

Figure 13. Re-gluing of the web-diagram in figure 13. The lines labelled 1, 2, 3, 4, 5, 6 and a are identified respectively.
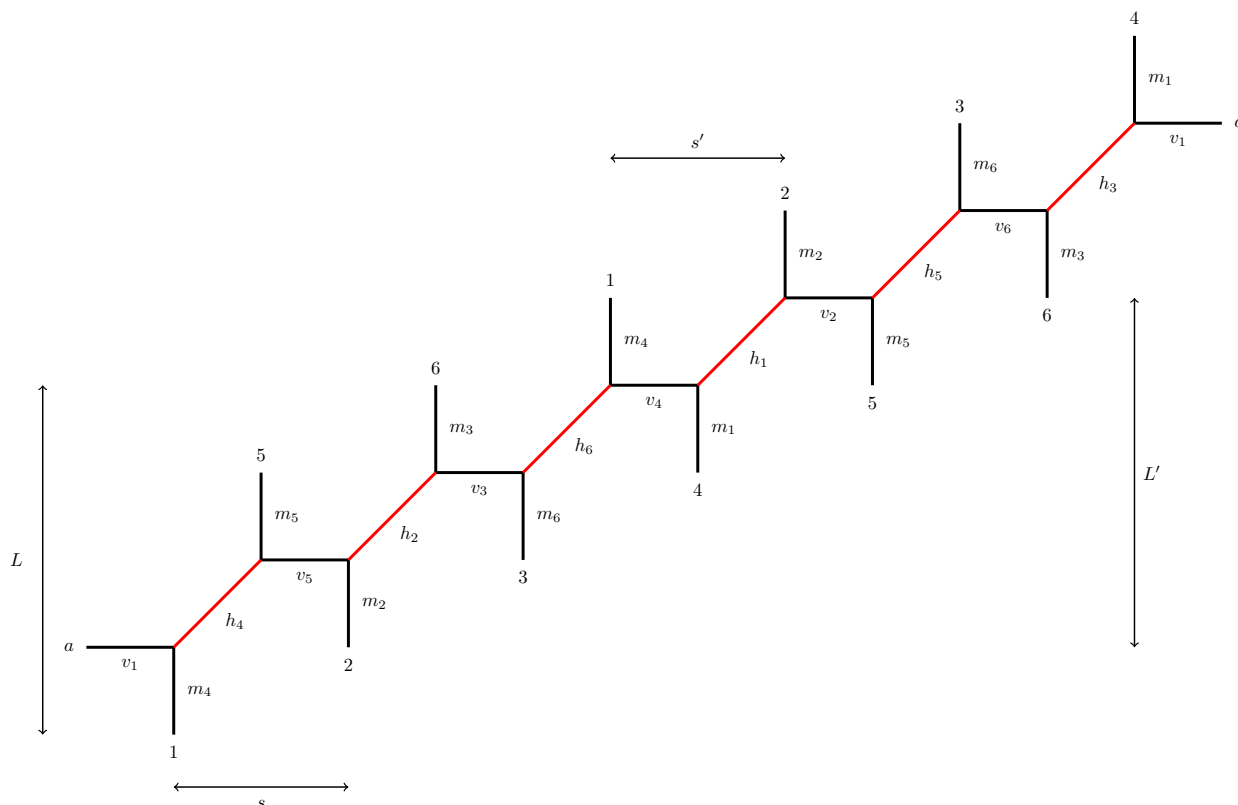
Figure 14. Diagram after the SL$(2, \mathbb{Z})$ transformation in equation (4.8). The red lines undergo a flop transition in the following step.

- The horizontal distance between the nodes 1 and 2 at the bottom of the diagram (denoted s in figure 14) has to be identical to the horizontal distance between the nodes 1 and 2 at the top of the diagram (denoted s' in figure 14). The same constraint has to hold for the nodes 2 and 3, 3 and 4, etc.

$$s = h_4 + v_5 = v_4 + h_1 = s', \qquad\qquad h_2 + v_3 = v_2 + h_5\,,$$
$$h_6 + v_4 = v_6 + h_3\,, \qquad\qquad h_1 + v_2 = v_1 + h_4\,,$$
$$h_5 + v_6 = v_5 + h_2\,, \qquad\qquad h_3 + v_1 = v_3 + h_6\,. \qquad (4.10)$$

The consistency conditions eq. (4.9) and eq. (4.10) are fully equivalent to the conditions eq. (4.2) through eq. (4.7), which guarantee that the original diagram in figure 11 is consistent.

The diagram in figure 14 looks already very similar to the $(N, M) = (6, 1)$ configuration, however, the identification of the vertical lines at the bottom of the diagram with the lines at the top of the diagram is different. Indeed, the latter are 'shifted' with respect to the former. However, through a series of further transformations, we can bring the diagram into the form of the $(6, 1)$ web, with the correct identification of the vertical lines. To this end, as a next step we perform a flop transition on all the lines drawn in red in figure 14. Using the general transformations as explained in (2.25) we can draw the new diagram in
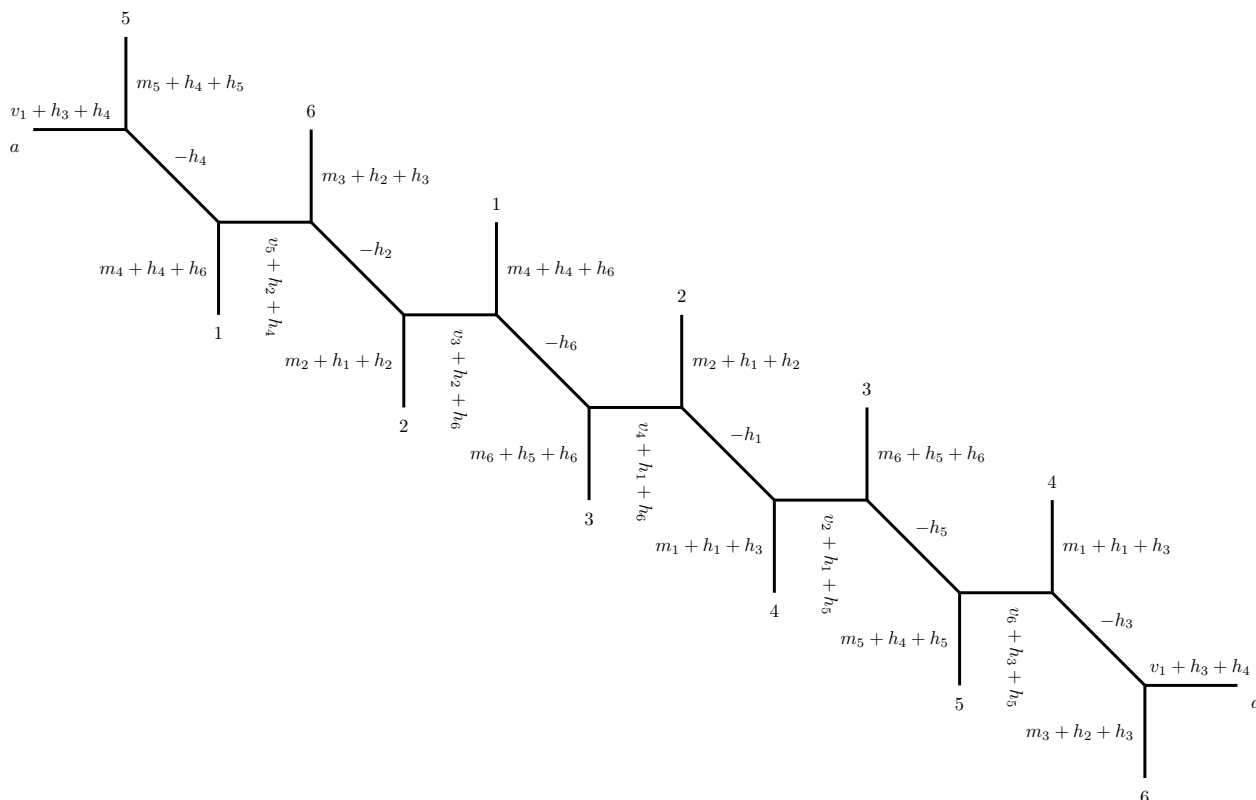
Figure 15. The final (p,q)-web diagram after six flop transformations.

figure 15. After undergoing the flop transformations, we can again check the consistency conditions for the diagram in figure 15. As before, we have to impose two different types of conditions

- The vertical length of the line connecting the upper node 1 with the lower node 1 ($L = m_4 + h_4 + h_6 - (-h_2)$) must be equal to the length of the line connecting the upper node 2 with the lower node 2 ($L' = m_2 + h_1 + h_2 - (-h_6)$) as well as 3 with 3 etc.:

$$m_4 + h_4 + h_2 + h_6 = m_2 + h_2 + h_6 + h_1 = m_6 + h_6 + h_1 + h_5 \tag{4.11}$$
$$= m_1 + h_1 + h_5 + h_3 = m_5 + h_5 + h_3 + h_4 = m_3 + h_3 + h_4 + h_2 \,.$$

These conditions are identical to equation eq. (4.9).

- The horizontal distance between the nodes 1 and 2 at the bottom of the diagram has to be identical to the horizontal distance between the nodes 1 and 2 at the top of the diagram. The same constraint has to hold for the nodes 2 and 3, 3 and 4, etc

$$\begin{aligned} h_4 + v_5 &= v_4 + h_1 \,, & h_2 + v_3 &= v_2 + h_5 \,, \\ h_6 + v_4 &= v_6 + h_3 \,, & h_1 + v_2 &= v_1 + h_4 \,, \\ h_5 + v_6 &= v_5 + h_2 \,, & h_3 + v_1 &= v_3 + h_6 \,. \end{aligned} \tag{4.12}$$

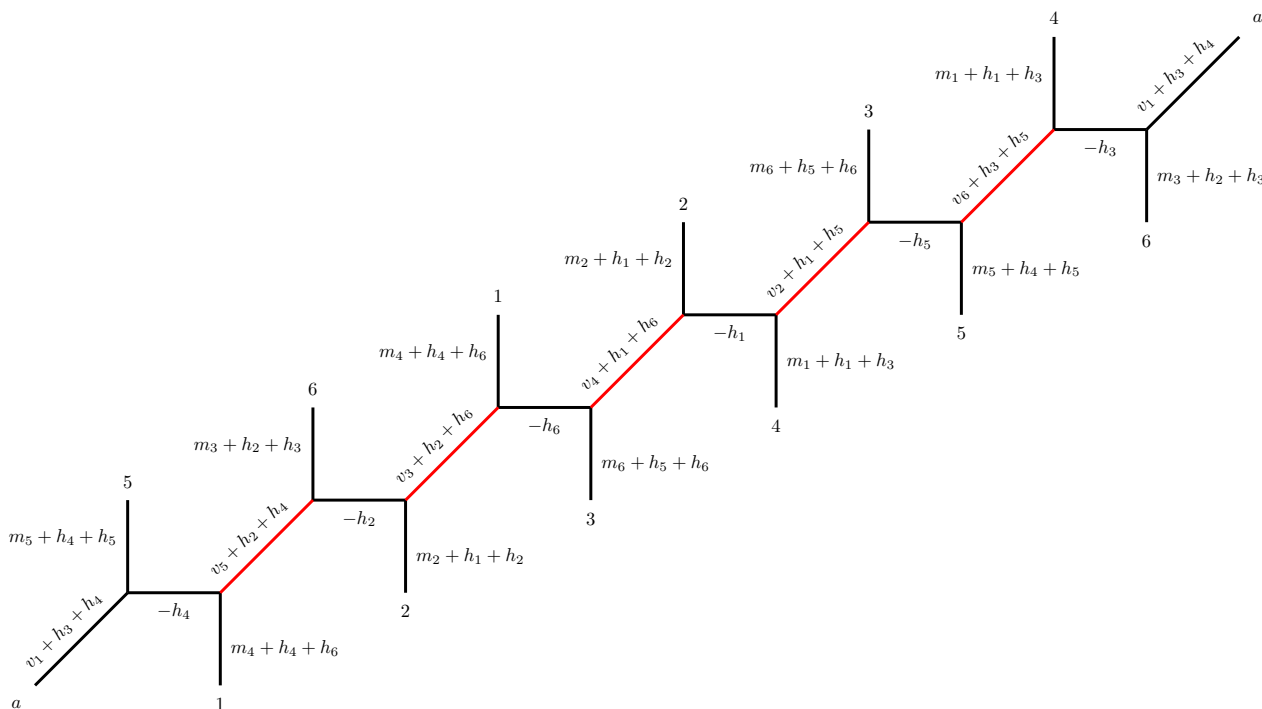These conditions are identical to equation (4.10).

Figure 16. Diagram after another SL$(2,\mathbb{Z})$ transformation. The red lines are to undergo a flop transition in the next step.

Thus, the consistency conditions eq. (4.11) and eq. (4.12) are still fully equivalent to the conditions eq. (4.2) through (4.7). This is to be expected, since the flop transformation does not change the overall length in the vertical or horizontal direction, as can be seen from eq. (2.25).

As a next step, we perform another SL$(2,\mathbb{Z})$ transformation to change the orientation of all lines in figure 15. Indeed, we transform

$$(1,0) \longrightarrow (1,-1), \qquad (0,1) \longrightarrow (0,1), \qquad (1,1) \longrightarrow (1,0), \qquad (4.13)$$

which changes horizontal lines into diagonal ones and vice versa, while leaving the vertical lines invariant. The resulting diagram is shown in figure 16. Since the SL$(2,\mathbb{Z})$ transformation does not modify the length of the individual lines (but only changes their orientation), the consistency conditions are also not altered, but remain eq. (4.11) and eq. (4.12).

As a next step we perform flop transitions on all the lines marked red in figure 16. Using the map of parameters in eq. (2.25), the new diagram takes the form of figure 17, where the vertical lengths $m'_{1,2,3,4,5,6}$ are given by

$$m'_1 = m_4 + v_3 + v_5 + 2(h_2 + h_4 + h_6),$$
$$m'_2 = m_2 + v_3 + v_4 + 2(h_1 + h_2 + h_6),$$
$$m'_3 = m_6 + v_2 + v_4 + 2(h_1 + h_5 + h_6),$$
$$m'_4 = m_1 + v_2 + v_6 + 2(h_1 + h_3 + h_5),$$
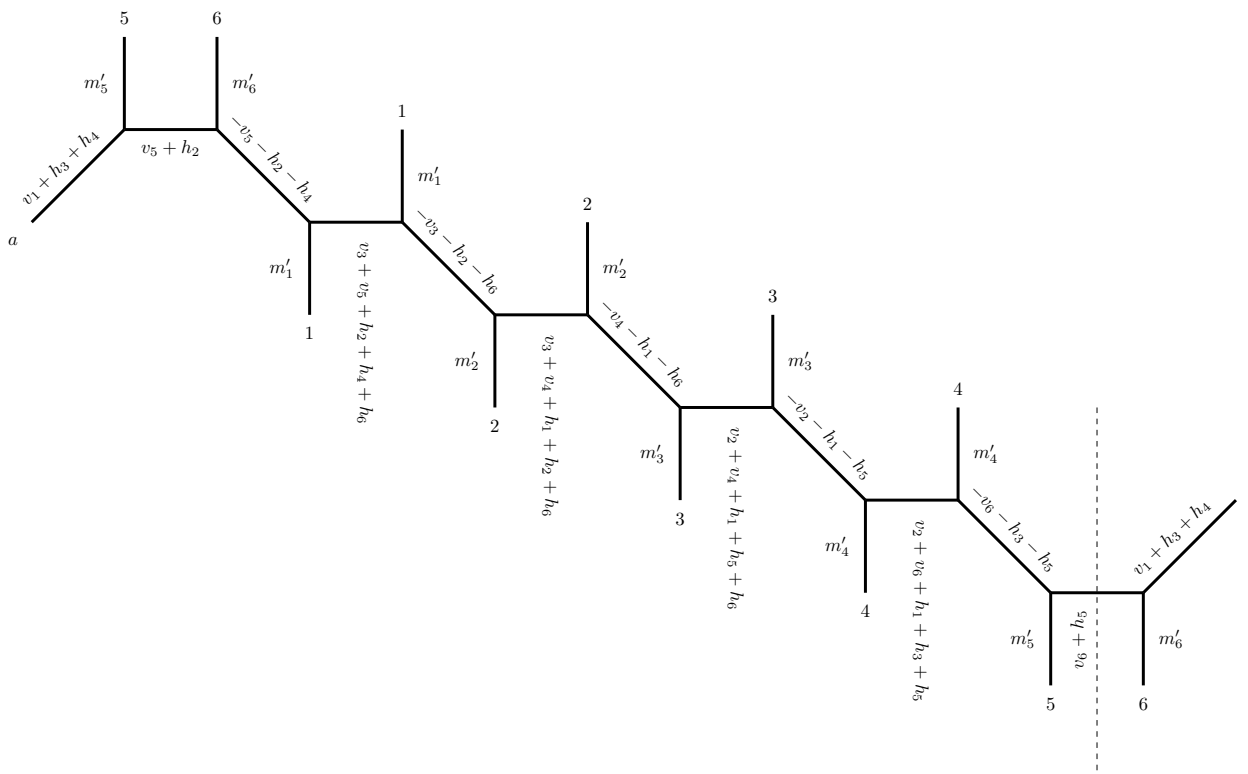$$m'_5 = m_5 + v_6 + h_3 + h_4 + 2h_5,$$

Figure 17. Diagram after five further flop transformations. The quantities $m'_{1,2,3,4,5,6}$ are given in eq. (4.14). The diagram will be cut along the dashed line in the following step.

$$m'_6 = m_3 + v_5 + 2h_2 + h_3 + h_4 \,. \tag{4.14}$$

As a next step we cut the diagram in figure 17 along the dashed line and glue it again along the diagonal line marked a. The result is shown in figure 18, for which we perform a flop transition for the line shown in red to arrive at figure 19. Here, the lines m''_5 and m''_6 have length

$$m''_5 = m'_5 + v_1 + h_3 + h_4 = m_5 + v_1 + v_6 + 2(h_3 + h_4 + h_5) \,,$$
$$m''_6 = m'_6 + v_1 + h_3 + h_4 = m_3 + v_1 + v_5 + 2(h_2 + h_3 + h_4) \,. \tag{4.15}$$

The consistency conditions for the diagram in figure 19 are the same as eq. (4.9) and eq. (4.10).

As a next step we perform an $\mathrm{SL}(2,\mathbb{Z})$ transformation which acts in the same manner as (4.13), i.e.

$$(1,0) \longrightarrow (1,-1) \,, \qquad (0,1) \longrightarrow (0,1) \,, \qquad (1,1) \longrightarrow (1,0) \,. \tag{4.16}$$

Thus, it transforms horizontal lines into diagonal ones and vice versa, while leaving vertical lines invariant. The resulting diagram is shown in figure 20. Finally, in order to obtain the familiar form of the $(N, M) = (6, 1)$ web (see [27]), we cut the diagram in figure 20 along the dashed line to arrive at figure 21. Comparing figure 21 with figure 14, we see that in
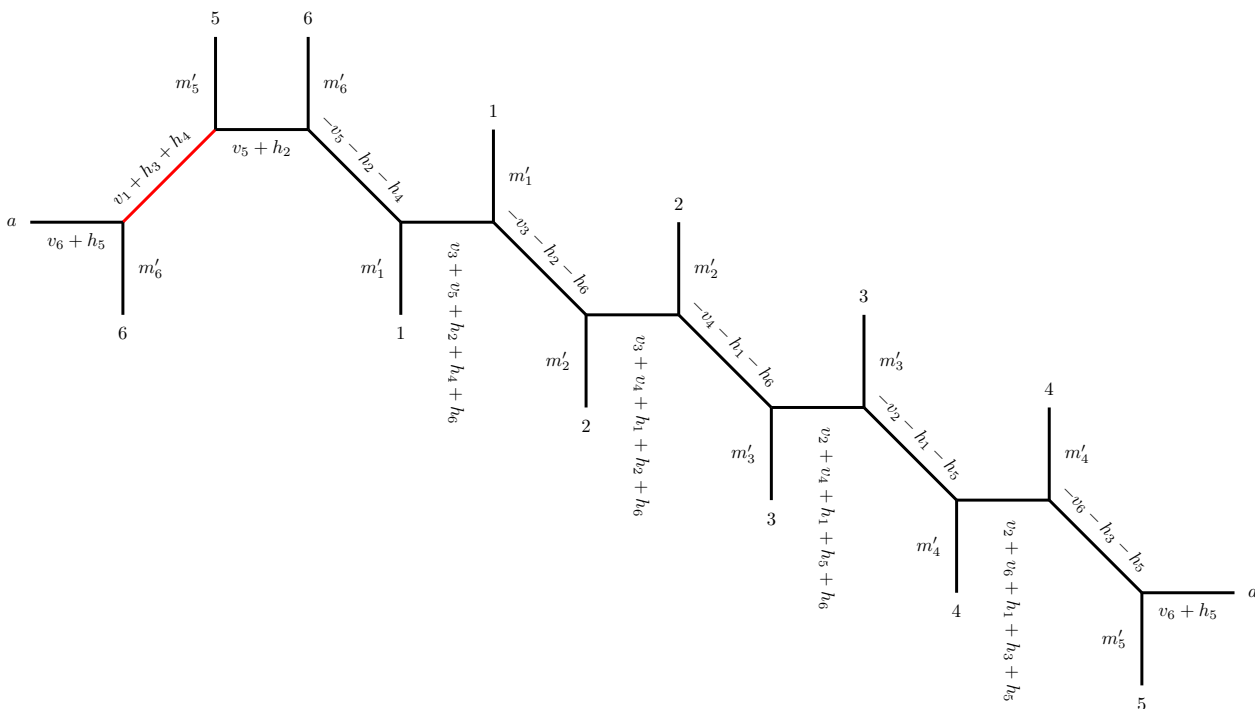
Figure 18. Re-gluing the diagram in figure 17. The red line will undergo a flop transition in the next step.

the former the vertical lines are directly above each other and not 'rotated' against each other as in the former. Therefore, the diagram in figure 21 indeed corresponds to the web $(N, M) = (6, 1)$. The consistency conditions are the same as in eq. (4.9) and eq. (4.10), which are equivalent to those in eq. (4.2) through eq. (4.7) in the original diagram in figure 10. Thus, by a series of flop transitions, we have been able to relate the Calabi-Yau threefold $X_{3,2}$ to $X_{6,1}$.

In the F-theory compactification, without m-deformation, the Calabi-Yau threefold $X_{3,2}$ gives rise to a little string theory with $\mathcal{N} = (1,0)$ supersymmetry, while the Calabi-Yau threefold $X_{6,1}$ gives rise to little string theory with $(2,0)$ supersymmetry. However, undeformed Calabi-Yau threefolds $X_{M,N}$ are singular, prohibiting us from performing flop transitions. In our construction, we thus always turned on the m-deformation. Hence, in the extended moduli space, these deformed theories retain the same $(1,0)$ supersymmetries and can be smoothly mapped to each other via flop transitions.

One would think that, since $X_{N,1}$ are related to $(2,0)$ little strings and $X_{N,M}$ to $(1,0)$ little strings, there is a jump in supersymmetry given by the duality discussed above. However, as we mentioned before, the deformation by $\mathrm{U}(1)_m$ commutes with the orbifold action on the transverse space and breaks the supersymmetry to $(1,0)$ in both sides. It is also not easy to see if the deformation by m can be turned off after performing the flop transitions since it mixes with other parameters of the theory in a non-trivial way. However, it is known that a situation exhibiting a phenomenon of supersymmetry do exist such as the one discussed in [59] in a different context, namely, M-theory compactifications on compact
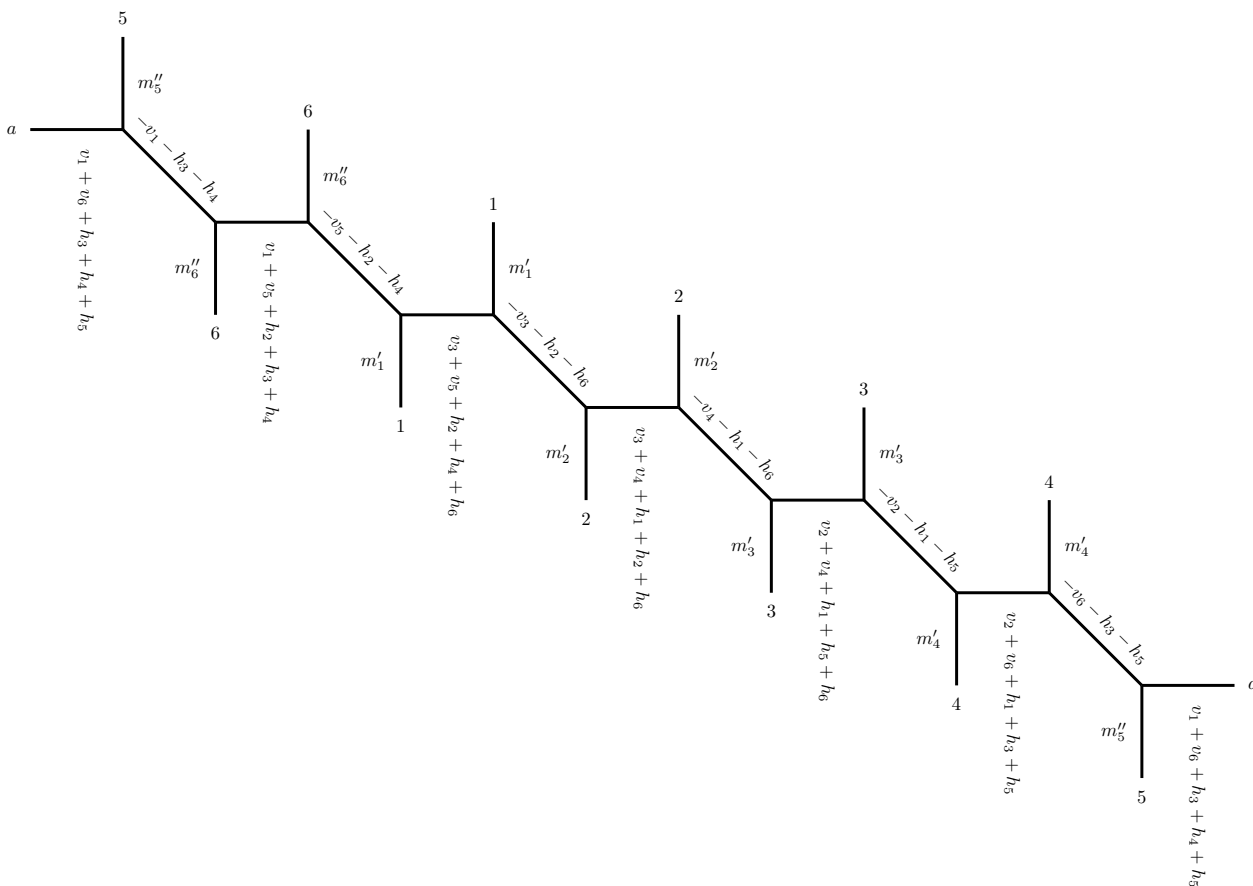
Figure 19. Diagram after a further flop transition. The parameters $m'_{1,2,3,4}$ are as in eq. (4.14) while $m''_{5,6}$ are defined in eq. (4.15).

Calabi-Yau threefolds. In this framework, flop transitions of birationally equivalent Calabi-Yau threefolds extend the Coulomb branch of five-dimensional $\mathcal{N} = 1$ theories. It was demonstrated in [59] through several lower-rank examples that the supercharges are well defined everywhere in this extended moduli space, but that the energy and the charges of BPS configurations are not differentiable everywhere: indeed, the number of residual supersymmetries often jumps across the walls of the Kähler cones (i.e. the locus where the flop transition takes place).

4.2.3 Simple check of the duality

As a simple check of the proposed relation between the partition functions of the $(N, M) = (3, 2)$ and the $(6, 1)$ brane webs, we consider the particular case

$$
\begin{aligned}
m &= m_1 = m_2 = m_3 = m_4 = m_5 = m_6\,, \\
v &= v_1 = v_2 = v_3 = v_4 = v_5 = v_6\,, \\
h &= h_1 = h_2 = h_3 = h_4 = h_5 = h_6\,.
\end{aligned}
\tag{4.17}
$$

which is a solution of eq. (4.2) through eq. (4.7) (and therefore also of eq. (4.9) and eq. (4.10)). Moreover, as has been proposed in [10] at this particular region in the moduli
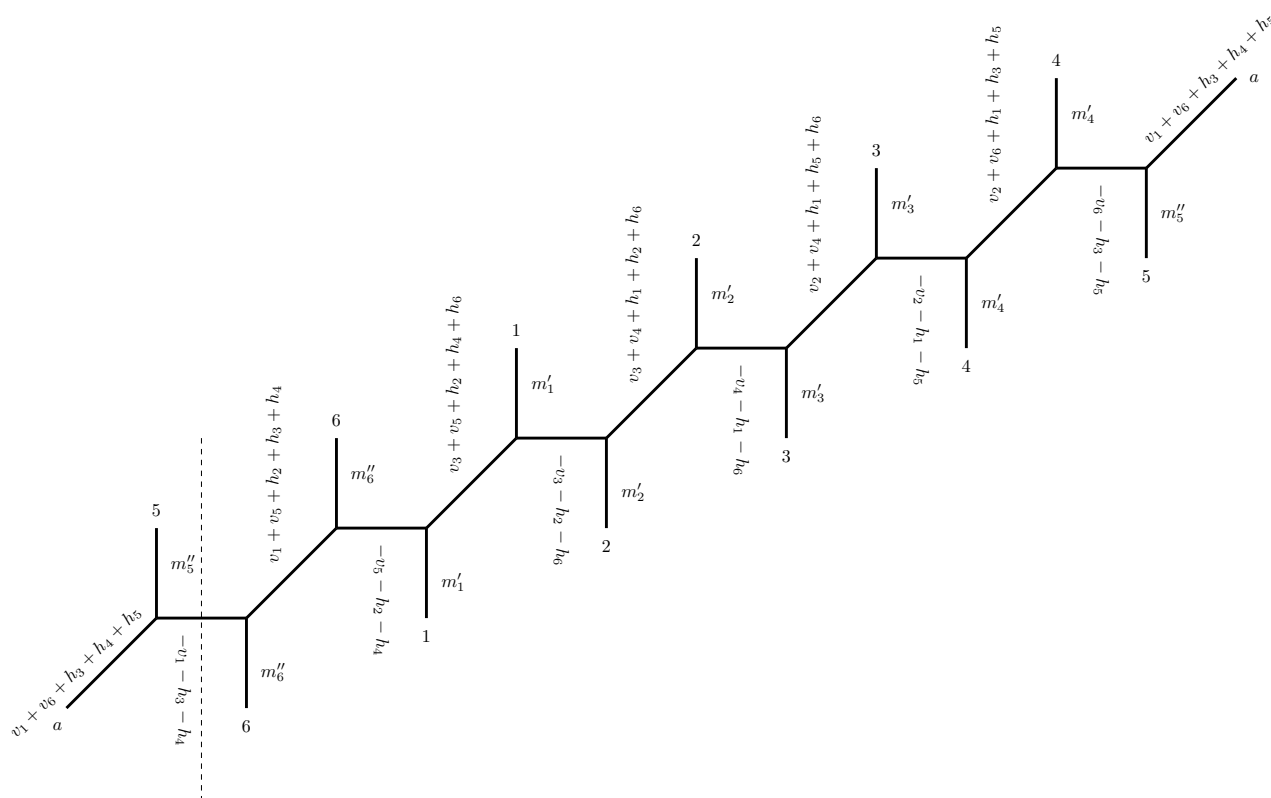
Figure 20. Diagram after another SL$(2,\mathbb{Z})$ transformation. In the final step, the diagram will be cut along the dashed line.
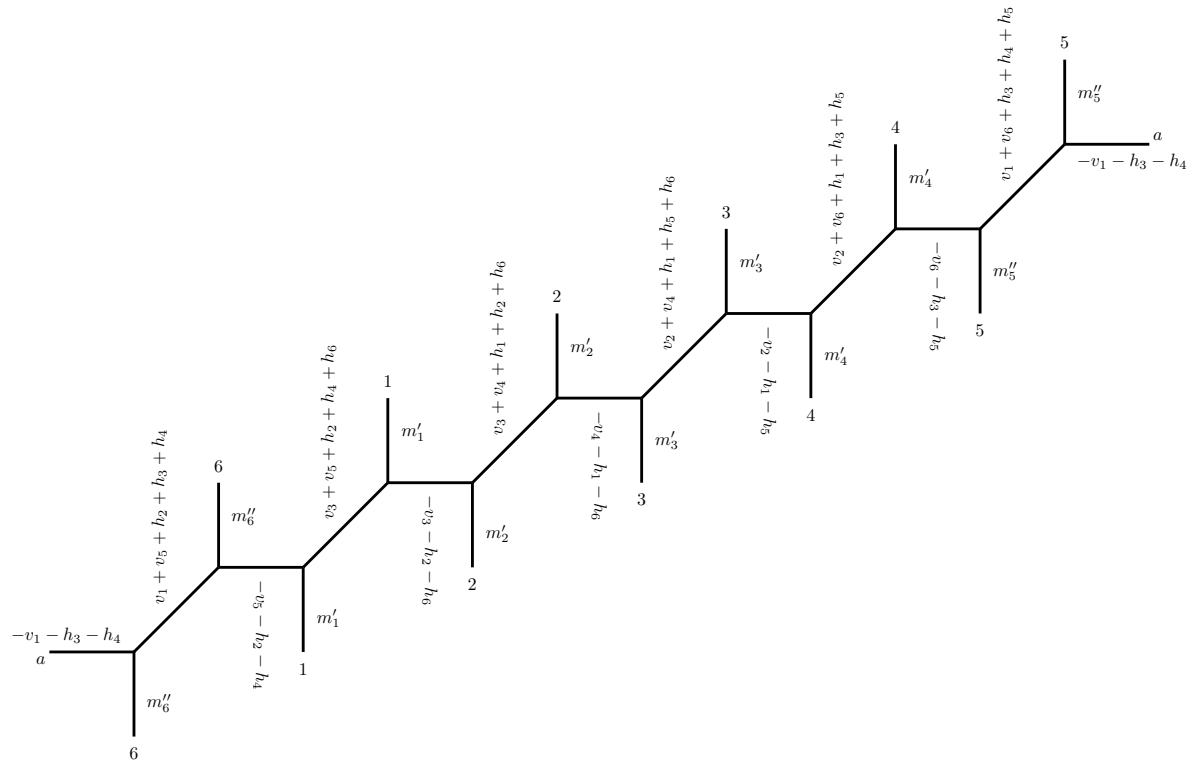

Figure 21. The final (p,q)-web diagram corresponding to $(N,M) = (6,1)$.

space, the Nekrasov-Shatashvili limit of the free energies of a generic (N, M) brane can be related to those of the web $(1, 1)$ (see eq. (3.11)). Thus, at eq. (4.17), the transformation of the parameters obtained by comparing figure 10 with figure 21 must be a symmetry of the partition function of the brane web $(1, 1)$. Our strategy of showing such an invariance is to show that this transformation is part of $\mathrm{Sp}(2, \mathbb{Z})$ which was proposed in [28, 54] to be a symmetry of the $(M, N) = (1, 1)$ case.

To this end, we start with the $(3, 2)$ web and introduce

$$\rho = 3m + 3h\,, \qquad \text{and} \qquad \tau = 2m + 2v\,. \tag{4.18}$$

which entails

$$h = \frac{1}{3}(\rho - 3m)\,, \qquad \text{and} \qquad v = \frac{1}{2}(\tau - 2m)\,. \tag{4.19}$$

Furthermore, we introduce the $(1, 1)$ period matrix

$$\Omega = \begin{pmatrix} \tau/2 & m \\ m & \rho/3 \end{pmatrix}\,. \tag{4.20}$$

Notice here the rescaling of the parameters, as is required to make contact with the configuration $(N, M) = (1, 1)$. We now want to compare Ω to a similar period matrix obtained from the $(6, 1)$ web. For the latter, we introduce in a similar fashion

$$\rho' = 6v + 6h\,, \qquad \tau' = m + 4v + 9h\,, \qquad m' = 2v + 3h\,. \tag{4.21}$$

which in terms of (ρ, τ, m) reads

$$\rho' = 3\tau + 2\rho - 12m\,, \qquad \tau' = 2\tau + 3\rho - 12m\,, \qquad m' = \rho + \tau - 5m\,. \tag{4.22}$$

We also introduce the $(1, 1)$ period matrix

$$\Omega' = \begin{pmatrix} \tau' & m' \\ m' & \rho'/6 \end{pmatrix} = \begin{pmatrix} 2\tau + 3\rho - 12m & \tau + \rho - 5m \\ \tau + \rho - 5m & \frac{1}{6}(3\tau + 2\rho - 12m) \end{pmatrix}\,. \tag{4.23}$$

The two period matrices Ω and Ω' are related through an $\mathrm{Sp}(2, \mathbb{Z})$ transformation

$$\Omega' = (A\Omega + B) \cdot (C\Omega + D)^{-1}\,, \tag{4.24}$$

with

$$A = \begin{pmatrix} 2 & -3 \\ 1 & -1 \end{pmatrix}\,, \qquad B = \begin{pmatrix} 0 & 0 \\ 0 & 0 \end{pmatrix}\,, \qquad C = \begin{pmatrix} 0 & 0 \\ 0 & 0 \end{pmatrix}\,, \qquad D = \begin{pmatrix} -1 & -1 \\ 3 & 2 \end{pmatrix}\,, \tag{4.25}$$

which satisfy eq. (2.21) (notice also that $\det\Omega = \frac{\rho\tau}{6} - m^2 = \det\Omega'$). This shows that $\mathcal{Z}_{X_{1,1}}$ is indeed invariant under the change of parameters implied by the above chain of dualities.[11]

---

[11]Notice that due to $\det(C\Omega + D) = 1$ for (4.25), a weight factor in the $\mathrm{Sp}(2, \mathbb{Z})$ transformation is irrelevant.

4.2.4 Vertex identification

We compare the diagrams in figure 11 and figure 21, where we identified vertices that are mapped into each other (see figure 22). We notice that the length of the horizontal and diagonal lines in the $(6,1)$ diagram can be read off as the distances (using only horizontal and vertical lines) between the same vertices in the $(3,2)$ web. As an example, we have highlighted the distance between the vertices E and H as well as L and K respectively. Notice that this rule does not only apply to neighboring vertices: e.g. the (shortest)[12] distance between vertices H and I is (again we only use horizontal and vertical lines)

$$h_4 = v_5 + h_2 + h_4 - v_1 - v_5 - h_2 - h_3 - h_4 + v_1 + h_3 + h_4 \,. \tag{4.26}$$

In section 5 we discuss how to generalise this observation to a general pattern that allows reconstructing the web $(\frac{NM}{k}, k)$ starting from a labelling of the vertices of the web (N, M).

4.3 Relation between $(N, M) = (2, 5)$ and $(10, 1)$

The next example is the web $(N, M) = (2, 5)$.

4.3.1 Duality transformation

A parametrisation of the $(N, M) = (2, 5)$ web is given in figure 23. Out of the 30 parameters (h_i, v_i, m_i) with $i = 1, \ldots, 10$, only 12 are independent. The remaining ones are fixed by consistency relations, as discussed above. Following a similar sequence of flop-transitions, cutting and re-gluing the diagram, as well as $\mathrm{SL}(2, \mathbb{Z})$ transformations, we can dualise the $(N, M) = (2, 5)$ to the $(10, 1)$ web with the parametrisation given in figure 24. Explicitly, the parameters $\bar{v}_i$ are given in terms of (h_i, v_i, m_i) as

$$\begin{aligned}
\overline{v}_1 &= m_1 + 4(v_1 + v_2 + v_4 + v_8 + v_{10}) + 3(h_2 + h_4 + h_8 + h_{10}) \,, \\
\overline{v}_2 &= m_{10} + 4(v_2 + v_4 + v_6 + v_8 + v_{10}) + 3(h_2 + h_4 + h_6 + h_8) \,, \\
\overline{v}_3 &= m_4 + 4(v_2 + v_4 + v_5 + v_6 + v_8) + 3(h_2 + h_5 + h_6 + h_8) \,, \\
\overline{v}_4 &= m_8 + 4(v_2 + v_5 + v_6 + v_8 + v_9) + 3(h_2 + h_5 + h_6 + h_9) \,, \\
\overline{v}_5 &= m_2 + 4(v_2 + v_3 + v_5 + v_6 + v_9) + 3(h_3 + h_5 + h_6 + h_9) \,, \\
\overline{v}_6 &= m_6 + 4(v_3 + v_5 + v_6 + v_7 + v_9) + 3(h_3 + h_5 + h_7 + h_9) \,, \\
\overline{v}_7 &= m_5 + 4(v_1 + v_3 + v_5 + v_7 + v_9) + 3(h_1 + h_3 + h_7 + h_9) \,, \\
\overline{v}_8 &= m_9 + 4(v_1 + v_3 + v_7 + v_9 + v_{10}) + 3(h_1 + h_3 + h_7 + h_{10}) \,, \\
\overline{v}_9 &= m_3 + 4(v_1 + v_3 + v_4 + v_7 + v_{10}) + 3(h_1 + h_4 + h_7 + h_{10}) \,, \\
\overline{v}_{10} &= m_7 + 4(v_1 + v_4 + v_7 + v_8 + v_{10}) + 3(h_1 + h_4 + h_8 + h_{10}) \,, \tag{4.27}
\end{aligned}$$

---

[12]Counting in the opposite direction in the $(6,1)$ web corresponds to $\rho' + h_4$, where ρ' is the length of the horizontal circle in the $(6,1)$ web.
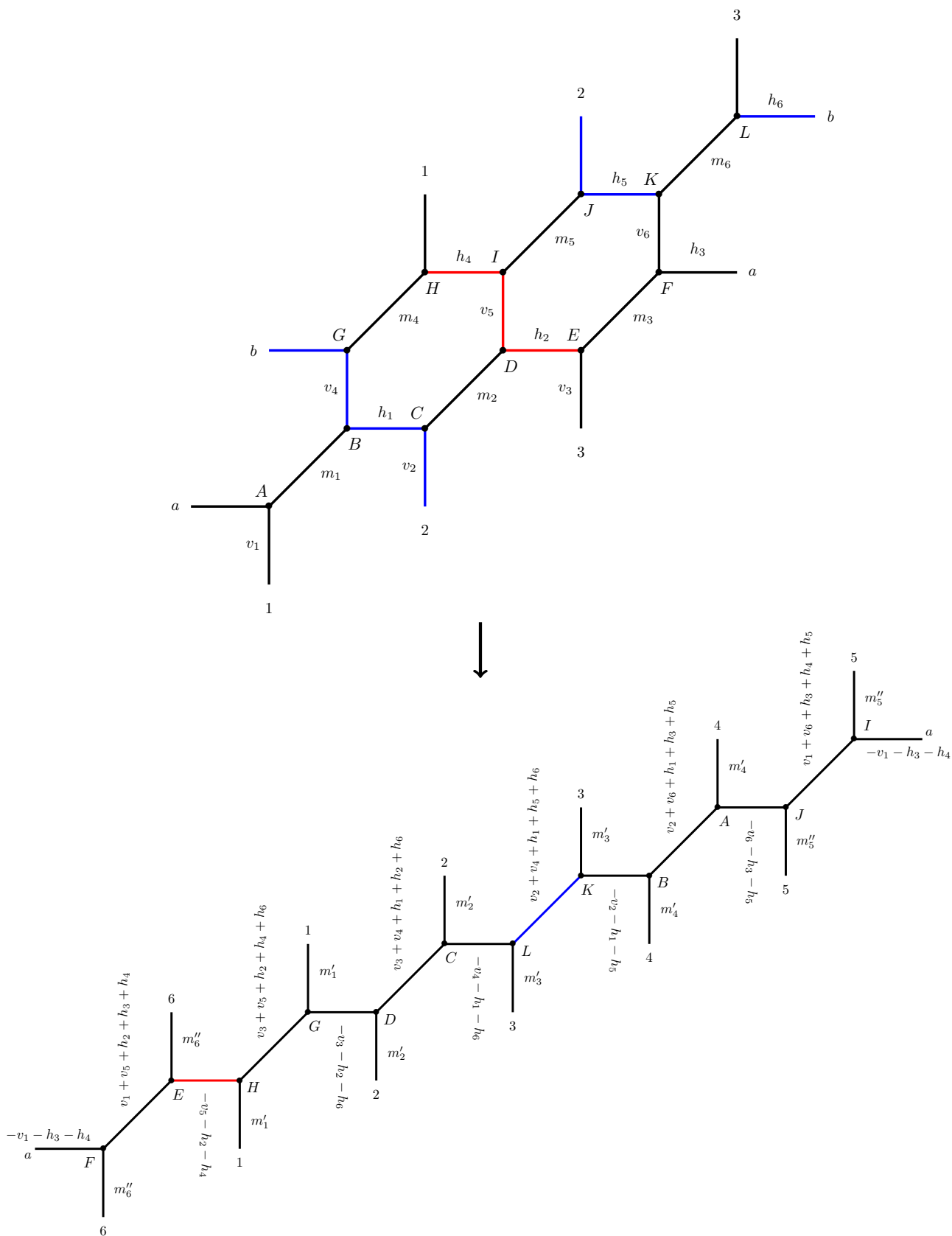
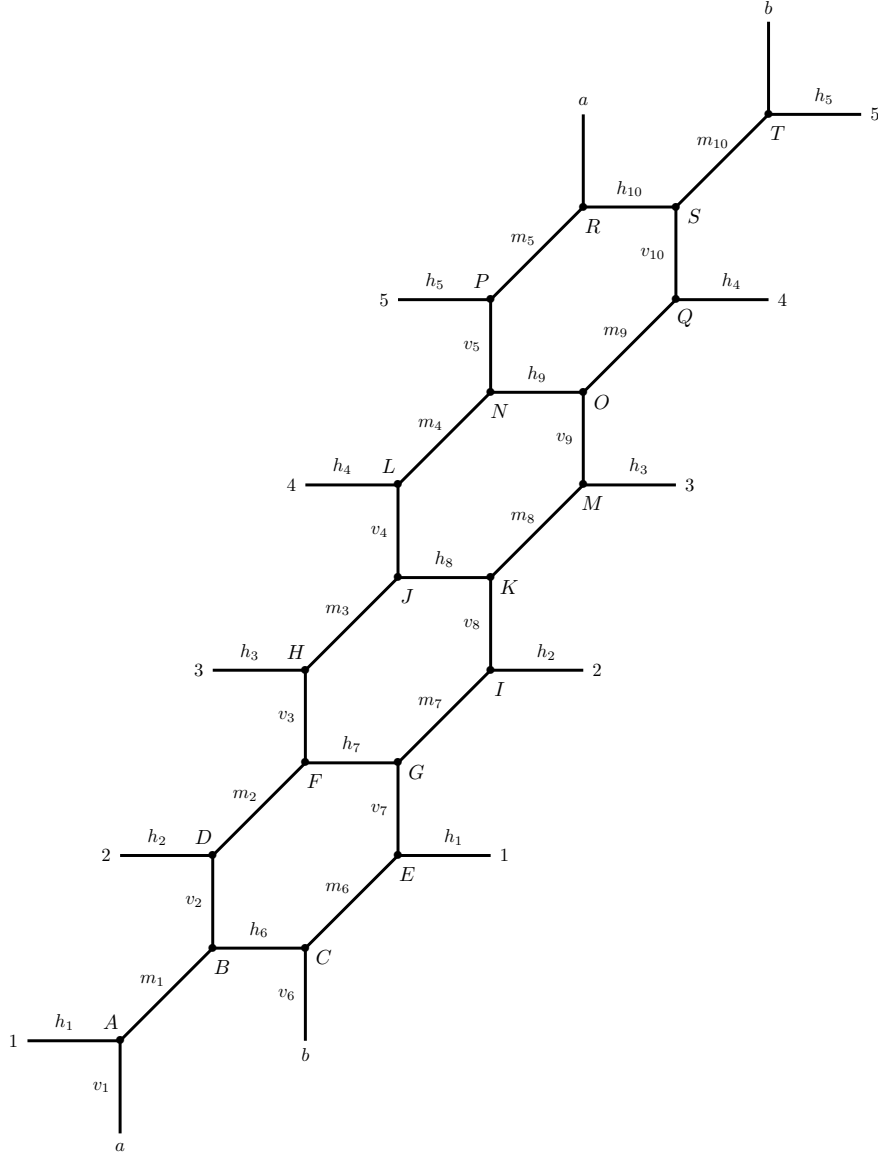**Figure 22**. Identifying vertices in the $(3, 2)$ and $(6, 1)$ webs.

Figure 23. Parametrisation of the $(N, M) = (2, 5)$ web and a labelling of the vertices.

while the parameters $\overline{h}$ are

$$\overline{h}_1 = -(v_2 + v_4 + v_8 + v_{10} + h_2 + h_4 + h_8), \quad \overline{h}_2 = -(v_2 + v_4 + v_6 + v_8 + h_2 + h_6 + h_8),$$
$$\overline{h}_3 = -(v_2 + v_5 + v_6 + v_8 + h_2 + h_5 + h_6), \quad \overline{h}_4 = -(v_2 + v_5 + v_6 + v_9 + h_5 + h_6 + h_9),$$
$$\overline{h}_5 = -(v_3 + v_5 + v_6 + v_9 + h_3 + h_5 + h_9), \quad \overline{h}_6 = -(v_3 + v_5 + v_7 + v_9 + h_3 + h_7 + h_9),$$
$$\overline{h}_7 = -(v_1 + v_3 + v_7 + v_9 + h_1 + h_3 + h_7), \quad \overline{h}_8 = -(v_1 + v_3 + v_7 + v_{10} + h_1 + h_7 + h_{10}),$$
$$\overline{h}_9 = -(v_1 + v_4 + v_7 + v_{10} + h_1 + h_4 + h_{10}), \quad \overline{h}_{10} = -(v_1 + v_4 + v_8 + v_{10} + h_4 + h_8 + h_{10}), \quad (4.28)$$
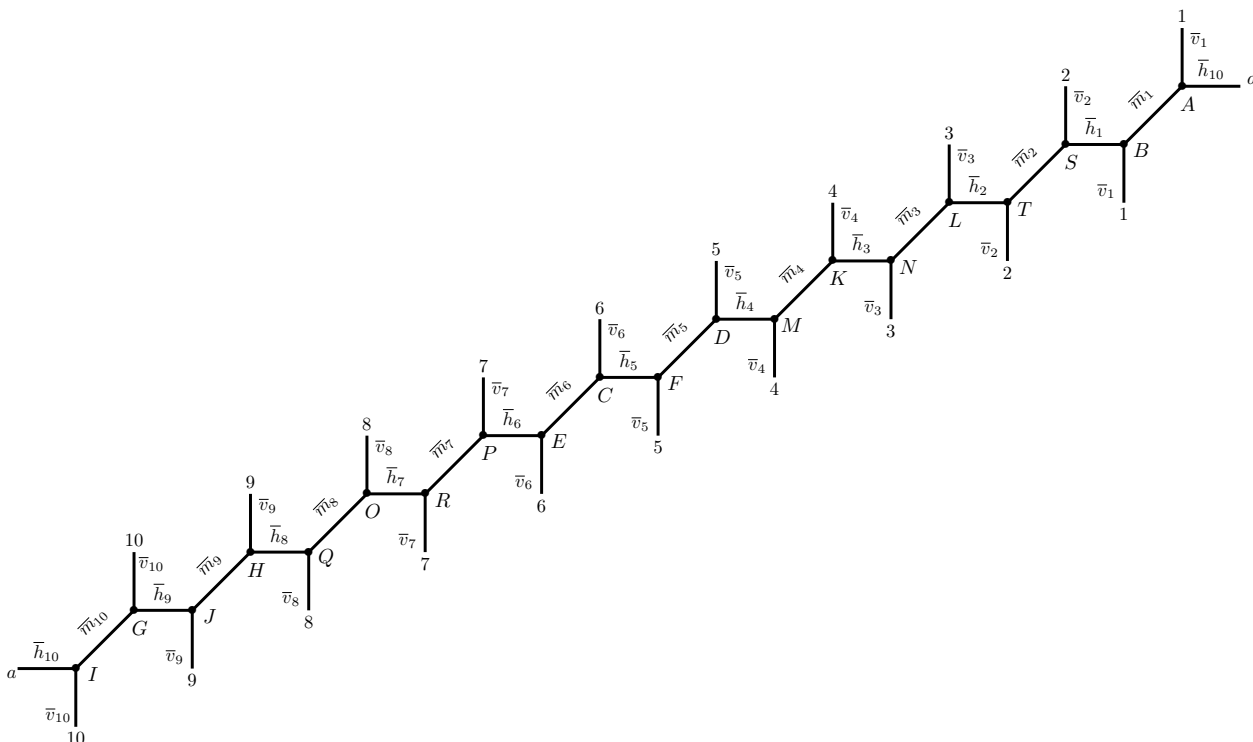
Figure 24. Parametrisation of the $(N, M) = (10, 1)$ web and a labelling of the vertices that is compatible with the one in figure 23.

and the parameters $\overline{m}$

$$\overline{m}_1 = (v_1 + v_2 + v_4 + v_8 + v_{10}) + (h_2 + h_4 + h_8 + h_{10}),$$
$$\overline{m}_2 = (v_2 + v_4 + v_6 + v_8 + v_{10}) + (h_2 + h_4 + h_6 + h_8),$$
$$\overline{m}_3 = (v_2 + v_4 + v_5 + v_6 + v_8) + (h_2 + h_5 + h_6 + h_8),$$
$$\overline{m}_4 = (v_2 + v_5 + v_6 + v_8 + v_9) + (h_2 + h_5 + h_6 + h_9),$$
$$\overline{m}_5 = (v_2 + v_3 + v_5 + v_6 + v_9) + (h_3 + h_5 + h_6 + h_9),$$
$$\overline{m}_6 = (v_3 + v_5 + v_6 + v_7 + v_9) + (h_3 + h_5 + h_7 + h_9),$$
$$\overline{m}_7 = (v_1 + v_3 + v_5 + v_7 + v_9) + (h_1 + h_3 + h_7 + h_9),$$
$$\overline{m}_8 = (v_1 + v_3 + v_7 + v_9 + v_{10}) + (h_1 + h_3 + h_7 + h_{10}),$$
$$\overline{m}_9 = (v_1 + v_3 + v_4 + v_7 + v_{10}) + (h_1 + h_4 + h_7 + h_{10}),$$
$$\overline{m}_{10} = (v_1 + v_4 + v_7 + v_8 + v_{10}) + (h_1 + h_4 + h_8 + h_{10}). \tag{4.29}$$

Using the assignment of vertices in figure 23 and figure 24, the parameters $\overline{h}$ and $\overline{m}$ can be read off from the two vertex diagrams in the same manner as in the case of $(N, M) = (3, 2)$.

The fact that the diagram in figure 23 can be transformed into figure 24 through a sequence of flops and $SL(2, \mathbb{Z})$ transformations shows that the web diagram $(N, M) = (2, 5)$ is indeed dual to the web diagram $(N, M) = (10, 1)$.

4.3.2 Simple check of the duality

As in section 4.2.3 for the case $(N, M) = (3, 2)$, we can perform a simple check of the duality found above. Indeed, we consider the following choice of the parameters

$$
\begin{aligned}
m_1 &= m_2 = \cdots = m_{10} = m \,, \\
h_1 &= h_2 = \cdots = h_{10} = h = \frac{\rho}{2} - m \,, \\
v_1 &= v_2 = \cdots = v_{10} = v = \frac{\tau}{5} - m \,,
\end{aligned}
\tag{4.30}
$$

which are compatible with all the consistency conditions. Furthermore, we introduce the three parameters (τ', ρ', m') for the $(10, 1)$ web

$$
\tau' = 5\tau + 8\rho - 40m \,, \qquad \rho' = 2\tau + 5\rho - 20m \,, \qquad m' = \tau + 2\rho - 9m \,.
\tag{4.31}
$$

and define the $(1, 1)$ period matrices

$$
\Omega = \begin{pmatrix} \tau/5 & m \\ m & \rho/2 \end{pmatrix} \,, \qquad \text{and} \qquad \Omega' = \begin{pmatrix} \tau' & m' \\ m' & \rho'/10 \end{pmatrix} \,,
\tag{4.32}
$$

These satisfy the relation

$$
\Omega' = (A\Omega + B) \cdot (C\Omega + D)^{-1} \,,
\tag{4.33}
$$

for the matrices

$$
A = \begin{pmatrix} 5 & -4 \\ 1 & -1 \end{pmatrix} \,, \qquad B = \begin{pmatrix} 0 & 0 \\ 0 & 0 \end{pmatrix} \,, \qquad C = \begin{pmatrix} 0 & 0 \\ 0 & 0 \end{pmatrix} \,, \qquad D = \begin{pmatrix} 1 & 1 \\ -4 & -5 \end{pmatrix} \,,
\tag{4.34}
$$

which satisfy as well the relations (2.21). This shows that (ρ, τ, m) and (ρ', τ', m') are related through an $\mathrm{Sp}(2, \mathbb{Z})$ transformation. Therefore, $\mathcal{Z}_{X_{1,1}}$ is indeed invariant under the change of parameters implied by the above chain of dualities.

4.4 Relation between $(N, M) = (3, 4)$ and $(12, 1)$

The next example is the case $(N, M) = (3, 4)$.

4.4.1 Duality transformation

A parametrisation of the web $(N, M) = (3, 4)$ is given in figure 25, which also shows an assignment of vertices. Of the 36 parameters in the web in figure 25, only 14 are independent on account of the consistency conditions. After going through a sequence of flop-transitions, cutting and re-gluing as well as $\mathrm{SL}(2, \mathbb{Z})$ transformations, we can bring this diagram to the form of the $(N, M) = (12, 1)$ web with the parametrisation given in figure 26. Specifically, the parameters $\overline{m}$ are given by

$$
\begin{aligned}
\overline{m}_1 &= h_2 + h_7 + h_{12} + v_2 + v_3 + v_5 + v_{12} \,, & \overline{m}_2 &= h_2 + h_4 + h_{12} + v_2 + v_5 + v_{11} + v_{12} \\
\overline{m}_3 &= h_2 + h_4 + h_9 + v_2 + v_5 + v_8 + v_{11} \,, & \overline{m}_4 &= h_4 + h_9 + h_{11} + v_1 + v_2 + v_8 + v_{11}
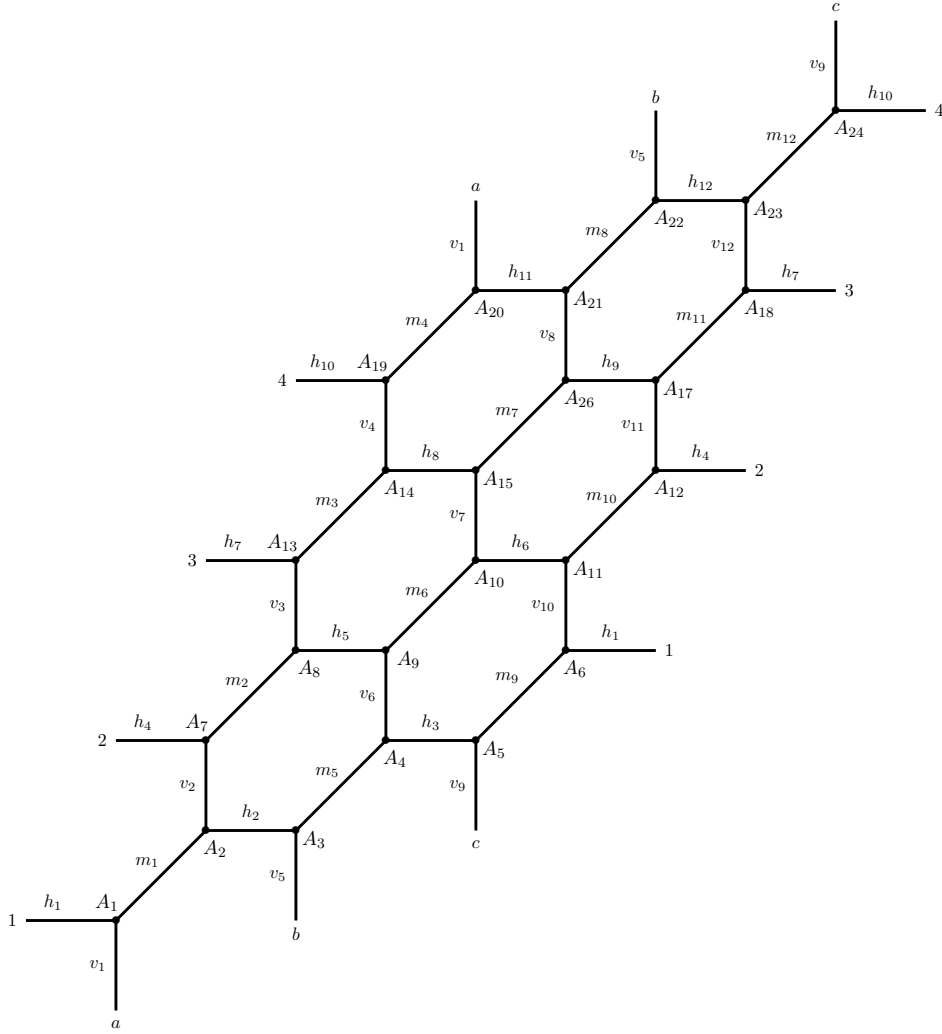\end{aligned}
$$

Figure 25. Parametrisation of the $(N, M) = (3, 4)$ web along with an assignment of vertices.

$$\overline{m}_5 = h_1 + h_9 + h_{11} + v_1 + v_8 + v_{10} + v_{11}, \qquad \overline{m}_6 = h_1 + h_6 + h_{11} + v_1 + v_7 + v_8 + v_{10},$$

$$\overline{m}_7 = h_1 + h_6 + h_8 + v_1 + v_4 + v_7 + v_{10}, \qquad \overline{m}_8 = h_6 + h_8 + h_{10} + v_4 + v_7 + v_9 + v_{10},$$

$$\overline{m}_9 = h_3 + h_8 + h_{10} + v_4 + v_6 + v_7 + v_9, \qquad \overline{m}_{10} = h_3 + h_5 + h_{10} + v_3 + v_4 + v_6 + v_9,$$

$$\overline{m}_{11} = h_3 + h_5 + h_7 + v_3 + v_6 + v_9 + v_{12}, \qquad \overline{m}_{12} = h_5 + h_7 + h_{12} + v_3 + v_5 + v_6 + v_{12}, \qquad (4.35)$$

while the parameters $\bar{h}$ are

$$\overline{h}_1 = -(h_2 + h_{12} + v_2 + v_5 + v_{12}), \qquad \overline{h}_2 = -(h_2 + h_4 + v_2 + v_5 + v_{11}),$$

$$\overline{h}_3 = -(h_4 + h_9 + v_2 + v_8 + v_{11}), \qquad \overline{h}_4 = -(h_9 + h_{11} + v_1 + v_8 + v_{11}),$$

$$\overline{h}_5 = -(h_1 + h_{11} + v_1 + v_8 + v_{10}), \qquad \overline{h}_6 = -(h_1 + h_6 + v_1 + v_7 + v_{10}),$$

$$\overline{h}_7 = -(h_6 + h_8 + v_4 + v_7 + v_{10}), \qquad \overline{h}_8 = -(h_8 + h_{10} + v_4 + v_7 + v_9),$$

$$\overline{h}_9 = -(h_3 + h_{10} + v_4 + v_6 + v_9), \qquad \overline{h}_{10} = -(h_3 + h_5 + v_3 + v_6 + v_9),$$

$$\overline{h}_{11} = -(h_5 + h_7 + v_3 + v_6 + v_{12}), \qquad \overline{h}_{12} = -(h_7 + h_{12} + v_3 + v_5 + v_{12}). \qquad (4.36)$$
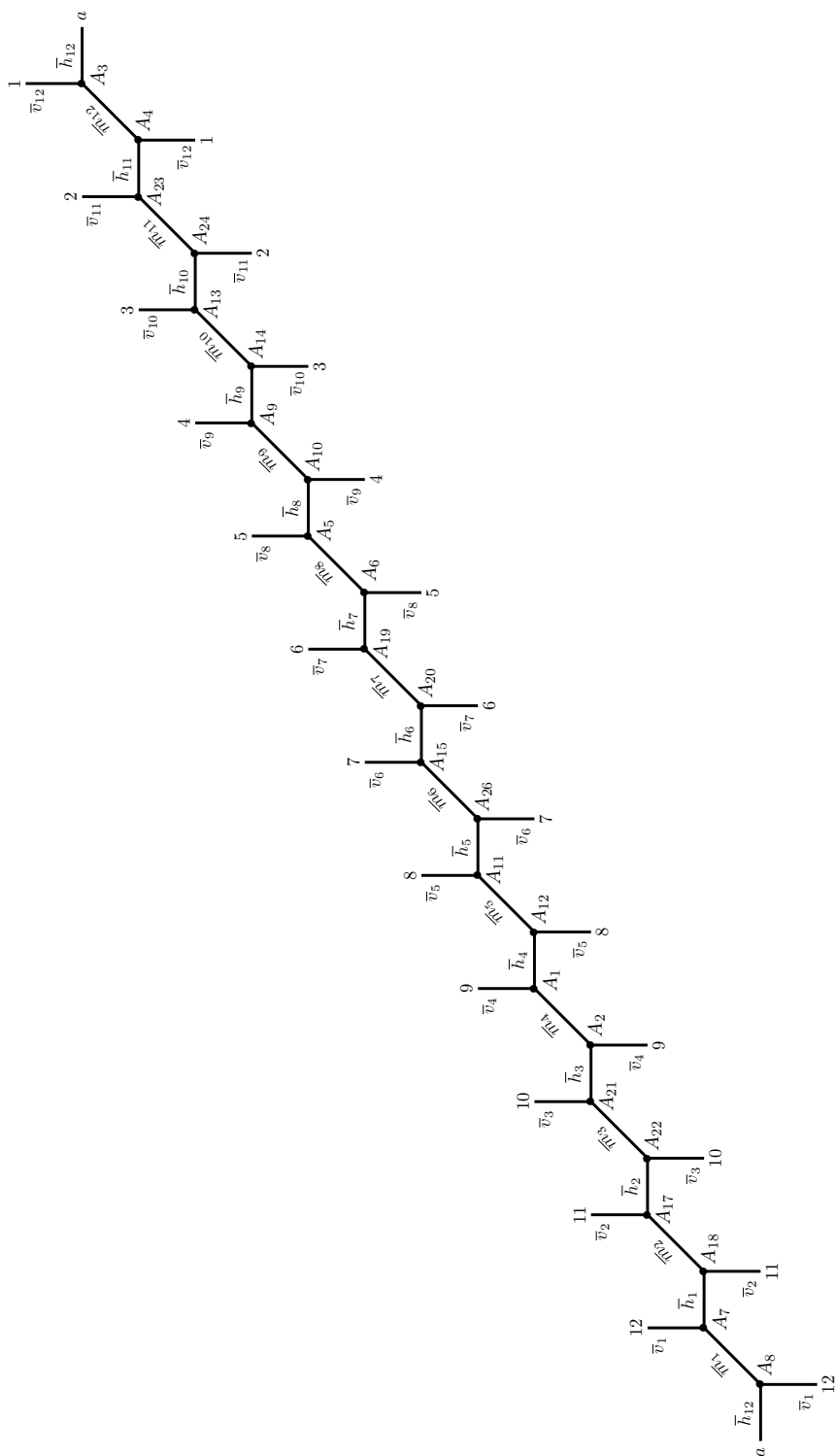
Figure 26. Parametrisation of the web $(N, M) = (12, 1)$web with an assignment of vertices compatible with figure 25.

and the parameters $\bar{v}$ are

$$\bar{v}_1 = m_2 + 2(h_2 + h_7 + h_{12}) + 3(v_2 + v_3 + v_5 + v_{12}) \,,$$

$$\bar{v}_2 = m_{11} + 2(h_2 + h_4 + h_{12}) + 3(v_2 + v_5 + v_{11} + v_{12}) \,,$$

$$\bar{v}_3 = m_8 + 2(h_2 + h_4 + h_9) + 3(v_2 + v_5 + v_8 + v_{11}) \,,$$

$$\bar{v}_4 = m_1 + 2(h_4 + h_9 + h_{11}) + 3(v_1 + v_2 + v_8 + v_{11}) \,,$$

$$\bar{v}_5 = m_{10} + 2(h_1 + h_9 + h_{11}) + 3(v_1 + v_8 + v_{10} + v_{11}) \,,$$

$$\bar{v}_6 = m_7 + 2(h_1 + h_6 + h_{11}) + 3(v_1 + v_7 + v_8 + v_{10}) \,,$$

$$\bar{v}_7 = m_4 + 2(h_1 + h_6 + h_8) + 3(v_1 + v_4 + v_7 + v_{10}) \,,$$

$$\bar{v}_8 = m_9 + 2(h_6 + h_8 + h_{10}) + 3(v_4 + v_7 + v_9 + v_{10}) \,,$$

$$\bar{v}_9 = m_6 + 2(h_3 + h_8 + h_{10}) + 3(v_4 + v_6 + v_7 + v_9) \,,$$

$$\bar{v}_{10} = m_3 + 2(h_3 + h_5 + h_{10}) + 3(v_3 + v_4 + v_6 + v_9) \,,$$

$$\bar{v}_{11} = m_{12} + 2(h_3 + h_5 + h_7) + 3(v_3 + v_6 + v_9 + v_{12}) \,,$$

$$\bar{v}_{12} = m_5 + 2(h_5 + h_7 + h_{12}) + 3(v_3 + v_5 + v_6 + v_{12}) \,.$$

As in the cases before, using the assignment of vertices in figure 25 and figure 26 the parameters $\bar{h}$ and $\bar{m}$ can be directly read off. Furthermore, the transformation above shows that the web diagrams $(N, M) = (3, 4)$ and $(12, 1)$ are indeed dual to each other.

4.4.2 Simple check of duality

In order to perform a check of the duality worked out above, we consider

$$m_1 = m_2 = \cdots = m_{12} = m \,,$$

$$h_1 = h_2 = \cdots = h_{12} = h = \frac{\rho}{3} - m \,,$$

$$v_1 = v_2 = \cdots = v_{12} = v = \frac{\tau}{4} - m \,. \tag{4.37}$$

Furthermore, we introduce the parameters in the $(12, 1)$ web

$$\tau' = 4\tau + 3\rho - 24m \,, \qquad \rho' = 3\tau + 4\rho - 24m \,, \qquad m' = \tau + \rho - 7m \,. \tag{4.38}$$

Next we also introduce the period matrices

$$\Omega = \begin{pmatrix} \tau/4 & m \\ m & \rho/3 \end{pmatrix} \,, \qquad \text{and} \qquad \Omega' = \begin{pmatrix} \tau' & m' \\ m' & \rho'/12 \end{pmatrix} \,, \tag{4.39}$$

which are related to each other by

$$\Omega' = (A\Omega + B) \cdot (C\Omega + D)^{-1} \,, \tag{4.40}$$

with the matrices

$$A = \begin{pmatrix} 4 & -3 \\ 1 & -1 \end{pmatrix} \,, \qquad B = \begin{pmatrix} 0 & 0 \\ 0 & 0 \end{pmatrix} \,, \qquad C = \begin{pmatrix} 0 & 0 \\ 0 & 0 \end{pmatrix} \,, \qquad D = \begin{pmatrix} 1 & 1 \\ -3 & -4 \end{pmatrix} \,, \tag{4.41}$$

which satisfy indeed the relations (2.21). This shows that (ρ, τ, m) and (ρ', τ', m') are related through an $\mathrm{Sp}(2, \mathbb{Z})$ transformation. Therefore, $\mathcal{Z}_{X_{1,1}}$ is indeed invariant under the change of parameters implied by the above chain of dualities.

4.5 Relation between $(N, M) = (4, 6)$ and $(12, 2)$

Our final example is the relation between the web diagrams $(N, M) = (4, 6)$ and $(12, 2)$. Notice that in this case the gcd is $\gcd(4, 6) = 2$ and it is therefore dualised to the web $(12, 2)$.

4.5.1 Duality transformation

A parametrisation of the web $(N, M) = (4, 6)$ is given in figure 27. Out of the 72 parameters in the diagram, only 26 are independent on account of the consistency conditions. By cutting and re-gluing the diagram in figure 27, we can bring it into a form which is very similar to the web $(N, M) = (12, 2)$, except that the lines at the top of the diagram are glued to the lines at the bottom in a twisted fashion (see figure 28). Next we perform a flop transition on the curves labelled by parameters v_i, which is carried out in both 'layers', as shown in the figure 29. The new parameters h'_i can be determined using figure 6 and are given by

$$
\begin{aligned}
h'_1 &= h_1 + v_2 + v_7 \,, & h'_9 &= h_9 + v_{10} + v_{15} \,, & h'_{17} &= h_{17} + v_{18} + v_{23} \,, \\
h'_2 &= h_2 + v_3 + v_8 \,, & h'_{10} &= h_{10} + v_{11} + v_{16} \,, & h'_{18} &= h_{18} + v_{13} + v_{24} \,, \\
h'_3 &= h_3 + v_4 + v_9 \,, & h'_{11} &= h_{11} + v_{12} + v_{17} \,, & h'_{19} &= h_{19} + v_1 + v_{20} \,, \\
h'_4 &= h_4 + v_5 + v_{10} \,, & h'_{12} &= h_{12} + v_7 + v_{18} \,, & h'_{20} &= h_{20} + v_{21} + v_2 \,, \\
h'_5 &= h_5 + v_6 + v_{11} \,, & h'_{13} &= h_{13} + v_{14} + v_{19} \,, & h'_{21} &= h_{21} + v_{22} + v_3 \,, \\
h'_6 &= h_6 + v_1 + v_{12} \,, & h'_{14} &= h_{14} + v_{15} + v_{20} \,, & h'_{22} &= h_{22} + v_{23} + v_4 \,, \\
h'_7 &= h_7 + v_8 + v_{13} \,, & h'_{15} &= h_{15} + v_{16} + v_{21} \,, & h'_{23} &= h_{23} + v_{24} + v_5 \,, \\
h'_8 &= h_8 + v_9 + v_{14} \,, & h'_{16} &= h_{16} + v_{17} + v_{22} \,, & h'_{24} &= h_{24} + v_6 + v_{19} \,.
\end{aligned} \tag{4.42}
$$

along with the parameters m'_i

$$
\begin{aligned}
m'_1 &= m_1 + v_1 + v_2 \,, & m'_2 &= m_2 + v_3 + v_2 \,, & m'_3 &= m_3 + v_3 + v_4 \,, \\
m'_4 &= m_4 + v_5 + v_4 \,, & m'_5 &= m_5 + v_5 + v_4 \,, & m'_6 &= m_6 + v_1 + v_6 \,, \\
m'_7 &= m_7 + v_8 + v_7 \,, & m'_8 &= m_8 + v_8 + v_9 \,, & m'_9 &= m_9 + v_{10} + v_9 \,, \\
m'_{10} &= m_{10} + v_{10} + v_{11} \,, & m'_{11} &= m_{11} + v_{12} + v_{11} \,, & m'_{12} &= m_{12} + v_{12} + v_7 \,, \\
m'_{13} &= m_{13} + v_{13} + v_{14} \,, & m'_{14} &= m_{14} + v_{15} + v_{14} \,, & m'_{15} &= m_{15} + v_{15} + v_{16} \,, \\
m'_{16} &= m_{16} + v_{17} + v_{16} \,, & m'_{17} &= m_{17} + v_{17} + v_{18} \,, & m'_{18} &= m_{18} + v_{13} + v_{18} \,, \\
m'_{19} &= m_{19} + v_{20} + v_{19} \,, & m'_{20} &= m_{20} + v_{20} + v_{21} \,, & m'_{21} &= m_{21} + v_{22} + v_{21} \,, \\
m'_{22} &= m_{22} + v_{22} + v_{23} \,, & m'_{23} &= m_{23} + v_{24} + v_{23} \,, & m'_{24} &= m_{24} + v_{24} + v_{19} \,.
\end{aligned} \tag{4.43}
$$

Now carrying out the flop transition on the curves labelled by h'_i in the web shown in figure 29 gives the web shown in figure 30 which is the standard untwisted $(12, 2)$ web.
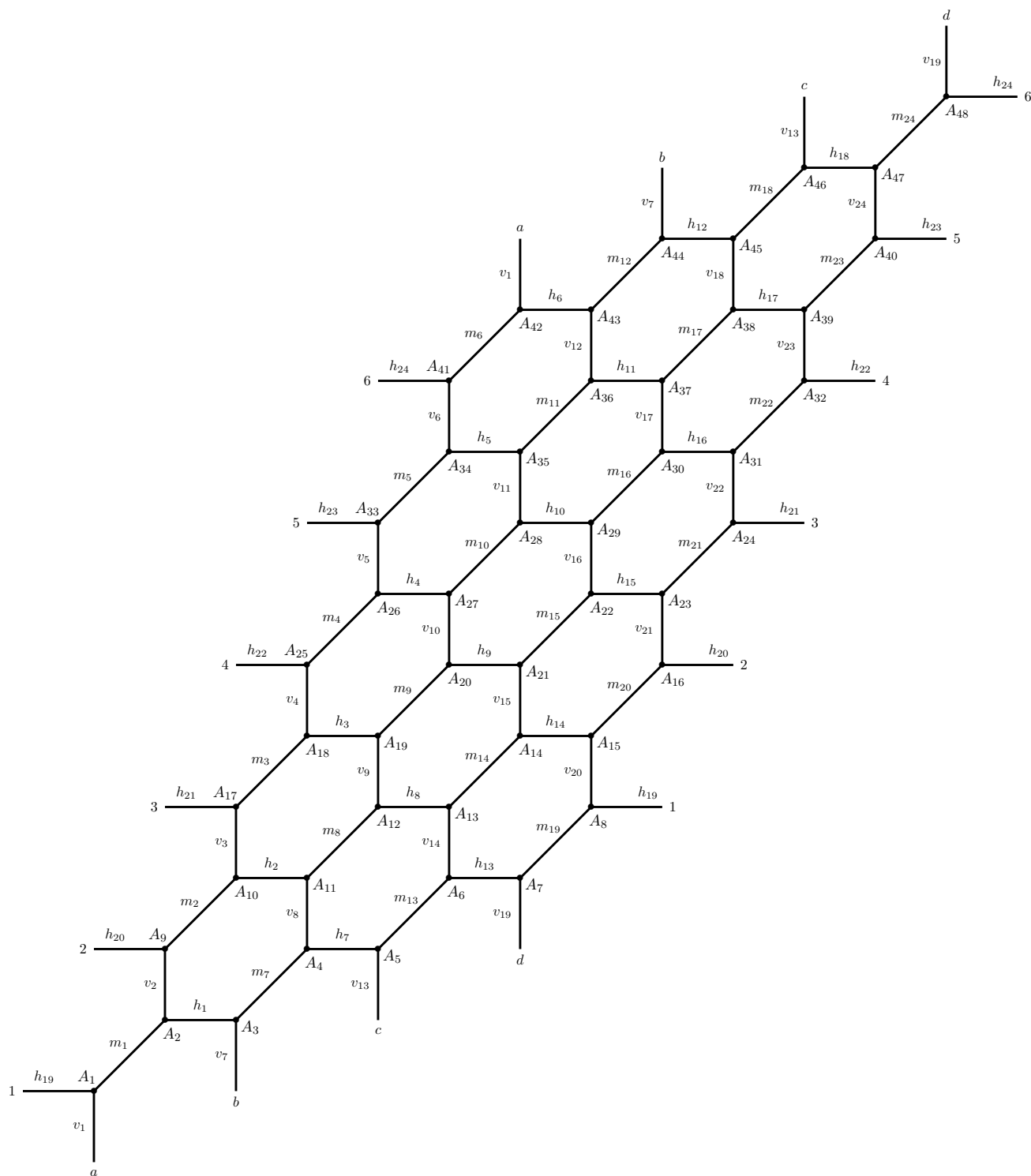
Figure 27. Parametrisation of the web $(N, M) = (4, 6)$ along with an assignment of vertices.
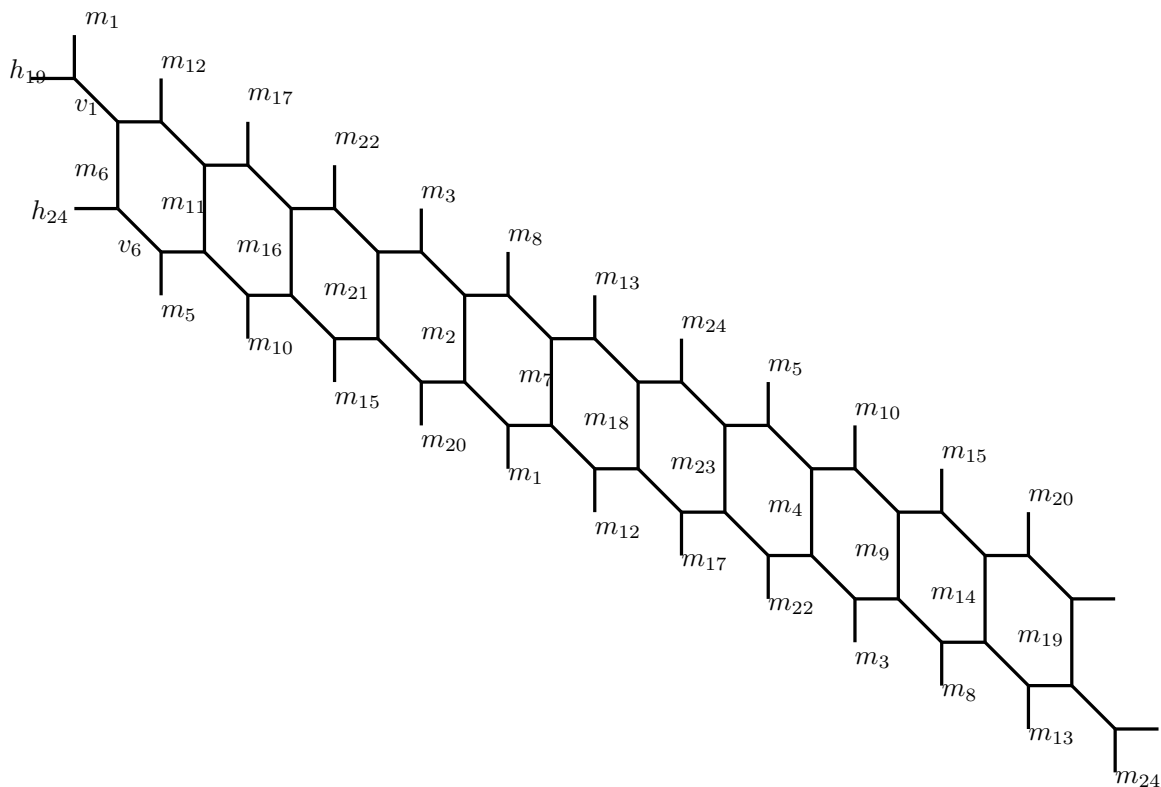
Figure 28. Twisted $(N, M) = (12, 2)$ web which is obtained from figure 27 by cutting and re-gluing different lines.
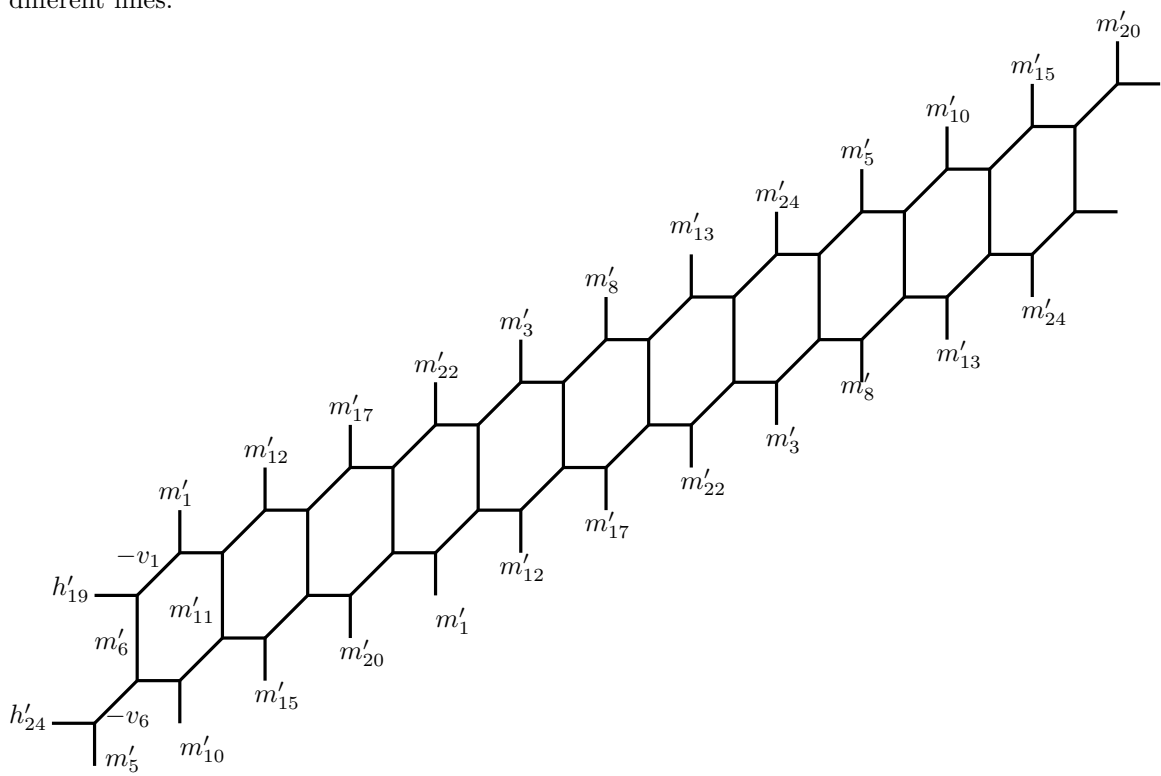

Figure 29. The twisted $(N, M) = (12, 2)$ web of figure 28 after flop transitions along the curves v_i.
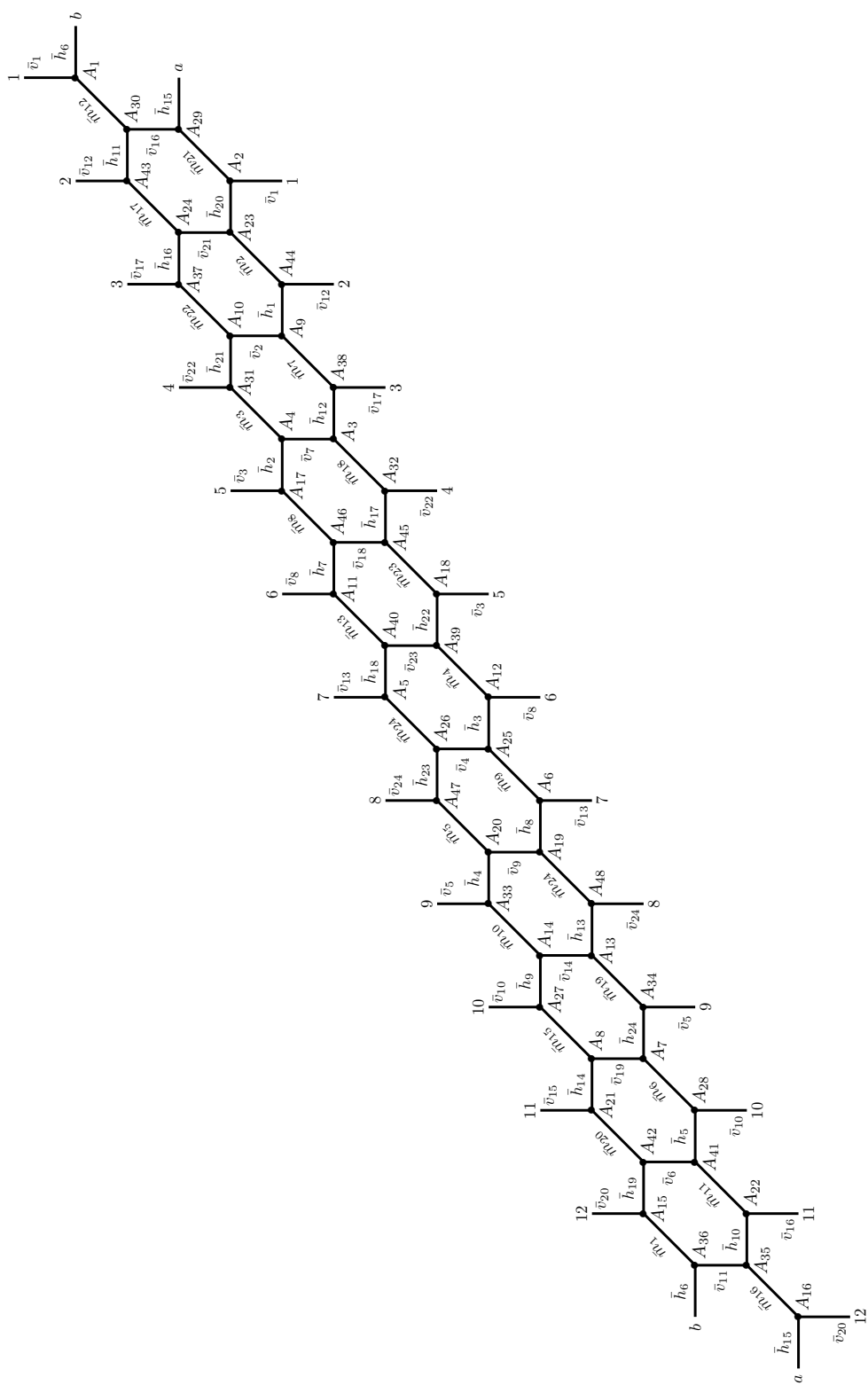
Figure 30. Parametrisation of the web $(N, M) = (12, 2)$ web along with an assignment of vertices.

The parameters $\overline{v}_i$ in terms of the parameters of the original $(4,6)$ web are given by

$$\overline{v}_1 = m'_1 + h'_6 + h'_{20}, \qquad \overline{v}_2 = m'_2 + h'_1 + h'_{21}, \qquad \overline{v}_3 = m'_3 + h'_2 + h'_{22},$$
$$\overline{v}_4 = m'_4 + h'_3 + h'_{23}, \qquad \overline{v}_5 = m'_5 + h'_4 + h'_{24}, \qquad \overline{v}_6 = m'_6 + h'_5 + h'_{19},$$
$$\overline{v}_7 = m'_7 + h'_{12} + h'_2, \qquad \overline{v}_8 = m'_8 + h'_7 + h'_3, \qquad \overline{v}_9 = m'_9 + h'_8 + h'_4,$$
$$\overline{v}_{10} = m'_{10} + h'_9 + h'_5, \qquad \overline{v}_{11} = m'_{11} + h'_{10} + h'_6, \qquad \overline{v}_{12} = m'_{12} + h'_{11} + h'_1,$$
$$\overline{v}_{13} = m'_{13} + h'_{18} + h'_8, \qquad \overline{v}_{14} = m'_{14} + h'_{13} + h'_9, \qquad \overline{v}_{15} = m'_{15} + h'_{14} + h'_{10},$$
$$\overline{v}_{16} = m'_{16} + h'_{15} + h'_{11}, \qquad \overline{v}_{17} = m'_{17} + h'_6 + h'_{20}, \qquad \overline{v}_{18} = m'_{18} + h'_{17} + h'_7,$$
$$\overline{v}_{19} = m'_{19} + h'_{14} + h'_{24}, \qquad \overline{v}_{20} = m'_{20} + h'_{19} + h'_{15}, \qquad \overline{v}_{21} = m'_{21} + h'_{16} + h'_{20},$$
$$\overline{v}_{22} = m'_{22} + h'_{21} + h'_{17}, \qquad \overline{v}'_{23} = m'_{23} + h'_{22} + h'_{18}, \qquad \overline{v}_{24} = m'_{24} + h'_{23} + h'_{13}, \qquad (4.44)$$

while the parameters $\overline{m}_i$ are

$$\overline{m}_1 = -v_1 + h'_{19} + h'_6, \qquad \overline{m}_2 = -v_2 + h'_{20} + h'_1, \qquad \overline{m}_3 = -v_3 + h'_{21} + h'_2,$$
$$\overline{m}_4 = -v_4 + h'_{22} + h'_3, \qquad \overline{m}_5 = -v_5 + h'_{23} + h'_4, \qquad \overline{m}_6 = -v_6 + h'_{26} + h'_5,$$
$$\overline{m}_7 = -v_7 + h'_1 + h'_{12}, \qquad \overline{m}_8 = -v_8 + h'_2 + h'_7, \qquad \overline{m}_9 = -v_9 + h'_3 + h'_8,$$
$$\overline{m}_{10} = -v_{10} + h'_4 + h'_9, \qquad \overline{m}_{11} = -v_{11} + h'_5 + h'_{10}, \qquad \overline{m}_{12} = -v_{12} + h'_6 + h'_{11},$$
$$\overline{m}_{13} = -v_{13} + h'_7 + h'_{18}, \qquad \overline{m}_{14} = -v_{14} + h'_8 + h'_{13}, \qquad \overline{m}_{15} = -v_{15} + h'_9 + h'_{14},$$
$$\overline{m}_{16} = -v_{16} + h'_{10} + h'_{15}, \qquad \overline{m}_{17} = -v_{17} + h'_{11} + h'_{16}, \qquad \overline{m}_{18} = -v_{18} + h'_{12} + h'_{17},$$
$$\overline{m}_{19} = -v_{19} + h'_{13} + h'_{26}, \qquad \overline{m}_{20} = -v_{20} + h'_{14} + h'_{19}, \qquad \overline{m}_{21} = -v_{21} + h'_{15} + h'_{20},$$
$$\overline{m}_{22} = -v_{22} + h'_{16} + h'_{21}, \qquad \overline{m}_{23} = -v_{23} + h'_{17} + h'_{22}, \qquad \overline{m}_{24} = -v_{24} + h'_{18} + h'_{23}, \qquad (4.45)$$

and the parameters $\overline{h}_i$ are

$$\overline{h}_1 = -(h_1 + v_2 + v_7), \qquad \overline{h}_2 = -(h_2 + v_3 + v_8), \qquad \overline{h}_3 = -(h_3 + v_4 + v_9),$$
$$\overline{h}_4 = -(h_4 + v_5 + v_{10}), \qquad \overline{h}_5 = -(h_5 + v_6 + v_{11}), \qquad \overline{h}_6 = -(h_6 + v_1 + v_{12}),$$
$$\overline{h}_7 = -(h_7 + v_8 + v_{13}), \qquad \overline{h}_8 = -(h_8 + v_9 + v_{14}), \qquad \overline{h}_9 = -(h_9 + v_{10} + v_{15}),$$
$$\overline{h}_{10} = -(h_{10} + v_{11} + v_{16}), \qquad \overline{h}_{11} = -(h_{11} + v_{12} + v_{17}), \qquad \overline{h}_{12} = -(h_{12} + v_7 + v_{18}),$$
$$\overline{h}_{13} = -(h_{13} + v_{14} + v_{19}), \qquad \overline{h}_{14} = -(h_{14} + v_{15} + v_{20}), \qquad \overline{h}_{15} = -(h_{15} + v_{16} + v_{21}),$$
$$\overline{h}_{16} = -(h_{16} + v_{17} + v_{22}), \qquad \overline{h}_{17} = -(h_{17} + v_{18} + v_{23}), \qquad \overline{h}_{18} = -(h_{18} + v_{13} + v_{24}),$$
$$\overline{h}_{19} = -(h_{19} + v_1 + v_{20}), \qquad \overline{h}_{20} = -(h_{20} + v_{21} + v_2), \qquad \overline{h}_{21} = -(h_{21} + v_{22} + v_3),$$
$$\overline{h}_{22} = -(h_{22} + v_{23} + v_4), \qquad \overline{h}_{23} = -(h_{23} + v_{24} + v_5), \qquad \overline{h}_{24} = -(h_{24} + v_6 + v_{19}). \qquad (4.46)$$

As in the previous cases, using the assignment of vertices in figure 27 and figure 30 the parameters $\overline{h}$ and $\overline{m}$ can be directly read off. Furthermore, the transformation above shows that the web diagrams $(N, M) = (4, 6)$ and $(12, 2)$ are indeed dual to each other.

4.5.2 Simple check of duality

In order to perform a check of the duality worked out above, we consider $(m_i, h_i, v_i) = (m, h, v)$ such that

$$\tau = 6(v + m) \implies v = \frac{\tau}{6} - m \tag{4.47}$$

$$\rho = 4(h + m) \implies h = \frac{\rho}{4} - m$$

In the $(12, 2)$ web the parameters (ρ', τ', m') are given by

$$\tau' = 2(\overline{v} + \overline{m}), \qquad \text{with} \qquad \rho' = 12(\overline{h} + \overline{m}), \tag{4.48}$$

with

$$\overline{v} = m + 2h + 6v, \qquad \text{and} \qquad \overline{h} = -(h + 2v), \qquad \text{and} \qquad \overline{m} = 2h + 3v. \tag{4.49}$$

This gives the following map between (τ, ρ, m) and (τ', ρ', m'):

$$\tau' = 3\tau + 2\rho - 24m, \qquad \rho' = 3\rho + 2\tau - 24m, \qquad m' = \frac{\tau}{2} + \frac{\rho}{2} - 5m. \tag{4.50}$$

Next, we also introduce the period matrices

$$\Omega = \begin{pmatrix} \tau/6 & m \\ m & \rho/4 \end{pmatrix}, \qquad \text{and} \qquad \Omega' = \begin{pmatrix} \tau'/2 & m' \\ m' & \rho'/12 \end{pmatrix}, \tag{4.51}$$

which are related to each other by

$$\Omega' = (A\Omega + B) \cdot (C\Omega + D)^{-1}, \tag{4.52}$$

with the matrices

$$A = \begin{pmatrix} 3 & -2 \\ 1 & -1 \end{pmatrix}, \qquad B = \begin{pmatrix} 0 & 0 \\ 0 & 0 \end{pmatrix}, \qquad C = \begin{pmatrix} 0 & 0 \\ 0 & 0 \end{pmatrix}, \qquad D = \begin{pmatrix} 1 & 1 \\ -2 & -3 \end{pmatrix}, \tag{4.53}$$

which satisfy indeed the relations (2.21). This shows that (ρ, τ, m) and (ρ', τ', m') are related through an $\mathrm{Sp}(2, \mathbb{Z})$ transformation. Therefore, $\mathcal{Z}_{X_{1,1}}$ is indeed invariant under the change of parameters implied by the above chain of dualities.

5 Map for arbitrary (N, M)

In the previous section, we have discussed a number of examples of how to transform a web (N, M) into a web $(\frac{MN}{k}, k)$, where $k = \gcd(M, N)$. While we have argued that such a transformation always exists, this does not fix the parameters of the new toric diagram $(\frac{MN}{k}, k)$ in terms of the parameters of the original one. However, based on the examples discussed before, we explain in this section that there exists a clear pattern, which we conjecture to hold for generic (N, M). In the following, without loss of generality, we assume that $M > N$.[13]

---

[13]In case $N > M$, a similar procedure applies, except that all v_i are replaced by h_i and vice versa.

5.1 Parameter map

The key in reconstructing the parameters $(\bar{h}_i, \bar{v}_i, \bar{m}_i)$ (for $i = 1, \ldots, MN$) of the web $(\frac{MN}{k}, k)$ in terms of the parameters (h_i, v_i, m_i) of the original web (N, M) is to find a matching between the vertices of the two webs. In this section, starting from a labelling $(A_1, A_2, \ldots, A_{2MN})$ of the vertices of the web (N, M) we construct a labelling of the vertices in the web $(\frac{MN}{k}, k)$, in other words, we explain how the vertices are mapped into each other. Furthermore, we provide a rule for the area for the curve connecting any two vertices in the web $(\frac{MN}{k}, k)$ in terms of the parameters of the original web.

5.1.1 Notation: vertices and paths

Before we describe the mapping of the parameters between the webs (N, M) and $(\frac{MN}{k}, k)$, we need to introduce some notation. We start from a labelling of the vertices of the web (N, M). There are two types of the former, depending on the orientation of the external leg along the direction $(1, 1)$, i.e.
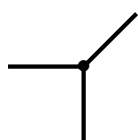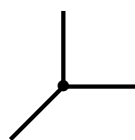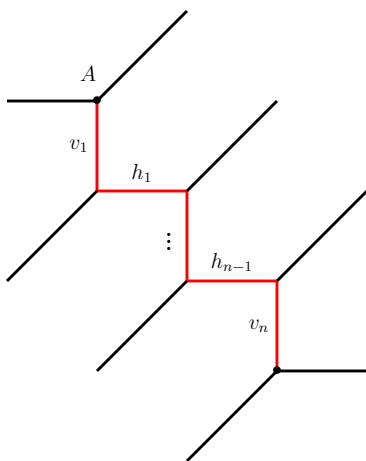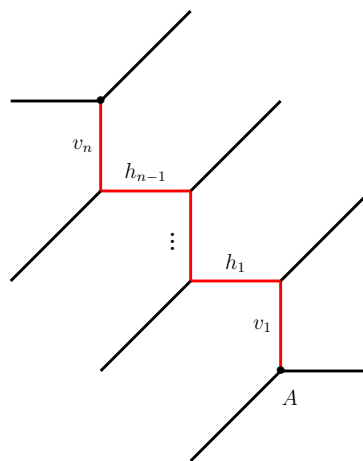

vertex of type 1   vertex of type 2

Furthermore, for $n \in \mathbb{N}$ we can define for each vertex A the path $\mathcal{P}(A, n)$ that starts at A and follows n vertical and $n - 1$ horizontal lines

path $\mathcal{P}(A, n)$ for a vertex of type 1   path $\mathcal{P}(A, n)$ for a vertex of type 2

Notice that $\mathcal{P}(A, n)$ connects a vertex of type 1 with a vertex of type 2 or vice versa. Finally, we call $\mathfrak{p}(A, n)$ the (ordered) $(2n - 1)$-tuple of parameters of the lines that form the path $\mathcal{P}(A, n)$, i.e. specifically with regards to the figures above

$$\mathfrak{p}(A, n) = (v_1, h_1, v_2, h_2, \ldots, h_{n-1}, v_n) \,. \tag{5.1}$$

5.1.2 Vertex mapping

As we have mentioned above, from a generic labelling of the (N, M) web, we conjecture that it is possible to directly reconstruct the labelling of the $(\frac{MN}{k}, k)$ web. The procedure we propose starts from any vertex of type 1 in the (N, M) web which we call A_1.[14] To find (one of) the neighbour(s) of this vertex in the $(\frac{MN}{k}, k)$ web, we follow $\mathcal{P}(A_1, \frac{M}{k})$, i.e. a path with $\frac{M}{k}$ vertical lines and $\frac{M}{k} - 1$ horizontal lines, that leads to a vertex of type 2 in the (N, M) web:
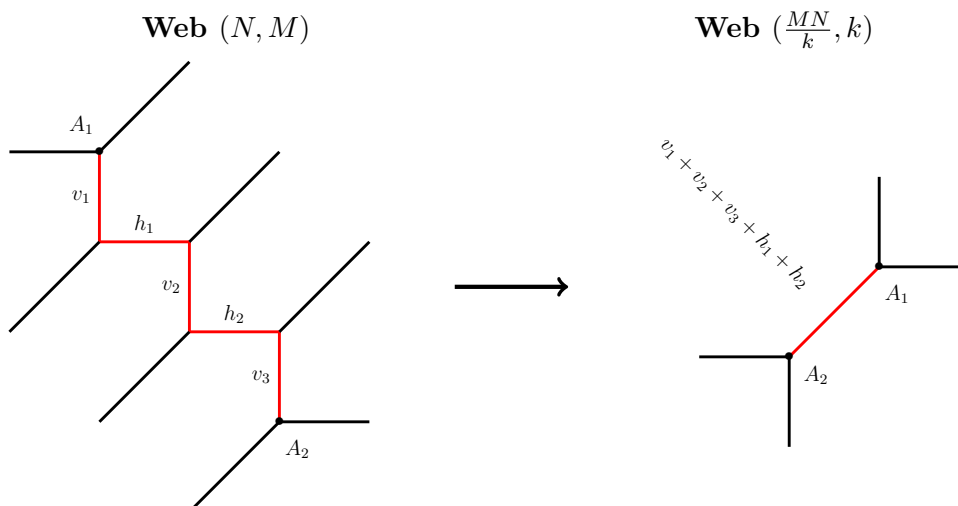
We conjecture that the parameter connecting the two vertices in the $(\frac{MN}{k}, k)$ web is the sum of all v_i's and h_i's we have followed,

$$\bar{m}_1 = \sum_{i=1}^{\frac{2M}{k}-1} \left(\mathfrak{p}(A_1, \tfrac{M}{k}) \right)_i . \tag{5.2}$$

From A_2, we follow $\mathcal{P}(A_2, \frac{M}{k} - 1)$, i.e. a path with $\frac{M}{k} - 1$ vertical lines and $\frac{M}{k} - 2$ horizontal lines, to a vertex of type 1 (which is different from A_1)

---
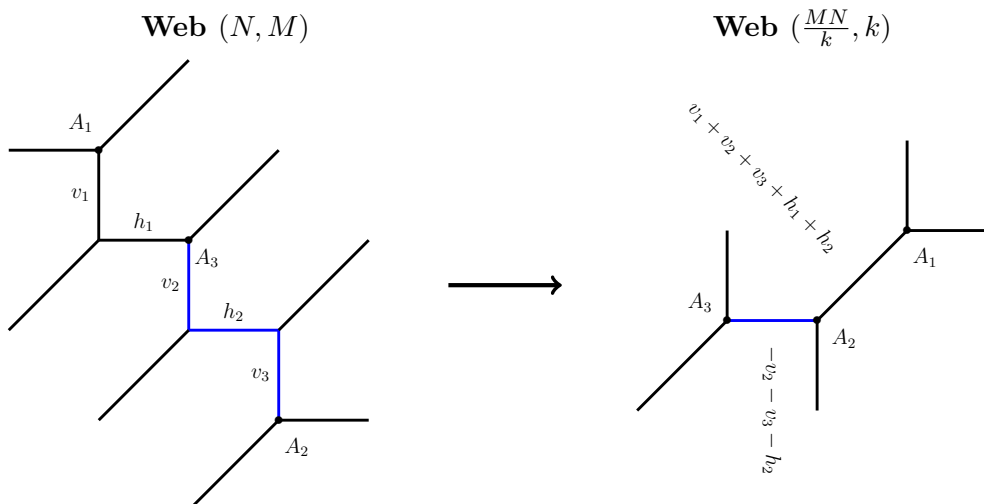
[14]As a possible source of confusion, we point out that vertices of type 1 in the web (N, M) will be mapped to vertices of type 2 in the web $(\frac{MN}{k}, k)$ and vice versa. Thus A_1 is of type 1 in the (N, M) web, but will be of type 2 in the $(\frac{MN}{k}, k)$ web.

The parameter connecting A_2 and A_3 in the web $(\frac{MN}{k}, k)$ show up as the negative sum of all v_i's and h_i's that we have followed, i.e.

$$\bar{h}_1 = - \sum_{i=1}^{\frac{2M}{k}-3} \left(\mathfrak{p}(A_2, \tfrac{M}{k}-1) \right)_i \tag{5.3}$$

Continuing from A_3 along $\mathcal{P}(A_3, \frac{M}{k})$, i.e. a path with $\frac{M}{k}$ vertical lines and $\frac{M}{k} - 1$ horizontal lines, we arrive at a new vertex A_4 of type 2. This procedure can be continued for $\frac{2MN}{k}$ steps passing through the vertices $A_1, A_2, \ldots, A_{\frac{2MN}{k}}$ in the (N, M) web. After this, we return to our original starting point, since at each step of the construction the vertex reached by the path
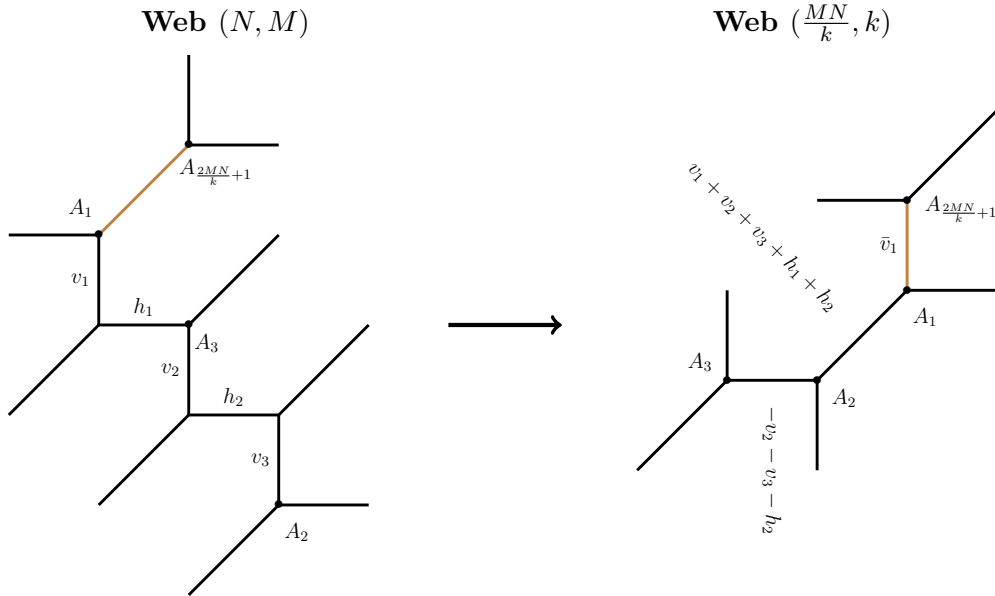
$$\mathcal{P}\left(A_1, \frac{M}{k}\right) \cup \mathcal{P}\left(A_2, \frac{M}{k}-1\right) \cup \mathcal{P}\left(A_3, \frac{M}{k}\right) \cup \mathcal{P}\left(A_4, \frac{M}{k}-1\right) \cup \ldots$$
$$\ldots \cup \mathcal{P}\left(A_{\frac{2MN}{k}-1}, \frac{M}{k}\right) \cup \mathcal{P}\left(A_{\frac{2MN}{k}}, \frac{M}{k}-1\right), \tag{5.4}$$

is A_1 itself. We therefore have constructed the first 'layer' of the $(\frac{MN}{k}, k)$ web, which at this point looks like
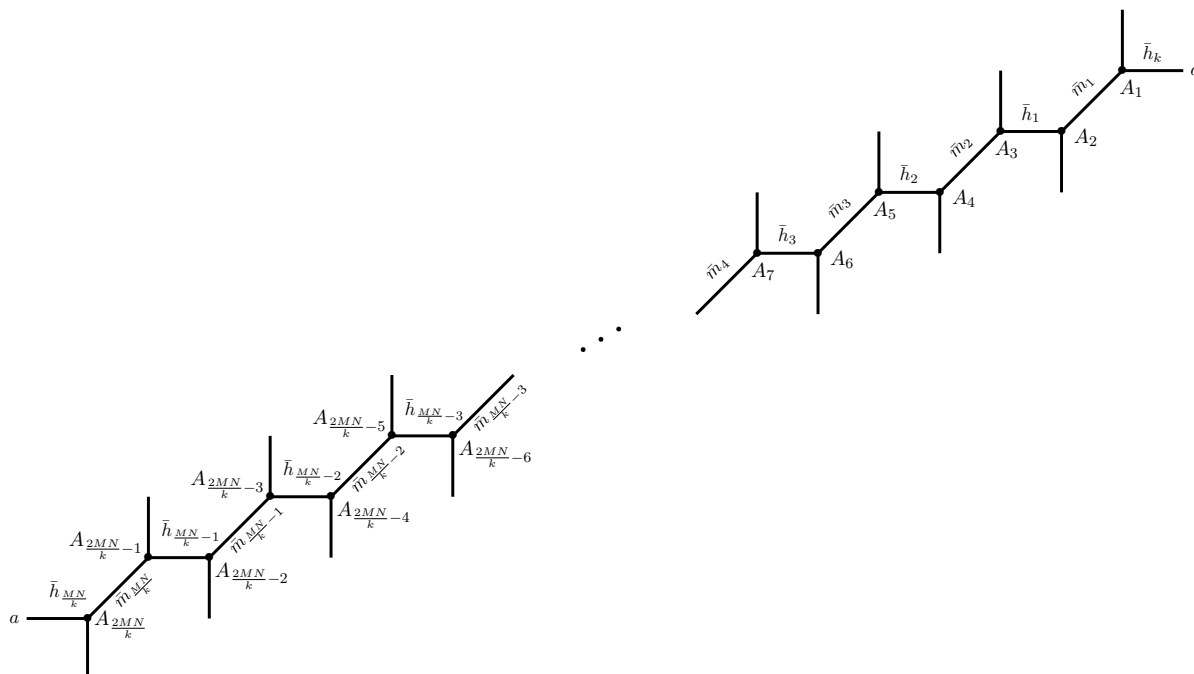
This web configuration is the counterpart of the diagonal path in figure 9. In order to find the remaining vertices, we return to (the type 1 vertex) A_1 in the (N, M) web and follow

the diagonal line

Web (N, M) **Web** $(\frac{MN}{k}, k)$

to arrive at the next vertex $A_{\frac{2MN}{k}+1}$ in the (N, M) web which is of type 2.[15] The parameter $\bar{v}_1$ is somewhat more involved to read off from the original (N, M) web. Indeed, calling the curve connecting A_1 and $A_{\frac{MN}{k}+1}$ in the (N, M) web $\mathcal{M}\left(A_1, A_{\frac{2MN}{k}+1}\right)$ (with parameter m), we consider the path

$$\mathcal{P}\left(A_1, \frac{M}{k} - 1\right) \cup \mathcal{M}\left(A_1, A_{\frac{2MN}{k}+1}\right) \cup \mathcal{P}\left(A_{\frac{2MN}{k}+1}, \frac{M}{k} - 1\right), \tag{5.5}$$

i.e. from the two vertices A_1 and $A_{\frac{2MN}{k}+1}$ we consider a curve that follows $\frac{M}{k} - 1$ vertical and $\frac{M}{k} - 2$ horizontal lines upwards and downwards. For illustrative purposes, we consider

---

[15]Notice, if $k = 1$, this vertex is in fact A_2 and the mapping of vertices is already complete. If $k > 1$, the vertex $A_{\frac{2MN}{k}+1}$ is different from the ones already encountered, i.e. $A_1, \ldots, A_{\frac{2MN}{k}}$.

the simple example $\frac{M}{k} = 4$ for which the total path is given in the following picture

$$(5.6)$$
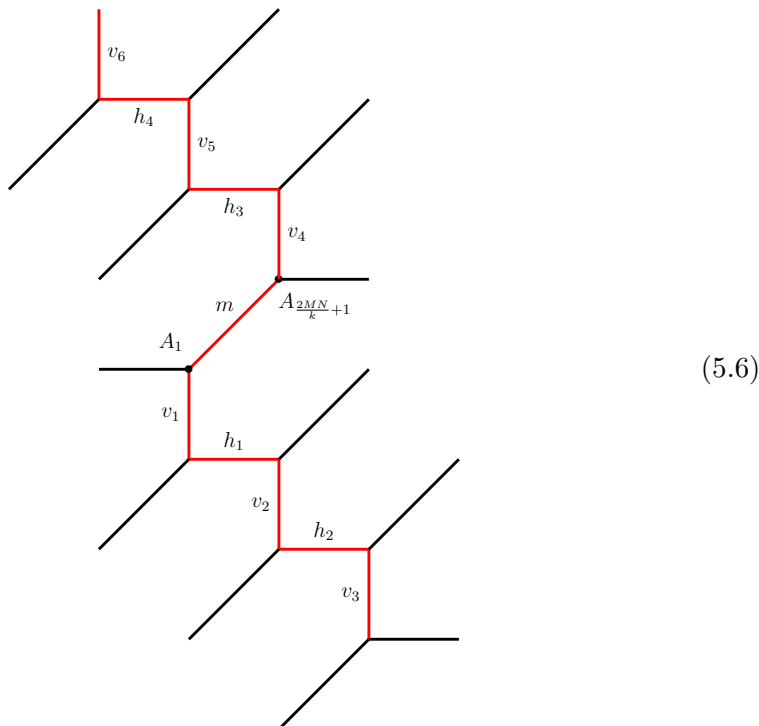
We then conjecture that the parameter $\bar{v}_1$ is given by the sum over all the parameters along this path, however, with factors that decrease the further we get away from the vertices A_1 and $A_{\frac{2MN}{k}+1}$:

$$
\begin{aligned}
\bar{v}_1 = m &+ \left(\frac{M}{k} - 1\right)\left[\left(\mathfrak{p}(A_1, \tfrac{M}{k} - 1)\right)_1 + \left(\mathfrak{p}(A_{\frac{2MN}{k}+1}, \tfrac{M}{k} - 1)\right)_1\right] \\
&+ \sum_{i=1}^{\frac{M}{k}-2}\left(\frac{M}{k} - 1 - i\right)\left[\left(\mathfrak{p}(A_1, \tfrac{M}{k} - 1)\right)_{2i} + \left(\mathfrak{p}(A_{\frac{2MN}{k}+1}, \tfrac{M}{k} - 1)\right)_{2i}\right] \\
&+ \sum_{i=1}^{\frac{M}{k}-2}\left(\frac{M}{k} - 1 - i\right)\left[\left(\mathfrak{p}(A_1, \tfrac{M}{k} - 1)\right)_{2i+1} + \left(\mathfrak{p}(A_{\frac{2MN}{k}+1}, \tfrac{M}{k} - 1)\right)_{2i+1}\right], \quad (5.7)
\end{aligned}
$$

e.g. for the case displayed in the diagram in eq. (5.6)

$$
\bar{v}_1 = m + (4 - 1)\left(v_1 + v_4\right) + (4 - 2)\left(h_1 + v_2 + h_3 + v_5\right) + (4 - 3)\left(h_2 + v_3 + h_4 + v_6\right). \tag{5.8}
$$

From the last vertex $A_{\frac{2MN}{k}+1}$, we can repeat all the previous steps to construct further vertices that make up the second 'layer' of the web $(\frac{MN}{k}, k)$. Indeed, following

$\mathcal{P}(A_{\frac{2MN}{k}+1}, \frac{M}{k}-1)$ we arrive at the next vertex $A_{\frac{2MN}{k}+2}$, which is[16]

Web (N,M) **Web** $(\frac{MN}{k}, k)$
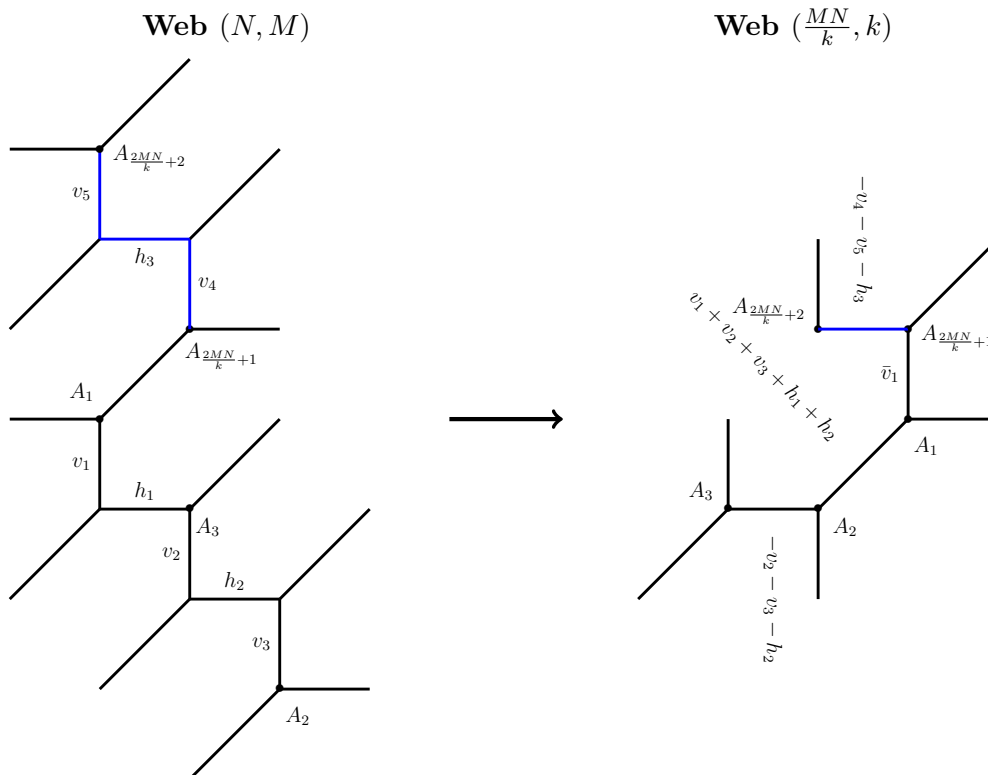
From here on, we can continue to map out the full $(\frac{MN}{k}, k)$ web: after a total of $2MN$ steps, this procedure is guaranteed to map all vertices of the (N,M) web to the $(\frac{MN}{k}, k)$ web. Moreover, while we have no general proof, the values for $(\bar{v}_i, \bar{h}_i, \bar{m}_i)$ we obtain in this manner are compatible with all the examples we have discussed so far.

5.2 $Sp(2, \mathbb{Z})$ transformation

Based on the expressions for $(\bar{v}_i, \bar{h}_i, \bar{m}_i)$ obtained in the previous subsection, we can check whether they correspond to an $Sp(2, \mathbb{Z})$ transformation for the partition function $\mathcal{Z}_{X_{1,1}}$, in the same manner as we did for all the examples in section 4. To this end, we set

$$v_i = v\,, \qquad h_i = h\,, \qquad m_i = m\,, \qquad \forall i = 1, \dots, MN\,, \qquad (5.9)$$

and hence identify all vertical, horizontal and diagonal parameters in the original (N,M) web. This leads to

$$\bar{v}_i = \bar{v}\,, \qquad \bar{h}_i = \bar{h}\,, \qquad \bar{m}_i = \bar{m}\,, \qquad \forall i = 1, \dots, MN\,, \qquad (5.10)$$

---

[16]For $k > 1$ the vertex $A_{\frac{2MN}{k}+1}$ is different from the vertices $A_1, \dots, A_{\frac{2MN}{k}}$ that we have previously constructed.

with

$$\bar{v} = m + 2\left[\sum_{n=1}^{\frac{M}{k}-1}\left(\frac{M}{k}-n\right)\right]v + 2\left[\sum_{n=1}^{\frac{M}{k}-2}\left(\frac{M}{k}-1-n\right)\right]h$$

$$= m + 2\left[\left(\frac{M}{k}\right)^2 - \frac{1}{2}\frac{M}{k}\left(\frac{M}{k}+1\right)\right]v + 2\left[\left(\frac{M}{k}-1\right)^2 - \frac{1}{2}\frac{M}{k}\left(\frac{M}{k}-1\right)\right]h$$

$$= m + \frac{M(M-k)}{k^2}v + \left(2 + \frac{M(M-3k)}{k^2}\right)h\,, \tag{5.11}$$

as well as

$$\bar{h} = -\left(\frac{M}{k}-1\right)v - \left(\frac{M}{k}-2\right)h\,, \qquad \text{and} \qquad \bar{m} = \frac{M}{k}v + \left(\frac{M}{k}-1\right)h\,. \tag{5.12}$$

Furthermore, we introduce

$$\rho = N(h+m)\,, \qquad \text{and} \qquad \tau = M(v+m)\,, \tag{5.13}$$

along with

$$\rho' = \frac{MN}{k}(\bar{h}+\bar{m}) = \frac{MN}{k}(h+v) = \frac{N}{k}\tau + \frac{M}{k}\rho - \frac{2MN}{k}m\,,$$

$$\tau' = k(\bar{v}+\bar{m}) = \frac{1}{k}\left[k^2 m + (M-k)^2 h + M^2 v\right] = \frac{M}{k}\tau + \frac{(M-k)^2}{Nk}\rho - \frac{2M(M-k)}{k}m\,,$$

$$m' = \bar{m} = \frac{\tau}{k} + \frac{1}{N}\left(\frac{M}{k}-1\right)\rho + \left(1 - \frac{2M}{k}\right)m\,. \tag{5.14}$$

With these parameters, we define the period matrices for the $(1,1)$ web

$$\Omega = \begin{pmatrix} \tau/M & m \\ m & \rho/N \end{pmatrix}\,, \qquad \text{and} \qquad \Omega' = \begin{pmatrix} \tau'/k & m' \\ m' & \rho'/\left(\frac{MN}{k}\right) \end{pmatrix}\,, \tag{5.15}$$

which have identical determinants

$$\det\Omega = \frac{\rho\tau}{MN} - m^2 = \det\Omega'\,. \tag{5.16}$$

In fact, Ω and Ω' are related by an $\mathrm{Sp}(2,\mathbb{Z})$ transformation in the following manner

$$\Omega' = (A\Omega + B)\cdot(C\Omega + D)^{-1}\,, \tag{5.17}$$

with

$$A = \begin{pmatrix} \frac{M}{k} & -\frac{M-k}{k} \\ 1 & -1 \end{pmatrix}\,, \quad B = \begin{pmatrix} 0 & 0 \\ 0 & 0 \end{pmatrix}\,, \quad C = \begin{pmatrix} 0 & 0 \\ 0 & 0 \end{pmatrix}\,, \quad D = \begin{pmatrix} 1 & 1 \\ -\frac{M-k}{k} & -\frac{M}{k} \end{pmatrix}\,, \tag{5.18}$$

which satisfy as well the relations eq. (2.21). This shows that (ρ,τ,m) and (ρ',τ',m') are related through an $\mathrm{Sp}(2,\mathbb{Z})$ transformation. Therefore, $\mathcal{Z}_{X_{M,N}}$ at this special locus is indeed invariant under the change of parameters implied by the above chain of dualities.

5.3 Extended moduli space of Calabi-Yau threefold

In the previous sections, we have compiled evidence that the web diagrams (N, M) and $(\frac{NM}{k}, k)$ with $k = \gcd(M, N)$ are dual to each other. This relation, however, also implies dualities between two different webs (N, M) and (N', M') with $MN = M'N'$ and $\gcd(M, N) = k = \gcd(M', N')$. We can give a characterisation of all such webs in the following manner: let $M, N \in \mathbb{N}$ with the following prime number decomposition

$$M = \left(\prod_{a=1}^{r} c_a^{h_a}\right) \left(\prod_{b=1}^{s} m_a^{p_a}\right), \qquad \text{and} \qquad N = \left(\prod_{a=1}^{r} c_a^{h_a}\right) \left(\prod_{b=1}^{t} n_a^{q_a}\right), \qquad (5.19)$$

with $r, s, t \geq 0$ and c_a, m_a and n_a prime numbers with multiplicities h_a, p_a and q_a, respectively. Furthermore, $m_a \neq n_b$ for $a = 1, \ldots, s$ and $b = 1, \ldots, t$ such that

$$k = \gcd(M, N) = \prod_{a=1}^{r} c_a^{h_a}. \qquad (5.20)$$

Finally, we define the disjoint sets

$$\mathcal{M} \subset \{m_1^{p_1}, m_2^{p_2}, \ldots, m_s^{p_s}, n_1^{q_1}, n_2^{q_2}, \ldots, n_t^{q_t}\}, \quad \mathcal{N} \subset \{m_1^{p_1}, m_2^{p_2}, \ldots, m_s^{p_s}, n_1^{q_1}, n_2^{q_2}, \ldots, n_t^{q_t}\}, \qquad (5.21)$$

such that

$$\mathcal{M} \cap \mathcal{N} = \{\}, \qquad \text{and} \qquad \mathcal{M} \cup \mathcal{N} = \{m_1^{p_1}, m_2^{p_2}, \ldots, m_s^{p_s}, n_1^{q_1}, n_2^{q_2}, \ldots, n_t^{q_t}\}, \qquad (5.22)$$

and we denote the product of all elements of $\mathcal{M}$ by $\mathfrak{m}$, and the product of all elements of $\mathcal{N}$ by $\mathfrak{n}$, respectively (notice that $\gcd(\mathfrak{m}, \mathfrak{n}) = 1$). With this notation in place, we propose that all webs of the form $(k\mathfrak{n}, k\mathfrak{m})$ are dual to each other, i.e. for two different $(\mathfrak{n}, \mathfrak{m})$ and $(\mathfrak{n}', \mathfrak{m}')$ we propose[17]

$$X_{k\mathfrak{n}, k\mathfrak{m}} \sim X_{k\mathfrak{n}', k\mathfrak{m}'}. \qquad (5.23)$$

In particular, as we have proposed above, the partition functions $\mathcal{Z}_{X_{k\mathfrak{n}, k\mathfrak{m}}}$ and $\mathcal{Z}_{X_{k\mathfrak{n}', k\mathfrak{m}'}}$ are identical after a judicious change of variables.

Notice that the 3×3 matrix of transformation U given by eq. (5.14),

$$\begin{pmatrix} \rho' \\ \tau' \\ m' \end{pmatrix} = U \begin{pmatrix} \rho \\ \tau \\ m \end{pmatrix}, \qquad U = \begin{pmatrix} \frac{M}{k} & \frac{N}{k} & -\frac{2NM}{k} \\ \frac{(M-k)^2}{Nk} & \frac{M}{k} & -\frac{2M(M-k)}{k} \\ \frac{1}{N}(\frac{M}{k} - 1) & \frac{1}{k} & 1 - \frac{2M}{k} \end{pmatrix}, \qquad (5.24)$$

has the property $U^2 = 1$. This property together with the fact that $\text{Tr}\, U = 1$ implies that the eigenvalues of U are $\{-1, 1, 1\}$. We can choose a new set of parameters α_1, α_2 and α_3 (which are a linear combination of ρ, τ and m), such that under the transformation in eq. (5.14),

$$\alpha_1 \mapsto -\alpha_1, \qquad \text{and} \qquad \alpha_{2,3} \mapsto \alpha_{2,3}. \qquad (5.25)$$

---

[17]As an example, we propose that the configurations $(30, 1) \sim (15, 2) \sim (10, 3) \sim (6, 5) \sim (5, 6) \sim (3, 10) \sim (2, 15) \sim (1, 30)$ are dual to each other.

The plane $\alpha_1 = 0$ is a wall of the (ρ, τ, m) Kähler cone and the flop transitions responsible for eq. (5.14) are reflections on this wall. In terms of (ρ, τ, m) the parameter α_1 is given by

$$\alpha_1 = N\Big(\rho + \frac{2M}{M-k}\tau - \frac{m}{M-k}\Big).\tag{5.26}$$

such that the wall $\alpha_1 = 0$ is given by,

$$(M-k)\rho + 2M\tau - m = 0.\tag{5.27}$$

The above codimension-one wall in the (ρ, τ, m) space has a form very similar to that of Humbert surfaces [60–62], although the corresponding invariant is negative.

6 Conclusions

In this paper, we have discussed a two-parameter family of little string theories that generically preserve eight supercharges. These theories are labelled by two integers (N, M) and are realised by a particular decoupling limit of M5-branes probing an orbifold geometry. The M5-branes are spread out on a circle of radius ρ, while compactified on a circle of radius τ with transverse space an A-type orbifold. The proposed duality that we discussed in the paper indicates that, as a consequence of this double compactification, this system of branes is dual to a setup with $\frac{NM}{k}$ M5-branes probing $\mathrm{ALE}_{A_{k-1}}$ (for $k = \gcd(N, M)$). Notice, however, that this new set of branes is compactified with new parameters (ρ', τ'), which are related to (ρ, τ) according to the duality map proposed in section 5. We recall that the duality does not hold in the limit $\rho \to \infty$ (i.e. the case that the M5-branes are arranged on $\mathbb{R}$ rather than S^1).

The M5-brane system was studied using a dual description in terms of toric Calabi-Yau threefolds $X_{N,M}$. These Calabi-Yau threefolds realise little string theories via F-theory compactification. We have indeed shown explicitly for a number of examples that $X_{N,M}$ and $X_{NM/k,k}$ can be related to each other through a series of flop transitions. They are thus just two different points in the extended moduli space and therefore the theories labelled by (N, M) and $(NM/k, k)$, with $k = \gcd(N, M)$, are dual to each other. This duality relates different members of the two-parameter class of $\mathcal{N} = (1, 0)$ little string theories studied in [9, 10]. However, it should be noted that the theories labelled by (N, M) and $(\frac{NM}{k}, k)$ live in different points of the parameter space of little string theories: indeed, as we have already seen in the dual description through M5-brane webs, the parameters ρ and τ are different in the two cases.[18] Furthermore, the little string partition function is invariant under flop transitions and, therefore, relates the BPS states of the two dual theories. We have generalised an emergent pattern of these examples to the generic case and have made a conjecture how to obtain the full duality map between the parameters of the two theories.

The duality we discussed has consequences for other systems as well which are related to little string theories. The partition function of the (N, M) little strings is related to the

---

[18]Notice in this regard, while the parameters (ρ, τ) are simply two Kähler parameters from the perspective of the Calabi-Yau manifold, the rather play the role of external parameters from the perspective of the LST. See [8, 10] for more explanations.

elliptic genus of a $(0, 2)$ sigma model with target space which is the product of M U(N) instanton moduli spaces of rank (of various charges) [25, 27, 28]. The duality between $X_{N,M}$ and $X_{NM/k,k}$ again implies that there are relations between sigma-models with different (N, M). However, since the duality map is rather complex and mixes in a non-trivial fashion the distances of the M5-branes, the duality relation at the level of the sigma-models is non-perturbative and will be explored elsewhere [56].

Acknowledgments

References

[1] J.A. Harvey, S. Murthy and C. Nazaroglu, *ADE Double Scaled Little String Theories, Mock Modular Forms and Umbral Moonshine*, *JHEP* **05** (2015) 126 [arXiv:1410.6174] [INSPIRE].

[2] O. Aharony, M. Berkooz and S.-J. Rey, *Rigid holography and six-dimensional* $\mathcal{N} = (2, 0)$ *theories on* $AdS_5 \times S^1$, *JHEP* **03** (2015) 121 [arXiv:1501.02904] [INSPIRE].

[3] Y.-H. Lin, S.-H. Shao, Y. Wang and X. Yin, *Interpolating the Coulomb Phase of Little String Theory*, *JHEP* **12** (2015) 022 [arXiv:1502.01751] [INSPIRE].

[4] J. Kim, S. Kim and K. Lee, *Little strings and T-duality*, *JHEP* **02** (2016) 170 [arXiv:1503.07277] [INSPIRE].

[5] M. Del Zotto, C. Vafa and D. Xie, *Geometric engineering, mirror symmetry and* $6d_{(1,0)} \to 4d_{(\mathcal{N}=2)}$, *JHEP* **11** (2015) 123 [arXiv:1504.08348] [INSPIRE].

[6] M. Aganagic and N. Haouzi, *ADE Little String Theory on a Riemann Surface (and Triality)*, arXiv:1506.04183 [INSPIRE].

[7] A. Giveon, J. Harvey, D. Kutasov and S. Lee, *Three-Charge Black Holes and Quarter BPS States in Little String Theory*, *JHEP* **12** (2015) 145 [arXiv:1508.04437] [INSPIRE].

[8] S. Hohenegger, A. Iqbal and S.-J. Rey, *Instanton-monopole correspondence from M-branes on* $\mathbb{S}^1$ *and little string theory*, *Phys. Rev.* **D 93** (2016) 066016 [arXiv:1511.02787] [INSPIRE].

[9] L. Bhardwaj, M. Del Zotto, J.J. Heckman, D.R. Morrison, T. Rudelius and C. Vafa, *F-theory and the Classification of Little Strings*, *Phys. Rev.* **D 93** (2016) 086002 [arXiv:1511.05565] [INSPIRE].

[10] S. Hohenegger, A. Iqbal and S.-J. Rey, *Self-Duality and Self-Similarity of Little String Orbifolds*, *Phys. Rev.* **D 94** (2016) 046006 [arXiv:1605.02591] [INSPIRE].

[11] N. Haouzi and C. Schmid, *Little String Origin of Surface Defects*, *JHEP* **05** (2017) 082 [arXiv:1608.07279] [INSPIRE].

[12] E. Witten, *Some comments on string dynamics*, `hep-th/9507121` [ɪɴSPIRE].

[13] P.S. Aspinwall, *Point - like instantons and the spin (32)/Z(2) heterotic string*, *Nucl. Phys.* **B 496** (1997) 149 [`hep-th/9612108`] [ɪɴSPIRE].

[14] P.S. Aspinwall and D.R. Morrison, *Point - like instantons on K3 orbifolds*, *Nucl. Phys.* **B 503** (1997) 533 [`hep-th/9705104`] [ɪɴSPIRE].

[15] N. Seiberg, *New theories in six-dimensions and matrix description of M-theory on T^5 and $T^5/\mathbb{Z}_2$*, *Phys. Lett.* **B 408** (1997) 98 [`hep-th/9705221`] [ɪɴSPIRE].

[16] N. Kim and S.-J. Rey, *M(atrix) theory on T_5/Z_2 orbifold and five-branes*, *Nucl. Phys.* **B 534** (1998) 155 [`hep-th/9705132`] [ɪɴSPIRE].

[17] K.A. Intriligator, *New string theories in six-dimensions via branes at orbifold singularities*, *Adv. Theor. Math. Phys.* **1** (1998) 271 [`hep-th/9708117`] [ɪɴSPIRE].

[18] A. Hanany and A. Zaffaroni, *Branes and six-dimensional supersymmetric theories*, *Nucl. Phys.* **B 529** (1998) 180 [`hep-th/9712145`] [ɪɴSPIRE].

[19] I. Brunner and A. Karch, *Branes at orbifolds versus Hanany Witten in six-dimensions*, *JHEP* **03** (1998) 003 [`hep-th/9712143`] [ɪɴSPIRE].

[20] O. Aharony, *A brief review of 'little string theories'*, *Class. Quant. Grav.* **17** (2000) 929 [`hep-th/9911147`] [ɪɴSPIRE].

[21] D.R. Morrison and C. Vafa, *Compactifications of F-theory on Calabi-Yau threefolds. 1*, *Nucl. Phys.* **B 473** (1996) 74 [`hep-th/9602114`] [ɪɴSPIRE].

[22] D.R. Morrison and C. Vafa, *Compactifications of F-theory on Calabi-Yau threefolds. 2.*, *Nucl. Phys.* **B 476** (1996) 437 [`hep-th/9603161`] [ɪɴSPIRE].

[23] D.R. Morrison and T. Rudelius, *F-theory and Unpaired Tensors in 6D SCFTs and LSTs*, *Fortsch. Phys.* **64** (2016) 645 [`arXiv:1605.08045`] [ɪɴSPIRE].

[24] S.B. Johnson and W. Taylor, *Enhanced gauge symmetry in 6D F-theory models and tuned elliptic Calabi-Yau threefolds*, *Fortsch. Phys.* **64** (2016) 581 [`arXiv:1605.08052`] [ɪɴSPIRE].

[25] B. Haghighat, C. Kozcaz, G. Lockhart and C. Vafa, *Orbifolds of M-strings*, *Phys. Rev.* **D 89** (2014) 046003 [`arXiv:1310.1185`] [ɪɴSPIRE].

[26] H. Ooguri and C. Vafa, *Two-dimensional black hole and singularities of CY manifolds*, *Nucl. Phys.* **B 463** (1996) 55 [`hep-th/9511164`] [ɪɴSPIRE].

[27] B. Haghighat, A. Iqbal, C. Kozcaz, G. Lockhart and C. Vafa, *M-Strings*, *Commun. Math. Phys.* **334** (2015) 779 [`arXiv:1305.6322`] [ɪɴSPIRE].

[28] S. Hohenegger and A. Iqbal, *M-strings, elliptic genera and $\mathcal{N} = 4$ string amplitudes*, *Fortsch. Phys.* **62** (2014) 155 [`arXiv:1310.1325`] [ɪɴSPIRE].

[29] S. Hohenegger, A. Iqbal and S.-J. Rey, *M-strings, monopole strings and modular forms*, *Phys. Rev.* **D 92** (2015) 066005 [`arXiv:1503.06983`] [ɪɴSPIRE].

[30] N.A. Nekrasov and S.L. Shatashvili, *Quantization of Integrable Systems and Four Dimensional Gauge Theories*, `arXiv:0908.4052` [ɪɴSPIRE].

[31] A. Mironov and A. Morozov, *Nekrasov Functions and Exact Bohr-Zommerfeld Integrals*, *JHEP* **04** (2010) 040 [`arXiv:0910.5670`] [ɪɴSPIRE].

[32] M. Reid, *The moduli space of 3-folds with $K = 0$ may nevertheless be irreducible*, *Math. Ann.* **287** (1987) 329.

[33] P.S. Green and T. Hubsch, *Connecting Moduli Spaces of Calabi-Yau Threefolds*, *Commun. Math. Phys.* **119** (1988) 431 [ɪɴSPIRE].

[34] P.S. Green and T. Hubsch, *Possible Phase Transitions among Calabi-Yau Compactifications*, *Phys. Rev. Lett.* **61** (1988) 1163 [ɪɴSPIRE].

[35] P. Candelas, P.S. Green and T. Hubsch, *Finite Distances Between Distinct Calabi-Yau Vacua: (Other Worlds Are Just Around the Corner)*, *Phys. Rev. Lett.* **62** (1989) 1956 [ɪɴSPIRE].

[36] P. Candelas, P.S. Green and T. Hubsch, *Rolling Among Calabi-Yau Vacua*, *Nucl. Phys.* **B 330** (1990) 49 [ɪɴSPIRE].

[37] C. Schoen, *On fiber products of rational elliptic surfaces with section*, *Math. Z.* **197** (1988) 177.

[38] T.J. Hollowood, A. Iqbal and C. Vafa, *Matrix models, geometric engineering and elliptic genera*, *JHEP* **03** (2008) 069 [hep-th/0310272] [ɪɴSPIRE].

[39] M. Aganagic, A. Karch, D. Lüst and A. Miemiec, *Mirror symmetries for brane configurations and branes at singularities*, *Nucl. Phys.* **B 569** (2000) 277 [hep-th/9903093] [ɪɴSPIRE].

[40] L.B. Anderson, X. Gao, J. Gray and S.-J. Lee, *Multiple Fibrations in Calabi-Yau Geometry and String Dualities*, *JHEP* **10** (2016) 105 [arXiv:1608.07555] [ɪɴSPIRE].

[41] O. Aharony, A. Hanany and B. Kol, *Webs of (p,q) five-branes, five-dimensional field theories and grid diagrams*, *JHEP* **01** (1998) 002 [hep-th/9710116] [ɪɴSPIRE].

[42] N.C. Leung and C. Vafa, *Branes and toric geometry*, *Adv. Theor. Math. Phys.* **2** (1998) 91 [hep-th/9711013] [ɪɴSPIRE].

[43] I. Smith, R.P. Thomas and S.T. Yau, *Symplectic conifold transitions*, *J. Diff. Geom.* **62** (2002) 209 [math/0209319] [ɪɴSPIRE].

[44] A. Strominger, *Massless black holes and conifolds in string theory*, *Nucl. Phys.* **B 451** (1995) 96 [hep-th/9504090] [ɪɴSPIRE].

[45] B.R. Greene, D.R. Morrison and A. Strominger, *Black hole condensation and the unification of string vacua*, *Nucl. Phys.* **B 451** (1995) 109 [hep-th/9504145] [ɪɴSPIRE].

[46] E. Witten, *Phase transitions in M-theory and F-theory*, *Nucl. Phys.* **B 471** (1996) 195 [hep-th/9603150] [ɪɴSPIRE].

[47] X. Rong and Y. Zhang, *Continuity of Extremal Transitions and Flops for Calabi-Yau Manifolds*, *J. Diff. Geom.* **89** (2011) 233 [arXiv:1012.2940] [ɪɴSPIRE].

[48] T. Hubsch, *Calabi-Yau Manifolds: A Bestiary for Physicists*, World Scientific, Singapore, (1994), [https://doi.org/10.1142/1410].

[49] A.C. Avram, M. Kreuzer, M. Mandelberg and H. Skarke, *The web of Calabi-Yau hypersurfaces in toric varieties*, *Nucl. Phys.* **B 505** (1997) 625 [hep-th/9703003] [ɪɴSPIRE].

[50] P. Candelas, X. de la Ossa, Y.-H. He and B. Szendroi, *Triadophilia: A Special Corner in the Landscape*, *Adv. Theor. Math. Phys.* **12** (2008) 429 [arXiv:0706.3134] [ɪɴSPIRE].

[51] P. Candelas and A. Constantin, *Completing the Web of Z_3 - Quotients of Complete Intersection Calabi-Yau Manifolds*, *Fortsch. Phys.* **60** (2012) 345 [arXiv:1010.1878] [ɪɴSPIRE].

[52] M. Eichler and D. Zagier, *The Theory of Jacobi Forms*, Birkhäuser (1985).

[53] J. Li, K. Liu and J. Zhou, *Topological string partition functions as equivariant indices*, [*Asian J. Math.* **10** (2006) 81](math/0412089) [math/0412089] [INSPIRE].

[54] R. Dijkgraaf, G.W. Moore, E.P. Verlinde and H.L. Verlinde, *Elliptic genera of symmetric products and second quantized strings*, [*Commun. Math. Phys.* **185** (1997) 197](hep-th/9608096) [[hep-th/9608096](hep-th/9608096)] [INSPIRE].

[55] T. Kawai, *K3 surfaces, Igusa cusp form and string theory*, [hep-th/9710016](hep-th/9710016) [INSPIRE].

[56] S. Hohenegger, A. Iqbal and S.-J. Rey, to appear.

[57] S.J. Rey, *On string theory and axionic strings and instantons*, in *Vancouver 1991, Proceedings, Particles and fields '91*, vol. 2, pg. 876–881, and SLAC Stanford, SLAC-PUB-5659, [https://doi.org/10.13140/2.1.4920.1605].

[58] S.-J. Rey, *The Confining Phase of Superstrings and Axionic Strings*, [*Phys. Rev.* **D 43** (1991) 526](INSPIRE) [INSPIRE].

[59] A.S. Chou, R. Kallosh, J. Rahmfeld, S.-J. Rey, M. Shmakova and W.K. Wong, *Critical points and phase transitions in $5 - D$ compactifications of M-theory*, [*Nucl. Phys.* **B 508** (1997) 147](hep-th/9704142) [[hep-th/9704142](hep-th/9704142)] [INSPIRE].

[60] G. Humbert, *Sur les fonctions abéliennes singulières. I*, J. Math. Pures Appl. **V** (1899) 233.

[61] G. Humbert, *Sur les fonctions abéliennes singulières. II*, J. Math. Pures Appl. **VI** (1900) 279.

[62] G. Humbert, *Sur les fonctions abéliennes singulières. III*, J. Math. Pures Appl. **VII** (1901) 97.